FINITE ELEMENT ANALYSIS OF MASONRY INFILL PANELS RETROFITTED WITH FERROCEMENT

A Thesis
by
M. Shahria Alam
Roll No. 100104333

Submitted to the Department of Civil Engineering, Bangladesh University of Engineering and Technology, Dhaka, in partial fulfillment of the degree of

MASTER OF SCIENCE IN CIVIL ENGINEERING (STRUCTURAL)

2004

FINITE ELEMENT ANALYSIS OF MASONRY INFILL PANELS RETROFITTED WITH FERROCEMENT

M. Sc. Thesis by

M. Shahria Alam
Roll No. 100104333

A Master of Science (M.Sc.) Thesis approved as to the style and content for the partial fulfillment of the requirement of the degree of Master of Science in Civil Engineering (Structural) on 23rd March 2004.

Dr. Khan Mahmud Amanat
Associate Professor
Dept. of Civil Engineering
BUET, Dhaka-1000.

Chairman (Supervisor)

Dr. Sk. Sekender Ali
Professor and Head
Department of Civil Engineering
BUET, Dhaka-1000.

Member (Ex-Officio)

Dr. Tahsin Reza Hossain
Associate Professor
Department of Civil Engineering
BUET, Dhaka-1000.

Member

Dr. Md. Afsar Ali
Assistant Professor
Department of Mechanical Engineering
BUET, Dhaka-1000.

Member (External)

DEDICATIONS

**To my *MOTHER*
who died just after the day I
defended my M.Sc. Thesis**

DECLARATION

It is hereby declared that except for the contents where specific reference have been made to the work of others, the studies contained in this thesis is the result of investigation carried out by the author. No part of this thesis has been submitted to any other University or other educational establishment for a Degree, Diploma or other qualification (except for publication).

Signature of the Candidate

(M. Shahria Alam)

ACKNOWLEDGMENT

Thanks to Almighty Allah for His graciousness, unlimited kindness and with the blessings of Whom the good deeds are fulfilled.

The author wishes to express his deepest gratitude to his supervisor Dr. Khan Mahmud Amanat, for his continuous guidance, invaluable suggestions, affectionate encouragement, generous help and unfailing enthusiasm at every stage of this study. His active interest in this topic and valuable advice was the source of author's inspiration.

The author is also grateful to Dr. Munaz A. Noor, Assistant Professor, Department of Civil Engineering, BUET for his help and valuable suggestions regarding this work. The author is also grateful to Ms. Anjuman Shahriar, Lecturer, Department of Civil Engineering, BUET for active co-operation.

The author also wishes to express his appreciation to his friends living abroad for supporting him with valuable journal papers and information.

A very special debt of deep gratitude is offered to his parents, brothers and his wife, who are always a constant source of inspiration throughout his life.

ABSTRACT

Retrofitting of damaged masonry infilled frame using ferrocement overlay as well as strengthening of existing infilled frames with ferrocement is a cost effective method in the context of Bangladesh, where many old structures need such retrofitting or strengthening works against possible earthquake hazards. However, virtually no mathematical or computational information is available to quantitatively estimate the effect of such retrofitting technique. The study presents a numerical investigation of the retrofitting effect of masonry-infilled reinforced concrete frames by ferrocement. The finite element technique has been effectively used to analyze bare RC frames, un-retrofitted masonry-infilled and retrofitted masonry-infilled frames. The proposed model accommodates the material nonlinearities of both concrete and masonry, and yielding of reinforcing bars.

The FE analyses procedure used in this study has been able to simulate test results on infilled RC frames verifying the effectiveness of such FE modeling. The same FE model was then used to simulate the test results of a retrofitted RC frame. It has been found that the lateral load carrying capacity of the damaged and retrofitted frame predicted by the FE model is in close agreement with the experimental results.

The FE analysis methodology has been proven to be an effective tool to reasonably estimate the load carrying capacity of the retrofitted infilled frames without resorting to expensive laboratory testing. This approach can now be effectively used in predicting the existing capacity of the building frames as well as the degree of strengthening that would be required to achieve if ferrocement overlay is applied as a retrofitting material.

TABLE OF CONTENTS

LIST OF TABLES

LIST OF FIGURES

Chapter 1

INTRODUCTION

1.1 BACKGROUND

The performance of masonry-infilled reinforced concrete (RC) frames under lateral loads is often much better than the bare frame structures. It is well established and has been reported that infill panel increases the stiffness of bare frame 4 to 20 times, [Comite Euro-International Du Beton, (1996)]. Although most of the RC buildings of our country consist of infill panels, still then many existing RC frame buildings are deficient to withstand moderate to severe earthquakes. Recent earthquakes in several parts of the country have repeatedly indicated that older RC frames suffered extensive damage. Typical damage was related to cracking of columns, beams and infill panels. Again, various components of reinforced concrete and masonry structures are often found to exhibit distress, even before their service life is over due to several causes. Defects, failure and general distress in the structure could be the result of the structural deficiency caused by erroneous design, poor workmanship or overloading. Moreover, structure may suffer deterioration of concrete as a result of inadequate cover to the reinforcement, presence of chloride or poor quality concrete. Fire damage may also weaken the structure as a whole as well as an individual member. The distressed structures require immediate attention, inquiry into the cause of distress and suitable remedial measure, so as to bring the structure into its service.

A study on seismic vulnerability of buildings of five major cities of Bangladesh was conducted by the Department of Civil Engineering of Bangladesh University of Engineering and Technology (BUET, 2002), sponsored by CARE. In this study the seismic damage prediction was made according to macro-seismic intensity scale. This assessment gives a vivid idea of how many buildings are susceptible to earthquake hazard and also the grade of damage they are going to suffer. The building evaluation showed that under an earthquake of intensity VIII (MMI), more than 60% of the buildings would be moderately or partially damaged and needed to be retrofitted, which would result in a large amount of money. Therefore, the development of effective and affordable retrofitting techniques for masonry elements is an urgent need for our country.

Researches conducted in the past have shown that the strength and ductility can be enhanced significantly in many ways but the employment of such methods would be costly and require highly skilled workers. Among a number of extensively studied strengthening techniques to enhance the performance of beams and columns of concrete frames, ferrocement has been found very effective and most economic. Even the effectiveness of ferrocement coating on masonry wall has also been proven through a series of experiments. Recently it has been demonstrated by experiment (Alam, 2003) that damaged masonry panel retrofitted with ferrocement can increase the inplane load resistance quite significantly. As the infrastructure continues to age, retrofitting of the existing structures is economically more viable than new construction. Increase in the cost of construction materials and construction itself has forced the engineers to look for economical and better methods for the repairs of damaged or distressed structures.

Before any retrofitting scheme is applied to a real structure it is necessary to analyze the existing structure to estimate its strength, which in turn helps to assess the required retrofitting work. Adequate knowledge is also required about the basic mechanics of ferrocement as a retrofitting material. Hence, development of a proper computational model is quite necessary to predict the performance of retrofitted structure and thereby helps in achieving an optimum and effective solution in this regard.

1.2 OBJECTIVES OF THE PRESENT STUDY

The objectives of the present study are as follows:

(i)   To analyze appropriate numerical model to simulate the behavior of a bare RC frame and unreinforced masonry infilled RC frame.

(ii)   To analyze appropriate numerical model to simulate the behavior of a damaged unreinforced masonry wall retrofitted with ferrocement.

(iii)   To identify the amount of contribution of the ferrocement in the infill in increasing the strength of the frame.

(iv)   To compare the experimental results with the predicted structural performance of the computational models.

1.3 SCOPE AND METHODOLOGY OF THE STUDY

The present research topic has been undertaken to study the behavior of damaged masonry infilled RC frame structures retrofitted with ferrocement overlay. To study this effect, finite element analysis (using a package software) has been carried out over bare RC frame, masonry infilled RC frame and finally over damaged infilled frame retrofitted with ferrocement. Here FE model of portal frames with and without masonry infill have been subjected to lateral load till failure. Then it is unloaded gradually. After this, ferrocement overlays are applied over the damaged infill panel and loaded again up to failure. The results obtained from this analysis are used to validate the available experimental data. The salient features within the scope may be summarized as below:

(i)   To determine the load carrying capacity of bare RC frame, masonry infilled RC frame and also the masonry infilled RC frame retrofitted with ferrocement.

(ii)   To predict the failure pattern of the retrofitted infill walls subjected to lateral loads.

(iii)   To predict the life cycle of the whole structure after retrofitting and this could help in achieving significant economy.

1.4 ORGANIZATION OF THE DISSERTATION

This dissertation is organized according to the stages followed for the development of the numerical investigation. Thus, Chapter 1 introduces a general statement of the problem and the objectives of this research. Chapter 2 reviews the available literature discussing various studies conducted on infilled frames. This chapter also includes a literature survey on the different techniques used for retrofitting masonry structures including the use of ferrocement as well as highlighting the structural application of the ferrocement in repairing/ strengthening/ retrofitting of reinforced concrete structures. At the end of this chapter an experimental program (Alam, 2003) has been described conducted in the concrete laboratory of BUET to evaluate the performance of masonry infilled RC frame retrofitted with ferrocement overlay. The next chapter discusses the computational model available on masonry infilled frame. Chapter 4 describes the development of the finite element (FE) model of the bare frame and the

masonry infilled frame with and without ferrocement coating. Assumptions and expressions used for the development of numerical model are also presented here. Chapter 5 presents the results obtained from the analysis of the FE models showing the load-deflection relationship of the RC frame with infill panels, original and the retrofitted one following step-by-step logical approximations based on and supported by experimental observations. Finally, Chapter 6 draws conclusion of the current work and discusses recommendations for future work in the area of masonry strengthening with ferrocement overlay.

Chapter 2

RETROFITTING OF INFILLED FRAMES

2.1 INTRODUCTION

Masonry infill panels have been used in reinforced concrete (RC) frame structures as exterior and interior partition walls for a long time. Although in traditional design the infills are not regarded as structural elements, these have a direct influence on structural characteristics such as stiffness and energy dissipation capacity. The effect of masonry infill panels in changing the stiffness, ultimate capacity and failure mode of framed structures has been one of the most interesting research topics in the last few decades. There had been a number of evidences of the contribution of masonry infill in resisting lateral loads during earthquakes, strong wind and tornadoes in the past. This proves the high rigidity of infill panels and explains the fact that presence of masonry infills confined within the frames provides strong lateral load resistance. Ever since these experiences, researchers throughout the world have been conducting successive investigations in determining the behavior of infilled frames. Various approaches have already been adopted starting from simple strength of materials approach, through trials to match experimental results using simple models. Methods, based on the theory of elasticity, equilibrium and energy approach, plastic analysis and finally finite element (FE) analysis have also been used.

The literature survey in this study is divided into four distinct sections. The first section highlights various experimental and theoretical studies conducted to date in the area of masonry infilled frames. The next section describes the extent of use of ferrocement as a retrofitting material. Then the later section shows some of the retrofitting techniques of infill panels. The final section depicts the experimental investigation of infill panels retrofitted with ferrocement of different researchers and particularly the research (Alam, 2003), which had been carried out in the Concrete laboratory of BUET.

2.2 WORKS ON INFILLED FRAMES

The behavior of infilled frames under lateral loads has been investigated by a number of researchers. Holmes (1961), Stafford Smith (1962, 1966, 1967), Mainstone and

Weeks (1970), McBridge (1984), Yong (1984), Amos (1986), and Richardson (1986) conducted experimental and analytical investigations on the lateral stiffness and strength of steel frames infilled with mortar and concrete panels. Dawe and Seah (1989), Flanagan et al. (1992), and Mander et al.(1993) studied the behavior of masonry infill steel frames under in plane and out of plane loads. Dhanasekar and Page (1986) developed finite element models of masonry infilled steel frames. Saneinejad and Hobbs (1995) developed equivalent diagonal strut method to predict the strength and stiffness of infilled steel frames as well as infill diagonal cracking load.

The behavior of masonry infilled RC frames, which is generally more complicated than that of infilled steel frames, has been examined by Fiorato et al.(1970), Kahn and Hanson (1979), Zarnic and Tomazevic (1990), Murty et al. (2000) and recently by Ghosh and Amde (2002), Al-Chaar (2002) and others. Both experimental and analytical studies have been carried out by Mehrabi et al. (1994, 1996, 1997) to investigate the performance of masonry infilled RC frames under in-plane lateral loadings under different design conditions. Based on tests and nonlinear finite element analyses, a unified plastic analysis for infilled frames with three types of interface conditions was proposed by Liauw and Kwan (1985). Unreinforced masonry walls used as infill panels in RC frames are vulnerable elements of buildings when subjected to earthquake loading and this has been studied either experimentally or analytically by Klingner and Bertero (1983), Bertero and Brokken (1983), Zarnic (1990), Mosalam et al. (1997), Kappos et al. (1998, 2002) and others. Manos et al. (2000) experimentally investigated the influence of masonry infills on the earthquake response of multi-story RC frames. Dey (2000) and later Waset (2002) worked on sway characteristics of masonry infilled RC building frames under lateral load. The study of Dymiotis et al. (2001) focused on the seismic reliability and probabilistic assessment of RC frames infilled with unreinforced masonry walls. Effect of randomly distributed infills on the vibration characteristics of reinforced concrete frames was investigated by Haque (2002).

2.3 USE OF FERROCEMENT AS A RETROFITTING MATERIAL

In the last few decades, incidences of failures of reinforced concrete structures have been seen widely because of increasing service loads and/or durability problems. The

defects and distresses in the structures are first noticed in the form of cracks, corrosion of reinforcing bars, spalling and scaling of concrete from the slabs, beams, columns, stairs, walls, which are frequently observed. This not only affects the appearance but also the strength and durability of the structures. Finally, the structure may collapse or need to be demolished for safety reasons. The economic losses in this regard are billions of dollars. Reconstruction is another expensive part. For this reason the size and form of repair and rehabilitation of structures has increased tremendously since there has been an increased emphasis on repair and retrofitting of structural defects over demolition and new construction.

Many factors contribute to the deterioration of reinforced concrete structures and affect their safety. Some of these are cracking due to impact and dynamic loading, creep, thermal cycling, inadequate design and faulty construction. Many investigations have been undertaken in strengthening and repairing of slabs, beams, columns but few research works are available for strengthening of infills. Because of its ease of application and low cost, especially in developing countries, ferrocement has been used for many days as a repair material for reinforced concrete and masonry elements as an alternative to the other highly expensive repair materials. Ferrocement is a type of thin wall reinforced concrete commonly constructed of hydraulic cement mortar reinforced with closely spaced layers of continuous and relatively small size wire mesh, made of metallic or other suitable materials. The close spacing and uniform dispersion of reinforcement within the matrix helps itself in possessing excellent mechanical properties in terms of crack control, impact resistance, and toughness. Moreover, it allows rapid construction with no heavy machineries and high-level skilled workers, imposes small additional weight and low cost construction. All these unique qualities of structural performance make ferrocement an ideal material for rehabilitation.

Research and development work on ferrocement has progressed at a tremendous pace during recent years and a variety of structures using innovative design and construction techniques have been built worldwide. As a result, a large volume of technical information is now available on various aspects of ferrocement design, construction, maintenance and repair. Increasing popularity and growing public acceptance have made it necessary to formulate design and working guidelines by

collecting the available information. Efforts have also been made in recent years to improve the performance of reinforced concrete elements by applying ferrocement overlay. The concept has been intuitively applied for repair and strengthening of distressed elements.

Iorns (1987) introduced laminated ferrocement as a new production technique of ferrocement. This technique has been used successfully for a wide variety of structural repairs and has proven to be impact and corrosion resistant. Water tanks and swimming pools could be renovated using an unbounded ferrocement laminate on the interior surface while pressure vessels and tanks were reinforced by an interior and exterior laminates containing high tensile wires between mesh layers.

2.3.1 Ferrocement in Retrofitting Beams

Anwar et al. (1991) investigated the rehabilitation technique for reinforced concrete structural beam elements using ferrocement. The technique involved strengthening of reinforced concrete beams by application of hexagonal chicken wire mesh and skeletal steel combined with ordinary plastering. The test result is in good compliance with the original design capacity of the beams. From the test result obtained a design chart has been developed to determine the parameters for rehabilitation of the beam elements.

Recent experimental studies of Andrews and Sharma (1988) have demonstrated the suitability of ferrocement for the repair of flexurally overloaded reinforced concrete beams. After straightening and removal of the fragmented concrete, the damaged length of longitudinal steel and any stirrups are replaced. The ferrocement encasing is then fixed in place, after which a cement rich mortar is applied to restore the original cross-sectional dimensions. On re-testing the beams repaired with ferrocement proved superior compared to those fixed with similar conventional reinforced concrete work, offering enhanced strength, reduced deflection and improved crack control.

Humayun and Robles-Austriaco (1991) used shotcrete ferrocement to strengthen existing reinforced concrete beams. This method has also proven effective at increasing flexural capacity and offers potential for enhancing shear capacity as well.

Lub and Wanroji (1988) reported that the strengthening of existing beams in reinforced concrete building structures could be done by means of shotcrete ferrocement. It was found that the mesh is fully effective and a monolithic condition of shotcrete layer and original concrete beam attained. The wire mesh was found to act as excellent shear reinforcement.

Kaushik and Dubey (1994) studied the performance of RC ferrocement composite beams through experimental investigation on RC beam cast on ferrocement and distressed beams rehabilitated by ferrocement jacking. They reported that the increase in ultimate strength compared to RC beams was 44% for composite beams and 39% for rehabilitated beams. This showed that composite beams and rehabilitated beams are capable of performing equally well. Moreover, the ultimate strength and stiffness of RC beam can be significantly increased by strengthening with precast ferrocement plates in the shear failure zone. Therefore, ferrocement can satisfactorily be used as the precast part of the composite in which RC beam is cast.

An experimental investigation was carried by Kadir et al. (1997) to study the ultimate load, flexural behavior and mode of failure at collapse of reinforced concrete beams using ferrocement permanent formwork (composite beams). The linkage between the two materials was achieved by placing shear connectors along the length of the beam. Test result showed that the reinforced concrete beams with ferrocement permanent formwork failed by flexure. The composite beam with shear connectors carried about 12% higher load and 10% reserved flexural strength and showed lower deflection when subjected to reinforced concrete beam without shear connectors. The ferrocement formwork with and without shear connectors contributed about 21%-75% and 16%-50% to the flexural strength respectively.

Fahmy et al. (1997) proposed a method for repairing reinforced concrete beams using ferrocement laminates as a viable alternative to steel plates which are directly glued to the cracked tension face of the beam by epoxy resins. Twenty-seven reinforced concrete beams were tested over simply supported one-meter span. Each specimen was first loaded with a central line load till collapse or up to (85%) of the ultimate load of the control specimen. After unloading, the damaged beam specimens were repaired by either one layer at the tension face, two layers at the tension face, or U-

shaped layer around the beam cross section. The experimental results of the repaired beams demonstrated that irrespective of the pre-loading level or the repair scheme, better cracking behavior for all test specimens could be achieved compared to their original behavior. Under short term loading conditions, all repaired specimens restored more than their original ultimate strengths. It was found that the ultimate strength of the repaired specimens is affected by the level of damage sustained prior to repairing. The ductility ratio and energy absorption properties were also improved by this method of repair.

Singh et al. (1988) suggested a simple procedure for the strengthening of brick masonry columns using ferrocement. Brick masonry column in old structure are usually used for low-rise structures. Although the performance of masonry columns under axial loads may be satisfactory, they possess a limited moment carrying capacity. Improving a moment carrying capacity become vital if the structure is subjected to modifications resulting in eccentric loads to be transferred to the columns. Ferrocement encasement of masonry column can considerably increase its capacity to resist axial loads and moments. Applying the ferrocement encasement, Singh et al. (1988) report the failure loads to be double that of uncased columns. Failure is due to failure in casing under combined bending and tension under lateral loads.

2.3.2 Ferrocement in Retrofitting Columns

Ferrocement coatings have also been used to increase bending capacity and improve the ductility of brickwork columns. This was investigated by Humayun and Robles-Austriaco (1991) and also by Yadunandan et al. (1992). The technique is used to enhance seismic resistance and flexural capacity where modifications to the structure have induced eccentric loading. Generally the mesh is fixed to the brickwork columns using wire shear connectors. Yadunandan et al. (1992) showed in his research that compared to plain brickwork columns, columns encased in a 25 mm thick ferrocement layer, reinforced with a chicken wire mesh, exhibited up to 275% increase in compressive strength, with improved ductility under axial loading. Adequate shear connection between the ferrocement coating and brickwork proved important in achieving full composite action.

Ahmed et al. (1994) carried out another interesting research work to investigate the possibility of using ferrocement as a retrofit material for masonry columns. Uniaxial compression test were performed on three uncoated brick columns, six coated brick columns with 25 mm plaster and another six columns coated with 25 mm thick layer of ferrocement. The study demonstrated that the use of ferrocement coating strengthens brick columns significantly and improves their cracking resistance.

Nedwell et al. (1994) conducted a preliminary investigation into the repair of short square columns using ferrocement. A short program was undertaken to provide some information regarding the effect of ferrocement repair on short columns subject to axial loading. It was found that the use of ferrocement retrofit coating increases the apparent stiffness of the columns significantly and improves the ultimate load carrying capacity.

Fahmy et al. (1999) proposed a method for repairing reinforced concrete columns using ferrocement laminates as a viable economic alternative to the highly expensive conventional jacketing methods by reinforcing concrete or steel jackets. Twenty-four RC column models were tested under concentric compression load. Each specimen was first loaded till failure or up to either 67% or 85% of the ultimate load of the control specimens. After unloading, the damaged column specimens were repaired by a complete jacket form of 10mm thick ferrocement around the four sides of the specimen. Three different types of reinforcing steel meshes were used, welded wire mesh and expanded meshes of two types. The experimental results of the repaired columns demonstrated that irrespective of the pre-loading level or the mesh type, better behavior and load carrying capacity for all test specimens could be achieved compared to their original behavior. Under short term loading conditions, all repaired specimens restored more than their original ultimate strengths. It was found that the ultimate load of the repaired columns specimens is affected by the level of damage sustained prior to repairing.

Takiguchi and Abdullah (2000, 2001) carried out an investigation on the strengthening of square reinforced concrete columns that are susceptible to shear failure by using circular ferrocement jackets. Based on 1:6 scale models, six identical RC columns were constructed. Two of these columns were tested under as-built

conditions, while the remaining four were strengthened with different numbers of layers of wire mesh before being tested. Unless failure occurred at an earlier stage, all columns were tested under cyclic lateral forces and constant axial load. From the test results, it was observed that both original columns suffered shear failure at low displacement ductility. But by providing circular ferrocement jackets over the entire length, the displacement ductility of the columns could be improved significantly.

2.3.3 Other Applications of Ferrocement

Other applications of ferrocement retrofit have included repair of concrete arches and domes, new linings for steel and concrete water storage tanks, sewer relining, repair of boats, and swimming pools which has been demonstrated by Romualdi (1987) and Humayun and Robles-Austriaco (1991). Advantages of this approach include increased strength, improved crack control, cost reduction, and enhanced corrosion protection.

The ability of ferrocement to fit snugly into curved surface makes it an ideal material for the rehabilitation of dome and shells. An example of such rehabilitation is the restoration of domes in the Widmill theatre in UK in 1988 (Rahman, 2002).

Sharma et al. (1984) rehabilitated an overhead circular water tank of 210000-litre capacity using ferrocement. The superior crack resistance properties made it suitable for water retaining satisfactorily. The tank was put out of service due to heavy leakage soon after its construction. The inspection of tank revealed the presence of a large cracked and honeycombed area in the center of tank wall, which was all along the wall periphery. At some point only coarse aggregate was deposited with no fine aggregate making it the major source of water leakage through the voids in such an area. After repairing by using ferrocement no leakage was observed and the tank seemed to be performing with full efficiency. The rehabilitated tank is currently under service.

Trikha et al. (1988) reported the process of repairing of damaged steel water tank using ferrocement. Steel water storage tank are widely used in every part of the world. One predominant problem associated with steel tank is that of corrosion. Due to the corrosion of steel tank have to replaced after an extra period of time. A common

remedial measure is to patch up to the corroded portion with new plates welded in place. But this option is not economical. The rehabilitation using ferrocement is quite economical and simple. The process consists of using the existing steel tank as a formwork while a new ferrocement inner lining is provided at hold water. The steel tank at student hostel of Roorkee University has been successfully rehabilitated using ferrocement inner linings, (Rahman, 2002).

The process of sanitary sewer relining using ferrocement to rehabilitate the sewer has already gained wide acceptance in UK. It is now being more commonly used in other countries as well. In sewer application it is important to pay attention to the type of and porosity of the mortar matrix used. This should pose no problems since there are a variety of formulations that provide adequate resistance to chemical attack. The cement used for mortar should be sulphate resistant.

Iorns (1987) studied the performance of ferrocement in construction and repair of boats trawlers. They showed that in fact, the most successful and convincing application of ferrocement has been in construction and repair of boats. Iorns suggests an open mold system to be used for better repair of boat. Instead of using no form the wire mesh layer is used directly.

The suitability of ferrocement as a retrofit (strengthening) material of unreinforced masonry wall has also been studied by a number of researchers, which will be discussed in the next section of this chapter.

For many repair and renovation programs of civil engineering structures, Chowdhury and Robles-Austriaco (1986) cite the suitability of ferrocement because of
1. Better cracking behavior.
2. Capacity of improving some of the mechanical properties of the treated structures.
3. Further modification or repair of ferrocement treatment is not difficult.
4. Imposition of little additional dead load requiring no adjustment of the supporting structures.
5. Ability to withstand thermal changes very efficiently.

6. Ability of achieving waterproofing property without providing any surface treatment.

7. Readily available constituent materials.

8. No need for special equipment.

9. Ability to be used in repair program with no distortion or down grading of architectural concept of the structures.

10. Flexibility of further modification.

2.4 RETROFITTING TECHNIQUES FOR INFILL PANELS

As one of the oldest material, masonry walls are being used either partially or entirely in the building structures throughout the world. Inclusion of infill panels within the RC frames is found to be an effective way to increase the stiffness and strength, and reduce lateral drift of the existing structures. Durrani et al. (1992), Islam et al. (1994), Pincheira et al. (1995, 1996) used the masonry infills themselves as a mean of retrofitting or strengthening existing framed buildings. Decanini et al. (1994) conducted an analytical study to investigate the effect of adding infill walls on reinforced concrete framed buildings. They concluded that the proper design of the infill should result in decreasing the bending moments in both the columns and the beams of the framed building. In fact, the addition of the infill distributes the moments more uniformly. Murty et al. (2000) in their experimental study on masonry infilled RC frames found that, due to infilling, the stiffness increases more than four times, the strength increases by 70%, the ductility increased four times. They also concluded that the inclusion of masonry infill drastically reduces the ductility demand on the RC frame members. This explained the excellent performance of many such buildings in moderate earthquakes even when the building is not designed or detailed to withstand the earthquake forces.

Infill panels play an important role in resisting lateral loads and overall strength of the structure. Therefore, it is very important to improve the condition of the distressed masonry infill panels. Several retrofitting techniques are available to increase the strength and the ductility of masonry infills. These can be categorized in two types, the first relates to adding structural elements such as steel or concrete frames to the existing building. This option presents some disadvantage such as adding significant weight to the building, which in turn may require foundation adjustments, resulting in

a higher retrofit costs as well as resulting in higher inertia forces in the event of an earthquake. Another disadvantage is that valuable space is lost to the framing elements, and in some cases disturbance of the occupants may occur. The second alternative is related to surface treatment. This alternative can be achieved in many ways. When the mortar is deeply eroded and the wall has hairline cracks, one of the surface treatments is re-pointing. It restores the physical and visual integrity of masonry. When reinforcement is used the technique is referred to as structural re-pointing. Grout and epoxy injection is also used to anchor other components or to strengthen the wall itself. It restores composite action of unreinforced masonry (URM) walls and also the integrity of previously damaged wall. But the problem is, it is applicable only to the faced and cavity walls. It also increases the weight and thus alters the dynamic response.

A standard procedure of retrofitting consists of removing one wythe/coating from the existing multi- wythe/coated wall and replacing it by a layer of reinforced concrete. In some cases, the walls are retrofitted with steel plates attached to the wall with steel anchors. Another way is to simply apply an external coating or overlay to one or both sides of the masonry wall. This includes the use of sprayed concrete, glass-reinforced concrete coating, steel fiber reinforced concrete coating or ferrocement coating.

2.4.1 Use of Steel Angles and Steel Strips in Retrofitting URM Walls

Steel bars or tension tendons inserted into holes up to 60 mm diameter drilled in the URM walls parallel to its plane improves in-plane and out-of-plane flexural behavior and also the connections between orthogonal walls at their intersections. This practice was widely applied in Europe for strengthening the historical buildings. However, it came under considerable criticism since the process is irreversible.

URM walls that develop tension due to either in-plane or out-of-plane bending can be strengthened using pre-stressing steel to create axial compression in the wall and increase its bending moment capacity. The significant effect of creep and rapid loss of post-tensioning effect limit its use widely.

Taghdi et al. (2000) suggested a method to increase the in-plane strength and ductility of masonry shear walls founded in low-rise buildings. In their testing they retrofitted

Fig. 2.1. The steel strip retrofitting techniques suggested
by Taghdi et al. (2000) for unreinforced masonry walls

the walls using vertical as well as vertical and diagonal steel strips. Steel angles and
anchor bolts were used to connect the steel strips to the foundation and the top-
loading beam. In essence, as shown in Fig. 2.2 the walls were transformed into a
masonry infilled frame with or without diagonal steel braces. The walls were
subjected to both gravity as well as cyclic in-plane loadings. It was noticed that the
retrofitting scheme increased both the ultimate strength as well as the ductility of the
wall many folds. It was also concluded that while the above upgrading technique is
effective, it requires a great deal of reparation work, its construction may disturb the
ongoing building functions, and the new structural elements may affect the
architectural aesthetics of the building. Hence, an alternative retrofitting technique is
worth considering.

2.4.2 Use of Fiber Reinforced Polymer in Retrofitting URM Walls

In a study conducted in the University of California-Berkeley by Tso et al. (1974)
Cagley et al. (1978), Clough et al. (1979), and Meli et al. (1980), masonry walls
coated with either reinforced plaster or fiberglass reinforced mortar were tested under
in-plane cyclic loading or under simulated earthquake loading, the strength of the
walls were nearly doubled and the coating increased the ductility of the system.

Weeks et al. (1994) reported one of the largest test programs conducted to date in the field of full scale testing of masonry structures at the University of California – San Diego. A full-scale five-story reinforced concrete masonry building was tested under simulated seismic loading. The damaged building was repaired subsequent to the original seismic test with carbon fabric overlay on the first two stories, ceramic foam injection of damaged hollow core floor blanks, and reconstruction of crushed wall toes in the first story wall with polymer concrete. The repaired building was retested using the same loading history applied to the original building. A direct comparison with the first test results showed that the repair improved the seismic deformation capacity by a factor of two and that particularly the polymer matrix based carbon fabric wall overlays proved to be highly effective in reducing shear deformations in the structural walls and in improving the overall structural ductility.

Laursen et al. (1995) tested URM shear walls with and without carbon fiber reinforced polymer (CFRP) retrofitting both under in-plane and out-of-plane loading. The carbon fibers doubled the ductility of the wall and increased its carrying capacity by 25%.

Ehsani et al. (1997) investigated the shear behavior of URM shear specimens retrofitted with fiber reinforced polymer (FRP) overlays as shown in Fig. 2.1. Two modes of failure were observed namely, the shear failure mode along the joint and, the delaminating of the fabric at the middle-brick region or fabric edges. They concluded that the type of failure was influenced by the fabric strength, whereas the shear failure was associated with the weaker fabric, and the delaminating occurred when a stronger fabric was used.
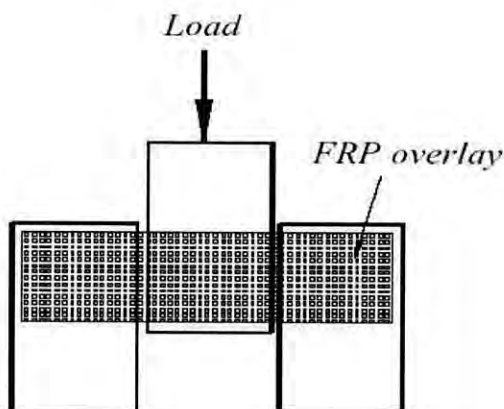
Fig. 2.2. The fiber reinforced polymer (FRP) retrofitted
shear specimen investigated by Ehsani et al. (1997)

Ehsani (1998) reported that composite materials are very effective in strengthening URM structures, where the tensile and shear capacity of the wall is negligible. Fabric of the composite material can be epoxy bonded to the exterior surface of the wall, similar to wallpaper. The fabrics can be easily cut to accommodate any opening. For an infill wall, even a thin fabric may be sufficient to contain the wall and prevent its collapse. The composite forces the whole wall to work integrally and increase the shear strength as well as the flexural out-of-plane strength and convert the URM into a ductile material.

Ehsani et al. (1999) studied the behavior of half-scale URM walls retrofitted with vertical FRP strips subjected to simulated earthquake out-of-plane loading. They concluded that although both URM walls and the FRP strips behave separately in a brittle manner, the combination resulted in a system capable of dissipating energy.

Traitafillou (1998) conducted a study to experimentally as well as analytically investigate the effect of strengthening masonry structures for out-of-plane bending, in-plane bending, and in-plane shear capacity all combined with axial loading. He came up with design equation and normalized interaction diagrams for the different loading cases. It was shown that the inclusion of the laminates increased the shear capacity three to five folds.

Kolsch (1998) presented a method for out-of-plane strengthening of masonry infills using carbon fiber embedded in a cement-based matrix. The technique prevented partial or complete out-of-plane collapse of the wall. The ultimate strength of the wall increased to 300% of that expected for the un-strengthened wall and the deformation capacity was also greatly enhanced.

Another type of research has been conducted in the area of retrofitting masonry infilled frames using glass fiber reinforced polymer (GFRP) laminates to enhance its in-plane behavior. The earliest research conducted in this field was that by Haroun et al. (1996). In this study, full scale hollow concrete block masonry infilled RC frames with and without FRP retrofitting were tested under cyclic in-plane loading. It was noted that the fiber composite increased the ultimate strength of the original frame by

35%, but more importantly, the ductility of the retrofitted frame was 280% more than the original infilled frame.

Colombo et al. (2000) conducted an experimental study on the effect of using a polymeric net embedded in plaster coating on improving the ductility and energy dissipation capability of masonry infilled steel frames. This technique is very close to the FRP application and it was found to be very effective in increasing the energy dissipation capacity.

Hakam (2000) conducted a preliminary study at Drexel University on GFRP retrofitted small-scale masonry infilled steel frames tested under diagonal monotonic loading. Figure 2.3 schematically shows the effect of the GFRP on the stiffness and the ultimate strength of the retrofitted infilled frames.

The study conducted by El-Dakhakhni (2002) focused on investigating the retrofitting effect of face shell mortar bedding hollow concrete masonry-infilled steel frames (CMISF) subjected to in-plane lateral loads using glass fiber reinforced plastic (GFRP) laminates that are epoxy-bonded to the exterior faces of the infill walls. The retrofitting technique using GFRP laminates aims at creating an engineered infill wall with a well-defined failure mode and a stable post peak behavior as well as containing
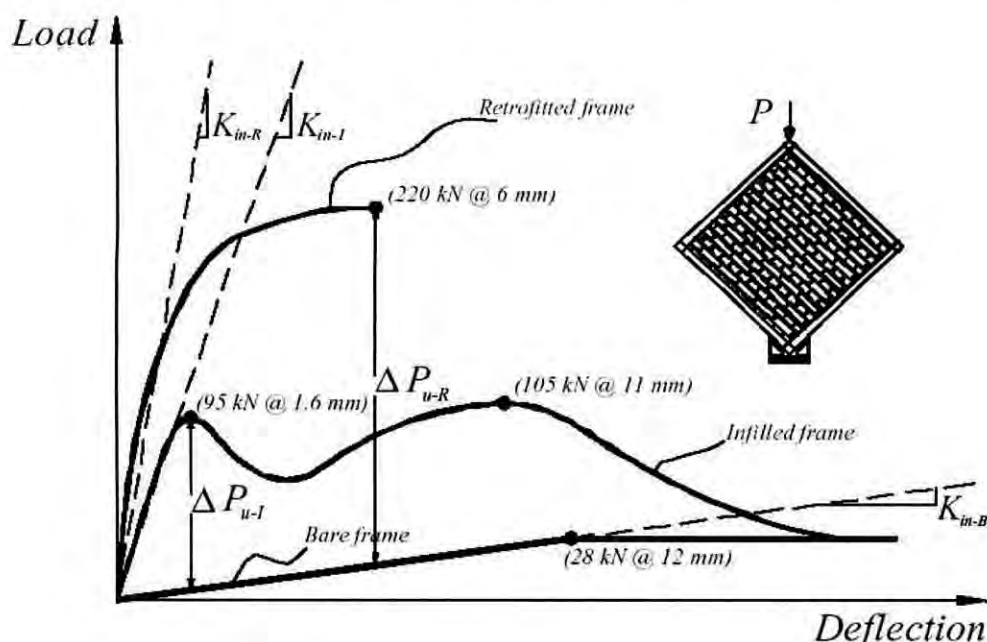
Fig. 2.3. The glass fiber reinforced polymer (GFRP) effect on the diagonally loaded masonry infilled steel frames tested by Hakam (2000)

the hazardous URM damage and preventing catastrophic failure. Results showed that the GFRP prevented both shear and tension cracking by supplying the required tensile strength. The GFRP also increased the lateral load capacity and enhanced the post peak behavior by means of stabilizing the masonry face shell and preventing its out-of-plane spalling. The stabilizing allows the wall to carry more loads and prevents sudden drop in the load carrying capacity.

2.4.3 Use of Ferrocement in Retrofitting URM Walls

The restoration of masonry constructions has been systematically studied since the 1960's decade. But very few of them dealt with retrofitting of masonry infilled frames using ferrocement laminates to enhance its in-plane behavior. Effectiveness of ferrocement as a retrofitting material for beams and columns has been extensively studied by various researchers, which has already been discussed in the previous section. This part will focus on retrofitting of masonry walls.

Hutchinson et al. (1984) conducted a research on the different methods used to reinforce unreinforced masonry walls subjected to in-plane cyclic loading, they used variety of techniques such as longitudinal prestressing, shotcrete on one surface, glass-reinforced cement on both surfaces, a combination of dowels, and steel-fiber reinforced coating on two surfaces, and the addition of a the ferrocement to one side of the wall. They came out with the conclusion that among all the methods considered, the solution involving spraying the concrete, and in particular the use of steel- fiber reinforced coating, were determined to be the most viable retrofitting method. This technique resulted in remarkably stable hysteresis loops.

Reinhorn et al (1985) tested a series of brick masonry walls strengthened with ferrocement layers. The 12.7 mm thick ferrocement coatings, applied to both faces, were reinforced using different mesh arrangements. The mesh was fixed in place using wire bond ties passing through the wall. Specimens were loaded by in-plane compression at opposing diagonal corners (diagonal split test). In tests where the bond ties proved adequate the walls failed in diagonal tension. However, in cases where bond ties failed, failure of the walls was less ductile as a result of local crushing and separation of the ferrocement coating. The strength, ductility and stiffness of the

coated walls was nearly double that of the uncoated walls. Strength enhancement, however, was little affected by mesh spacing.

Irimies and Crainic (1993) tested 6 models of masonry walls with flanges at the edges, models were previously damaged and two rehabilitation procedures were applied, one by time or both at the same time. The first one involved the injection of cement paste into the cracks and the second consisted of the application of 30 mm thickness reinforced mortar (that can be understood as a kind of under-reinforced ferrocement) overlays. The reinforcing steel mesh had 6 or 4 mm diameter wires spaced at 250 or 200 mm, depending on the case. The models were submitted to combination of vertical and horizontal loads up to the collapse. The authors observed that both rehabilitation techniques might be applied to retrofit damaged masonry walls.

Jabarov et al. (1985) worked out on similar masonry walls but with 2 rectangular openings each. The previously damaged wall was coated with a 25 mm reinforced mortar overlays. Additional steel bars in diagonal directions were placed in some parts of the walls to test the efficiency of different reinforcement arrangements. Amongst other conclusions, the authors observed that the strength and rigidity of the rehabilitated walls depend on the overlay thickness, the mortar strength and the reinforcement ratio.

Kahn (1984) analyzed the influence of reinforced overlays on the seismic performance of unreinforced masonry walls. Seventeen masonry walls made of solid bricks were tested under diagonal compression according to ASTM E 519-93. Fifteen panels were coated with sprayed mortar, guided over the welded mesh reinforced wall surface. Bonding conditions and the efficiency of steel connections were also tested. The author concluded that the ferrocement overlays increase the load capacity under shear and tension actions, also the deformation limit.

Alcocer et al. (1996) analyzed the effect of ferrocement overlays on the performance of non-bearing masonry walls under seismic actions. Full-scale models of masonry walls confined by reinforced concrete beams and columns were previously damaged

and rehabilitated. It was observed that rehabilitation technique improved the shear strength, the stiffness, the crack distribution and the ductility.

Mander and Nair (1994) tested medium scale clay masonry infilled steel frame sub-assemblages with and without retrofitting under in-plane quasi-static cyclic loading. The retrofitting scheme involved the use of ferrocement overlays with and without diagonal reinforcing bars. They concluded that the URM infills can act as a ductile lateral load resisting element in multi-story frames. Including the ferrocement overlay increased the ductility even more, and the enhancement of the ferrocement using the diagonal reinforcing bars resulted also in increasing the strength as well as the energy dissipation capabilities of the system. The diagonal bars also helped in preventing the out-of-plane buckling of the ferrocement layer. They suggested that such rehabilitation technique could be used in the lower story of multi- story frames where most of the plastic hinging would normally occur under earthquake loading.

Oliveria (2001) accomplished an extensive study on the application of reinforced mortar overlays in masonry construction rehabilitation. The experimental program involved axial compression, shear and bending tests on concrete hollow block panels with different kinds of mortar overlays. The type of mortar overlays used in these series were weak (low compression strength) mortar; strong (high compression strength) mortar; polypropylene fiber reinforced mortar; steel fiber reinforced mortar; steel mesh reinforced mortar without steel connectors; steel mesh reinforced mortar with type are 20 mm thick. Also a quite full-scale model series were tested to observe the efficiency of the embedded mesh reinforced mortar overlays in a situation of combined compression, shear and tension stresses. The general conclusion is that the application of mortar overlays is a powerful rehabilitation technique for masonry infill panels.

2.5 EXPERIMENTAL INVESTIGATION OF INFILL PANELS RETROFITTED WITH FERROCEMENT

An experimental program was carried out in the concrete laboratory of BUET by Alam (2003) on one half-scale masonry infilled reinforced concrete frame and rehabilitated frame. The frame was subjected to one point lateral load by hydraulic jack in the laboratory up to failure. The distressed frame was rehabilitated by using

ferrocement overlay. The experiments were performed to investigate the performance of ferrocement overlay in strengthening of distressed masonry infilled reinforced concrete frame subjected to lateral load. For each test initial cracking load, failure load, crack pattern and deflection were observed. The results obtained from this test have been used in this study to simulate the retrofitted infilled-frame into the numerical model so as to predict the peak load.

2.5.1 Experimental Program

The sketch of reaction frame diagram is shown in Fig. 2.4, which consists of base BC and two columns AB and CD. The base was stiff enough to withstand any bending failure during testing of the reinforced concrete infill frame. Fig. 2.5 shows the placement of reinforcement in to the base and reaction frame. The properties of concrete and compressive test result are shown in Table 2.1. The tensile test results of reinforcement are shown in shown in Table 2.2. Hydraulic jacks are mounted at the top of column, which is supported by column cantilever element projected from top of the column shown in Fig. 2.4. The bending resistance of the column was not sufficient to withstand the reaction of the hydraulic jack. Therefore a pair of tie rods on each side of the frame was used to tie the column top to the farthest point of the base as shown in 2.4. To prevent the bending of the tie anchor, (25mm bar put across the column) additional clamping was arranged.
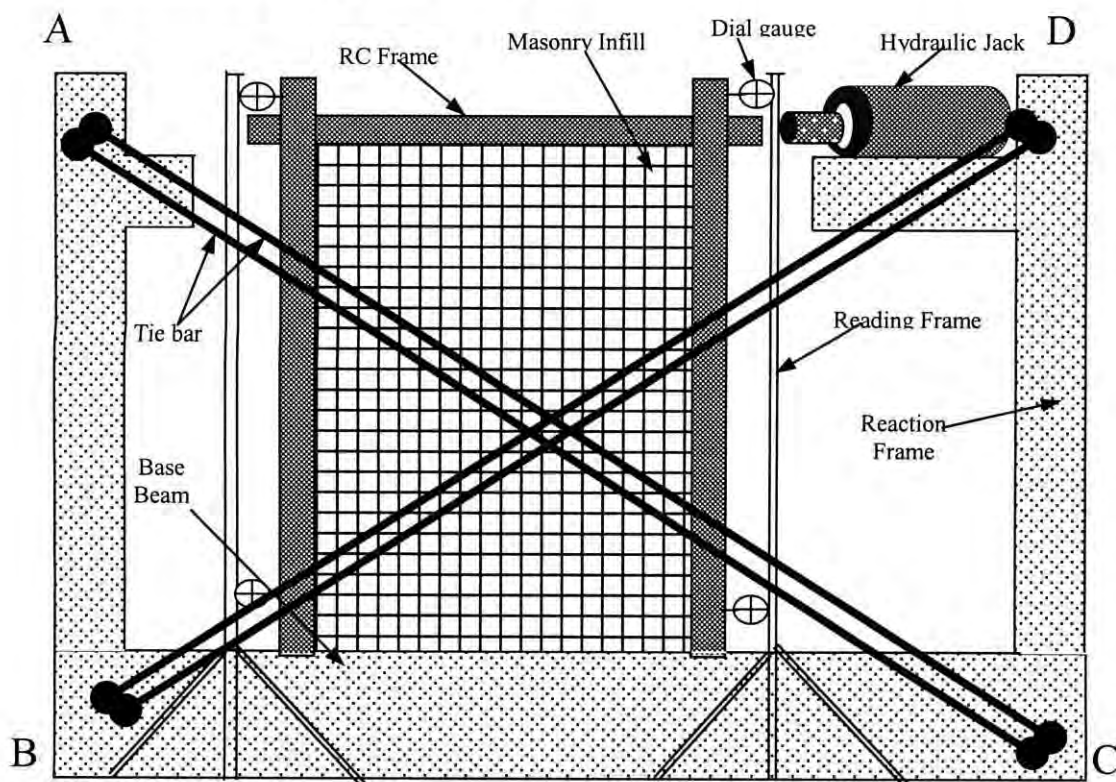
Fig. 2.4. Schematic elevation of Masonry infilled RC Frame and test setup by Alam (2003).

Masonry infilled reinforced concrete frame is constructed monolithically with the reaction frame base BC that is shown in Fig. 2.4. As an ordinary building having column and beam size of 300mm x 300mm and floor height 3.049m, the frame had been modeled in half scale. So for the experimental purpose column and beam has been taken as 150mm x 150mm and a height 1.5245m has been chosen. Again masonry infill size 110 mm × 55 mm × 35 mm was chosen. The infill material is half scale model. Therefore half scale masonry elements are used in testing. The common-

LONG -SECTION

SECTION: A-A   SECTION: B-B
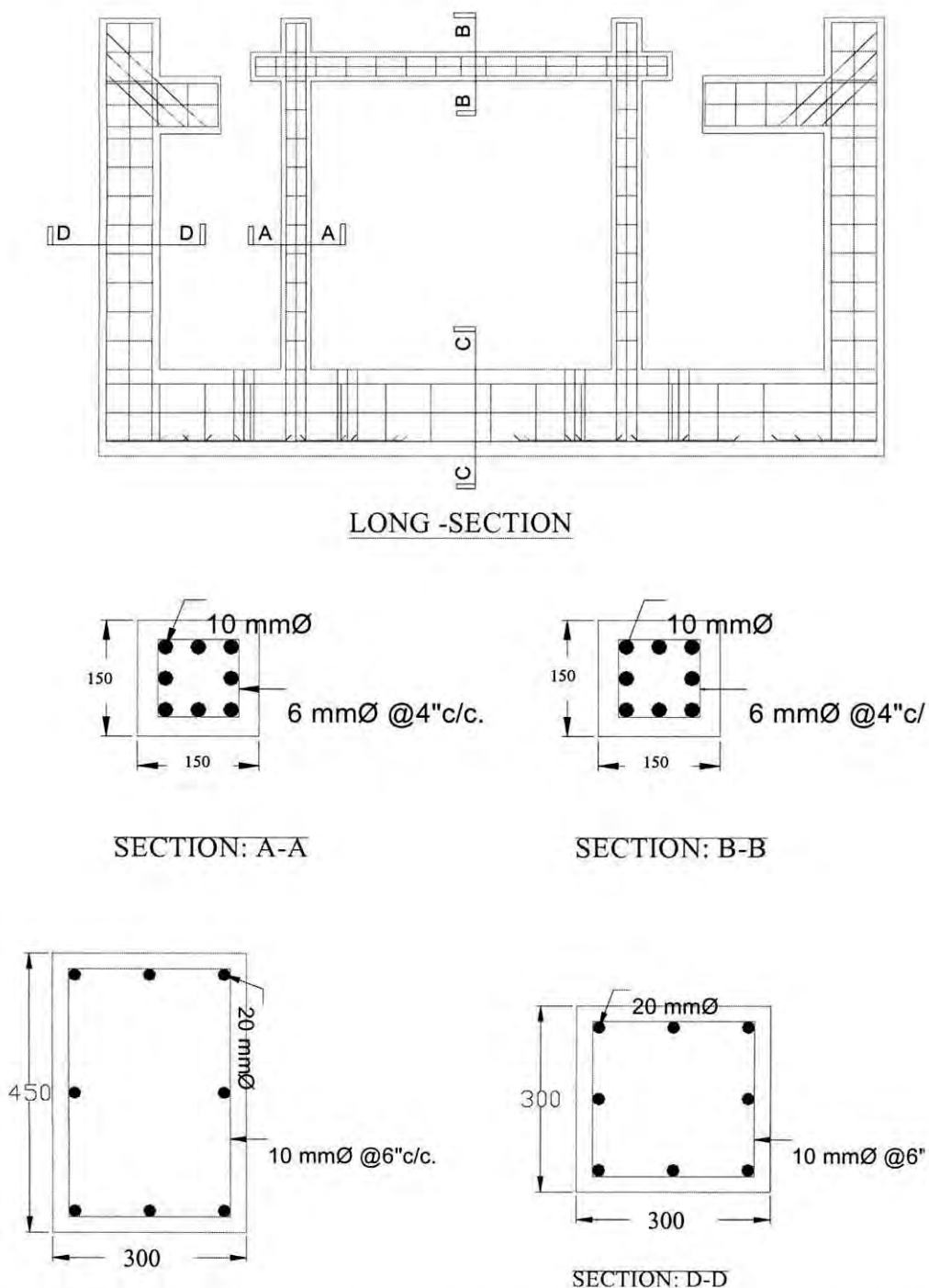
SECTION: D-D

Fig. 2.5. Long and cross-section of test setup of masonry infilled RC frame by Alam (2003)

ly used size of brick mass is 250mm × 125mm × 81mm. Therefore half scale brick specimens are obtained by slicing a normal size brick using a diamond saw. Five half-scale bricks high stack bonded prisms with plywood capping at top and bottom were loaded in uniaxial compression perpendicular and parallel to the joint to failure. The test results are shown in Table 2.3.

The half scale infilled RC frame was tested by hydraulic jack machine (compression) of capacity 50 ton (50,000kg) or 500 kN, applying lateral load at the top of the RC column up to initiation of failure. The surface of masonry infill (both sides) and all the sides of column were white and yellow colored respectively to facilitate the viewing of cracks. The frame was subjected to one point loading by hydraulic jack (compression) testing machine at the top of the column as shown in Fig. 2.4. Loads were increased at uniform rate of 1000kg (or 1Ton) or 10kN until the failure occurred. Applied loads were recorded using machine dial gauges. To measure corresponding deflection of frame four dial gauges, two at the top of the frame and the other two at bottom of both left and right side of the frame were placed. The cracking load, failure load, failure pattern and deflection at top and bottom of the frame for each incremental load had been observed and recorded during testing.

Table: 2.1. Properties of concrete (used in casting of columns and beams)

Type of Coarse Aggregate	Size of Coarse Aggregate (mm)	Water cement ratio	Mix Ratio (by volume) C:FA:CA	Average Compressive strength (MPa)
Brick chips	20 (down graded)	0.5	1:2:4	16.40

NB: 10.034 kg per sq cm = 1 MPa

Table: 2.2. Tensile test Result of Reinforcement (used in beam & column)

SL. No.	Dia. of Bar (mm)	Area of Bar (cm)	Yield load (kg)	Yield Strength (MPa)	Ultimate load (kg)	Tensile Strength (MPa)	Elongation
1	16	2.0	8863.63	441.68	11227.27	559.46	18%
2	10	0.785	2500	317.39	3454.54	438.57	18%
3	6	0.2827	1954.54	689	2545.45	897.35	21%

NB: 1MPa = 10.034 kg per sq cm

Table: 2.3. Compression test of Brick Prism

Arrangement of the prism	Average Compressive strength (MPa)
a) Load perpendicular to the joint	18
b) Load parallel to the joint	14

NB: 10.034 kg per sq cm = 1 MPa

Table: 2.4. Properties of mortar (used in ferrocement)

Type of Cement	Fineness Modulus of sand	Water cement ratio	Mix Proportion C : FA	Average Compressive strength (MPa)
Ordinary Portland Cement	2.65	0.45	1:2.5	33.81

NB: 10.034 kg per sq cm = 1 MPa

After testing of infilled RC frame to failure, the frame was ready for repairing by ferro-wrapping. Before any mesh was applied to the infill and frame it was carefully dismantled of plaster from the infill and the column. Laitance and any loose concrete cased by the damaging process were also removed. It was then washed with water to ensure removal of all dust. The distressed masonry infilled RC frame was then repaired with ferrocement overlay (the properties of mortar used for ferrocement as shown in Table 2.4), two layers of wire mesh were placed on column and one layer mesh was placed on the infill on both sides of the surface of masonry infill. All the sides of columns were white and yellow colored to facilitate viewing of cracks. The repaired frame was again tested using hydraulic jack in the laboratory with the previous test setup. One point loading was applied over the top of the frame and results were recorded. Four dial gauges were also used for recording the top and bottom deflection.

2.5.2 Test Results

Results from the original frame

When the original frame was tested with the incremental load, first crack appeared along bottom right corner of masonry infills. The crack propagated diagonally upward as the load was gradually increased and the numbers of cracks were also increased with the increase in loadings. Both faces of the infilled RC frame (top to bottom) showed similar crack pattern. At a stage of load of 19ton the infill frame failed with a major diagonal crack. It was observed that cracks went through masonry, which

means that brick failure occurred. After the full failure of the frame and infill the loading was stopped and frame was kept for repairing. The load-deflection curves of the original frame are shown in Fig. 2.6, 2.7, 2.8 and 2.9.
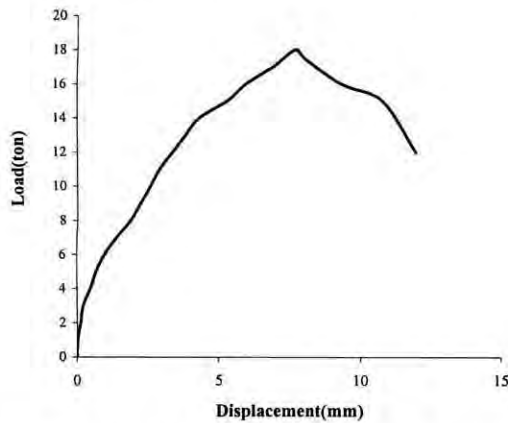
Fig. 2.6. Load vs. deflection diagram at the top right corner of the original frame by Alam (2003)
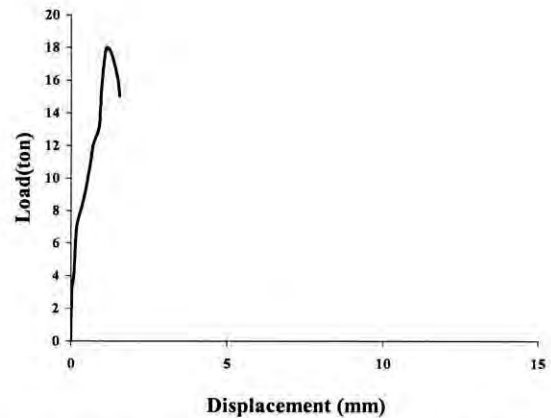
Fig. 2.7. Load vs. deflection diagram at the bottom right corner of the original frame by Alam (2003)
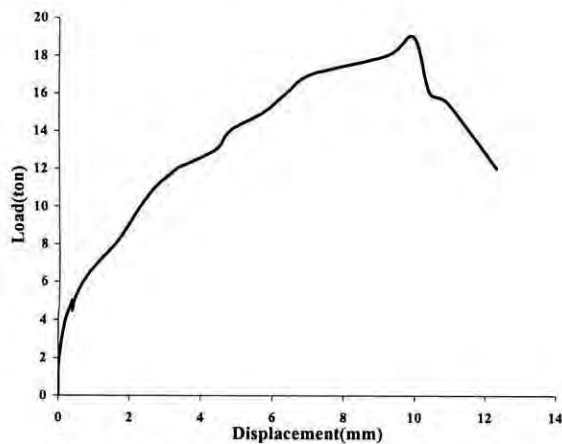
Fig. 2.8. Load vs. deflection diagram at the top left corner of the original frame by Alam (2003)
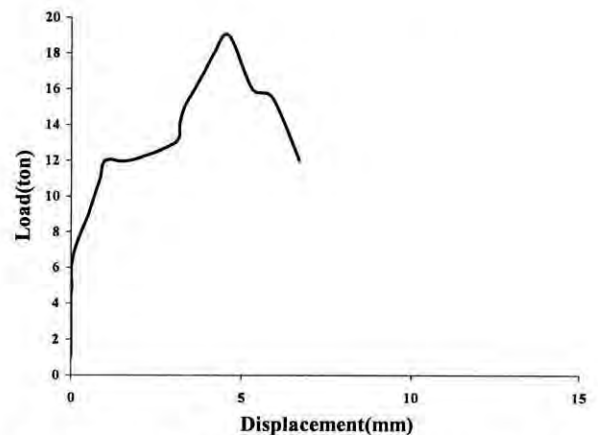
Fig. 2.9. Load vs. deflection curve at the bottom left corner of the original masonry infilled RC frame by Alam (2003).

Results from the repaired frame

After repairing the distressed infilled RC frame with ferrocement overlay it was tested in the same fashion as the original one. The first crack was formed at the bottom at a load of 16ton. The corresponding deflections at the top and bottom were 5.99mm and 1.87mm respectively, which are less than those obtained for the original frame (6.38mm and 3.63 m respectively). These cracks propagated vertically upward as the load was gradually increased. At a stage of loading of 23ton the repaired frame was diagonally failed, shown. Again the diagonal cracks were observed at top of the column at windward side and bottom of leeward side also. During testing of original

frame as well as rehabilitated frame, the deflection was measured at top and bottom of the frame by setting four different dial gauges. The typical load deflection curves at top and the bottom for the rehabilitated frame are shown in Fig.2.10 to 2.13. From test results it was found that the deflection of rehabilitated frame is less than the original frame. This indicates that more strength can be attained in a distressed RC frame by using ferrocement overlay.
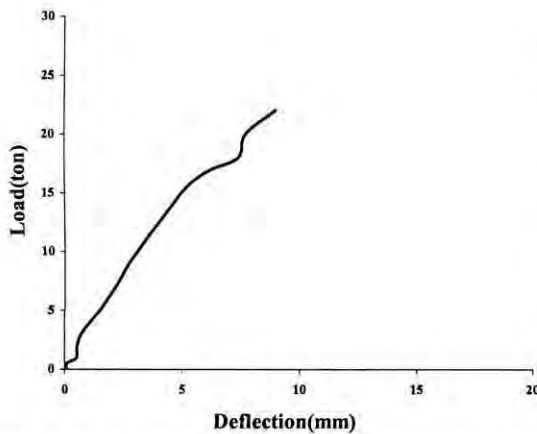
Fig. 2.10. Load vs. deflection at the top right corner of the repaired masonry infilled frame by Alam (2003)
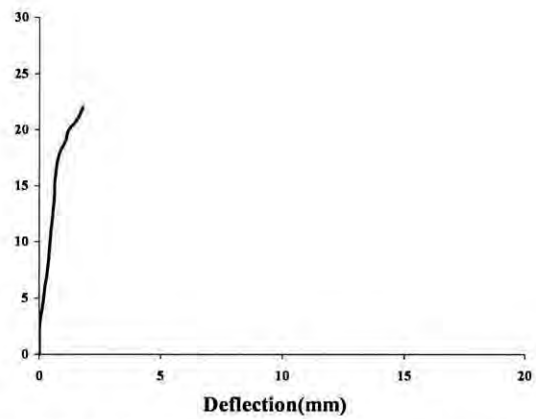
Fig. 2.11. Load vs. deflection at the bottom right corner of the repaired masonry infilled frame by Alam (2003)
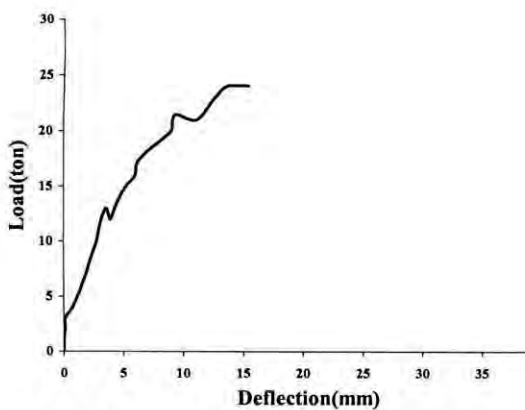
Fig. 2.12. Load vs. deflection at the top left corner of the repaired masonry infilled frame by Alam (2003)
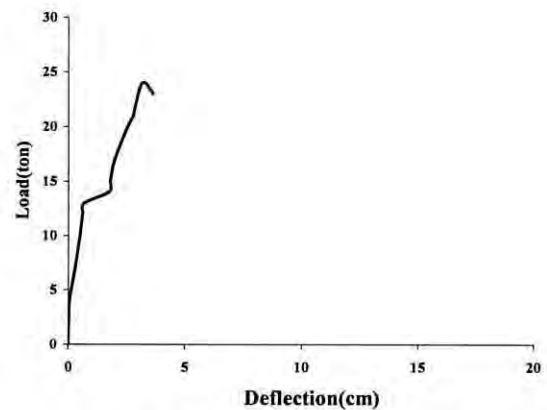
Fig. 2.13. Load vs. deflection at the bottom left corner of the repaired masonry infilled frame by Alam (2003)

2.6 REMARKS

Various research works on infilled-frame structures and the importance of infill panels have been discussed in this chapter. At the same time several retrofitting techniques for improving the performance of infill panels have also been focused in the present chapter. The beneficial effect of using ferrocement laminates in retrofitting

masonry and concrete structural element is clearly established in this literature. Significant changes in the behavior of such retrofitted structure are clear. It has been shown that ferrocement is a low cost but highly effective retrofitting material. Strength of the original structure can be restored easily using ferrocement. Although such advantageous properties of ferrocement are established through experiment, there is a lack of computational technique to assess such beneficial properties of ferrocement. It is practically not possible to conduct laboratory experiment for each and individual structure. Instead a computational procedure, if available, shall enable us to estimate the restorable strength of a damaged structure quickly and easily at a low cost. In view of the growing demand to retrofit existing masonry and concrete structures or to facilitate the inclusion of the infills in the analysis and design of new structures, there is an urgent need to establish a modeling technique for retrofitted masonry-infilled RC frames with ferrocement overlay.

The objective of this research work is to predict the ultimate load carrying capacity of the unreinforced masonry infill panels confined in reinforced concrete frame structures strengthened with ferrocement overlays and thereby help in achieving a great economy in the design of retrofitting schemes.

Chapter 3

COMPUTATIONAL MODELING OF INFILL PANEL

3.1 INTRODUCTION

The computational modeling of infilled frames has been described in this chapter. The effect of masonry infilled panels in changing the behavior of RC frame has long been an interesting topic to the researchers for the last few decades. The contribution of the masonry panel confined within RC frame in the stiffness and ultimate load carrying capacity (in-plane) has been investigated by various researchers and numerous computational models have been established in this regard. This part states the numerous computational models that are available on infill panels.

3.2 AVAILABLE COMPUTATIONAL MODEL

Modeling of RC structures as well as infill panels is based mainly on finite element methods and sophisticated material models. The modeling of infill panel with reinforced concrete frame can be broadly categorized into two approaches: a) equivalent diagonal strut approach and b) continuum approach.

3.2.1 Equivalent Diagonal Strut Approach

The first published research on modeling of infill panel as an equivalent diagonal strut was by Holmes (1961). He proposed a method for predicting the deformations and strength of infilled frames based on the equivalent diagonal strut concept. He assumed that the infill wall acts as a diagonal compression strut, as shown in Fig. 3.1(a), of the same thickness and elastic modulus as the infill with a width equal to one-third the diagonal length. He also concluded that, at the infill failure, the lateral deflection of the infilled frame is small compared to the deflection of the corresponding bare frame. Also, the frame members remained elastic up to the failure load. By equating the elastic deformation of the frame diagonal to the shortening of the equivalent diagonal strut at failure, Holmes derived an equation to determine the ultimate lateral load carrying capacity as shown in Eqn. 3.1.

$$H = \frac{24 E I e_c{}' d}{h^3 \left(1 + \dfrac{I}{I_0} \cot\theta \right)\cos\theta} + A f_c \cos\theta \tag{3.1}$$
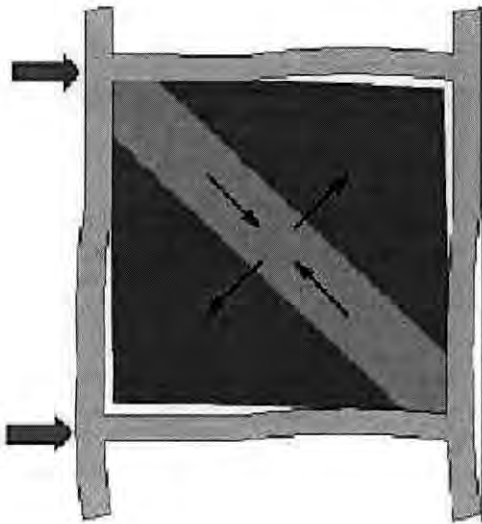
Fig. 3.1(a). The Diagonal Compression
Strut of Masonry Infill
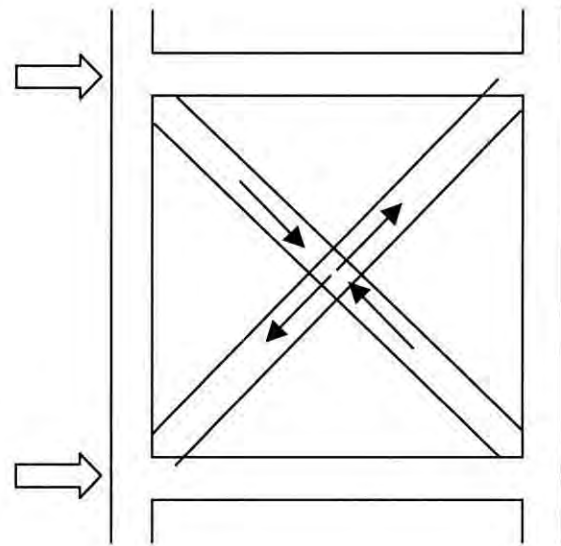
Fig. 3.1(b). Material Modeling of
Masonry infill as Diagonal Strut

Here, H is the horizontal load at failure, I is the moment of inertia of the column of the frame, I_o is the moment of inertia of the beam of the frame, E is the modulus of elasticity of frame members, e_c is the uniaxial compressive strain of the infill material at failure, h is the height of the infill, d is the diagonal length of the infill, θ is the angle of inclination of the diagonal strut to the horizontal, A is the sectional area of the equivalent diagonal strut and f_c is the ultimate compressive strength of the equivalent diagonal strut. Holmes showed that a value of $td/3$, where t and d are the thickness and diagonal length of the infill, respectively, best represents the value of A for strength prediction. However, the analytical predictions of deflection at ultimate load were generally lower than those measured experimentally. Later, Holmes (1963), based on test results of model steel frames with concrete infills, proposed semi-empirical methods to predict the behavior of infilled frames subjected to lateral and vertical loadings.

Smith (1962) conducted a series of tests on laterally loaded square mild steel frame models infilled with micro-concrete. Monitoring the model deformations during the tests showed that the frame separated from the infill over three quarters of the length of each frame member. These observations led to the conclusion that, the wall could be replaced by an equivalent diagonal strut connecting the loaded corners. The load-deformation relation recorded showed a high increase in stiffness of the infilled frame

compared to the bare frame. Another series of tests were conducted on unframed mortar walls loaded diagonally and measuring the strains along the loaded diagonal. In order to find a theoretical method to predict the experimental results, a stress function was solved for a number of nodes on the wall using the finite difference method and the theoretical results were in good agreement with the experimental observations. The theoretical results were translated into what was termed an *effective width* of the wall, which is the width of an equally stiff uniform strut whose length is equal to the diagonal of the wall and whose thickness is the same as the wall. It was determined that the effective width of the equivalent strut was dependent only on the wall's aspect ratio.

Further tests revealed that the above assumption, which was made, based on loading unframed walls, is invalid. The effective width of infill was found to depend on the length of contact between the infill and the frame, which itself was found to be highly dependent on the relative stiffness between the frame and the infill. In 1966 Smith conducted a series of tests on diagonally loaded small-scale square mild steel frames infilled with micro-concrete. Using equilibrium and energy considerations of the frame and infill, Smith (1966) was able to establish the length of contact, αh, between the frame column and the infill; α is given in Eqn. 3.2 in terms of λ, where λh is a *dimensionless* parameter expressing the relative stiffness of the frame and the infill given in Eqn. 3.3.

$$\alpha = \frac{\Pi}{2\lambda} \tag{3.2}$$

$$\lambda h = h \left(\frac{E_m t}{4EIh} \right)^{1/4} \tag{3.3}$$

Here, E_m is the elastic modulus of the infill, t is thickness of the infill, EI is the column rigidity and h is the height of the infill. After deriving the length of contact, it became possible to isolate the frame from the infill in order to evaluate the load carried by each component of the infilled frame system. Smith (1966) used a finite difference technique to evaluate stress and strain in the infill and to derive a theoretical effective width of the equivalent diagonal strut. Smith (1966) found the theoretical effective width to be consistently less than the experimentally measured values. He attributed

this discrepancy to higher strain due to stress concentration and nonlinear load-deformation behavior of the mortar infill at the loaded corner. In view of this finding, he recommended the use of experimental curves to estimate the effective width. Smith and Carter (1969) extended the work on square infilled frames to include rectangular walls. In a manner similar to that of the square infilled frames, the equivalent strut width is expressed as a function of λh, where the equation is as given below.

$$\lambda h = h \left(\frac{E_m t}{4EIh} \sin 2\theta \right)^{1/4} \tag{3.4}$$

In the above equation, θ is the angle of inclination of the diagonal to the horizontal member. They concluded that the lateral stiffness of an infilled frame may be obtained by statically analyzing the equivalent pin-jointed frame in which the infill is replaced by an equivalent diagonal strut. They also found that the effective width of an infill acting as a diagonal strut was influenced by many factors. Some of the most influencing factors were the relative stiffness of the infill and the frame, the aspect ratio of the wall, the stress strain relationship of the infill material and the magnitude of the diagonal load on the infill. Provided that the frame members possess adequate strength, the authors suggested that an infill consisting of concrete or mortar may fail by either tension cracking along the loaded diagonal and/or crushing of the infill at the loaded corners. In addition to the above modes of failure, a masonry infill may also fail by a third mode, namely, the shear cracking along the interface between brick and mortar. They also concluded that column stiffness can influence the stiffness and strength of the infill rather than the beam stiffness, which have been shown to have little effect, and that whatever the beam stiffness is, the length of beam in contact is always roughly half the span. Experimental results also showed that the bending moments in an infilled frame relative to the same non- filled frame subjected to similar forces are greatly reduced. They suggested design charts corresponding to the mentioned three failure modes, from these charts; the failure load in the equivalent diagonal strut can be obtained.

Mainstone (1971) presented results of series of tests on model frames with infills of micro-concrete and model brickwork along with a less number of full-scale tests. He found that factors such as the initial lack of fit between the infill and the frame and variation in the elastic properties and strength of the infill can result in a wide

variation in behavior even between nominally identical specimens. Mainstone also adopted the concept of replacing the infill with an equivalent pin-jointed diagonal strut; although he believed the concept can only be justified for behavior prior to first cracking of the infill. He plotted the aforementioned test results against the stiffness parameter, λh, and empirically formulated three equivalent diagonal strut widths to evaluate the stiffness, first crack load, and ultimate composite strength of the infilled frame.

Based on the analytical and experimental studies conducted by Kadir (1974), Hendry (1981) proposed a semi-empirical relation for the equivalent width of the diagonal strut as,

$$w = \frac{1}{2}\sqrt{\left(\alpha_l^2 + \alpha_h^2\right)} \tag{3.5}$$

where, w is the effective width of the infill wall, α_l is the contact length between the beam of the frame and the infill wall, α_h is the contact length between the column of the frame and the infill wall The above equation assumes that the contact stress has a triangular distribution, and idealizes it into a uniform distribution of half the maximum value of the triangular one. The contact lengths were obtained using Smith method (1969) after modifying Eqn. 3.4 to suit the beam also and using Eqn. 3.2 to obtain the column as well as the beam contact lengths.

Paulay and Priestley (1992) suggested treating the infill walls as diagonal bracing members connected by pins to the frame members. They also suggested calculating the stiffness of the structure and hence its natural period based on considering the effective strut width to be one quarter the wall diagonal.

Saneinejad and Hobbs (1995) proposed a method of analyzing masonry infilled steel frames subjected to in-plane loading. The method utilized the data generated from previous experiments as well as the results of a series of non-linear FE analyses. The proposed method accounts for both the elastic and the plastic behavior of infilled frames and predicts the strength and stiffness of the infilled frames. The method also accounted for various parameters like different wall aspect ratios and different beam-to-column stiffness and strength. The method was based on using equilibrium and elasticity equations to generate various parameters governing the behavior of the

infilled frame system like the contact stresses and lengths along with the initial stiffness of the infilled frame as well as the secant stiffness at failure. The authors also assumed that at failure, full plastification occurs at the loaded corners of the frame as well as the part of the infill in contact with the frame. The authors suggested that the resistance to lateral loads was offered by three components. These components are the force induced due to shear stresses on the beam-wall interface, the force generated by the normal stresses on the column-wall interface and finally the force developed in the steel frame itself as a result of its own stiffness to horizontal loads. Having derived the ultimate load, the area of the diagonal strut was easily derived. The collapse load and the initial stiffness as predicted by the proposed method was compared to tests conducted by others and was found to give satisfactory results.

Madan et al. (1997) further extended the work of Saneinejad and Hobbs (1995) by including a smooth hysteretic model for the equivalent diagonal strut. The proposed analytical development assumes that the contribution of masonry infill panel as shown in Fig. 3.2 to the response of the infilled frame can be modeled by replacing the panel by a system of two diagonal masonry compression struts as shown in Fig. 3.3. The stress strain relationship for masonry in compression as shown in Fig. 3.4 is used to determine the strength envelope of the equivalent strut. The individual masonry struts are considered ineffective in tension. But the combination of both diagonal struts pro-
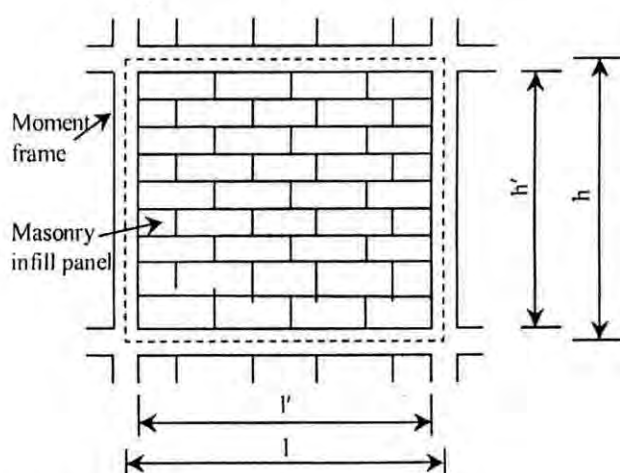
Fig. 3.2. Masonry infill frame sub-assemblage in
masonry infill panel frame structures.
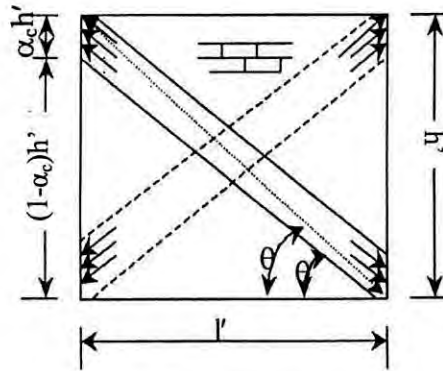
Fig. 3.3. Masonry infill panel in frame structure

$$f_m = \frac{f'_m \varepsilon_m r}{r - 1 + \varepsilon'_m} \quad \text{where}$$

$$r = \frac{E_m}{E_m - E_{sec}}$$
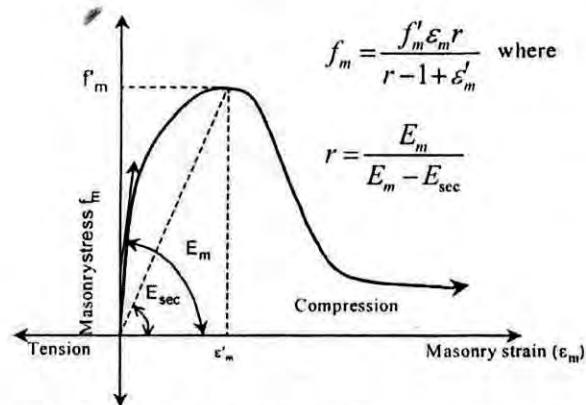
Fig. 3.4. Constitutive model for masonry infill
panel by Madan et.al. (1997)
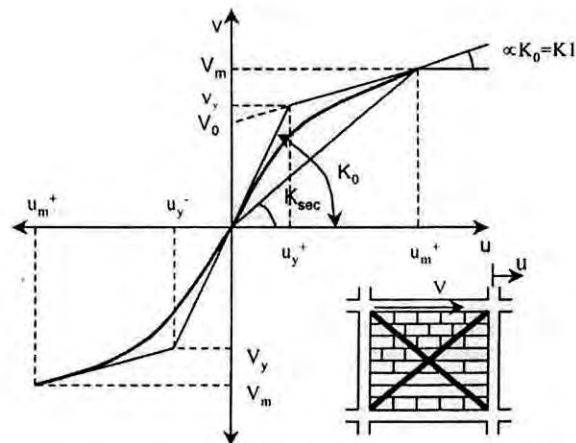
Fig. 3.5. Strength envelope for masonry infill
panel by Madan et.al. (1997)

ide a lateral load resisting mechanism for the opposite lateral directions of loading. The lateral force-deformation relationship for the structural masonry infill panel is assumed to be a smooth curve bounded by a bilinear strength envelope with an initial elastic stiffness until the yield force V_y and there on a degraded stiffness until the maximum force V_m is reached shown in Fig. 3.5. The corresponding lateral displacement values are denoted as u_y and u_m respectively.

Flanagan et al. (1999) reported the results of a number of full-scale clay infilled steel frames tested under in-plane loading. A piecewise linear equivalent diagonal strut was used to model the infill. The behavior of the structural clay tile infills was correlated with the absolute story drift rather than the non-dimensional story drift. The area of the strut, A, was given by Eqn. 3.6

$$A = \frac{\Pi t}{C\lambda \cos\theta} \tag{3.6}$$

where, t, λ and θ are defined in Eqn. 3.4 and C is an empirical constant depending on the in-plane drift displacement.

El-Dakhakhni (2000, 2002), El-Dakhakhni et al. (2001) suggested a modeling technique for concrete masonry infilled steel frames, as shown in Fig. 3.6. The technique is based on replacing the infill wall by one diagonal and two off-diagonal struts. It is based on making use of the orthotropic behavior of the masonry wall as well as some experimental observation, and analytical simplifications, in order to simplify the nonlinear modeling of these structures.
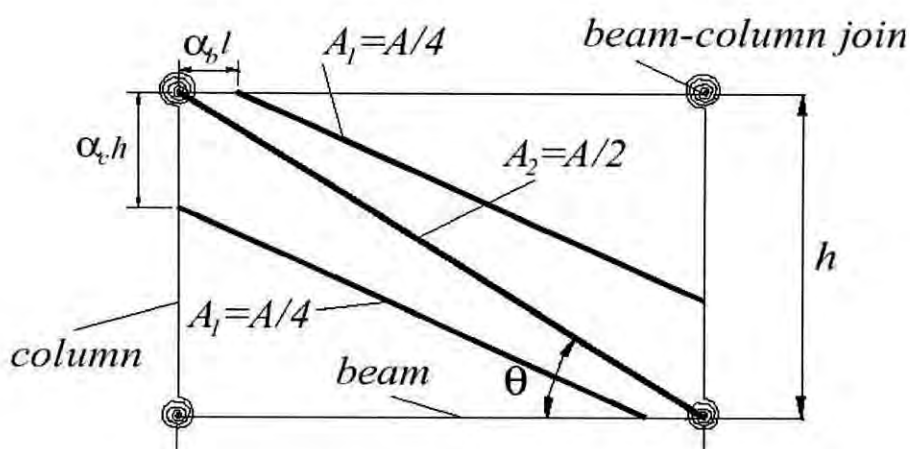
Fig. 3.6. The infilled frame model proposed by El-Dakhakhni (2000)

3.2.2 Continuum Approach

In the period of very early ages of studying infill panels, experimental work was conducted by Thomas (1953) and Wood (1958) in the United Kingdom and test results provided ample testimony that a relatively weak infill can contribute significantly to the stiffness and strength of an otherwise flexible frame. Sachanski (1960) performed tests on model and prototype infilled frames. Based on his test results, he proposed an analytical model in which he analyzed contact forces between the frame and the infill by assuming their mutual bond to be replaced by thirty redundant reactions. The forces were determined by forming and solving the equations for the compatibility of displacements of the frame and the infill. He treated the infill as an elastic membrane and stiffness coefficients of the infill were determined by integrating the stresses determined by using a finite difference technique. Having found the contact forces, he then proposed a stress function for the stress analysis of the infill. It should be pointed out that the theoretical approach of Sachanski can only be applied to an integral infill frame where separation between the infill and the frame is prevented. Additionally, the infill was assumed to be isotropic, homogeneous, and elastic and these assumptions are not applicable for the non-homogeneous and anisotropic masonry infills.

Riddington and Smith (1977) conducted an extensive series of plane stress finite element analyses of laterally loaded infilled frames. The interaction between the frame and the infill was modeled by introducing a linking matrix, representing the contact interface, connecting each two adjacent nodes in the frame and the infill wall. This forced the nodes on the frame and infill to undergo the same displacement if they are in contact. When sliding occurs between the two nodes due to the presence of tension force in the interface, the linking matrix forced the two nodes to have the equal displacement only perpendicular to the interface. They gave empirical equations based on the conducted stress analyses in order to estimate shear stress, diagonal tension and vertical compression at the center of the wall.

Mallick and Severn (1967) introduced an iterative technique whereby the points of separation between the frame and the infill, as well as the stress distribution along the length of contact between the frame and the infill, were obtained as an integral part of

the solution. Slip between the frame and the infill was also taken into account. Standard beam elements were used to model the frame while plane stress rectangular elements were used for the infill. The contact problem was solved by initially assuming that the infill and frame nodes have the same displacement. Having determined the nodal displacement, the load along the periphery of the infill is determined and checked for tension. If a tension force is found, separation is assumed to have occurred and the corresponding nodes on the frame and infill are allowed to move independently in the next iteration. This procedure is repeated until a pre-described tolerance for convergence is achieved. The effect of slip and interface friction was considered by introducing shear forces along the length of contact. The authors ignored the axial deformations of the columns in their formulation. Barua and Mallick (1977) used FE to analyze infilled frames and their technique was similar to the method proposed by Sachanski (1960) except that a finite element technique was used to determine stiffness coefficients of the boundary nodes of the infill. Unlike Sachanski; Barau and Mallick allowed for the separation between the infill and frame and included the effect of slip.

Liauw and Kwan (1983, 1985) developed a plastic theory of non-integral (without shear connectors) infilled frames in which the stress redistribution towards collapse was taken into account and the friction is neglected for strength reserve. The theory was based on the findings from non-linear finite element analysis and experimental investigation. The results from the theory have been shown to compare favorably with the experimental results given by many researchers on small-scale model tests. Series of equations defining the ultimate load capacity as governed by various modes of failure was suggested by Liauw and Kwan. The parameters involved in these equations were the beam and column strength, the aspect ratio of the wall as well as its mechanical properties. Liauw and Lo (1988) conducted a series of tests on a number of small-scale models of micro concrete infilled steel frames. The frame members were hot-rolled mild steel solid rectangular bars. FE analysis was used to model the test specimens, taking into account the nonlinearity of material, cracking in the wall and separation-friction-slip at the interface between the wall and the frame. In order to simulate the frame-wall interface, each pair of adjacent nodes in the frame and wall elements were connected by an interface element.

Dawe and Charalambous (1983) presented a finite element technique where standard beam and membrane elements were used to model the frame and the infill wall, respectively. Static condensation was then used to eliminate the interior degrees of freedom of the infill leaving only the degrees of freedom associated with nodes adjacent to the frame nodes. The interface between the frame and the infill was modeled with rigid links and an iterative solution technique was adopted. At the end of each iteration, these rigid links were checked, and for a link in tension, a static condensation technique was used to eliminate the stiffness of this link.

Mehrabi and Shing (1997) developed a cohesive dilatant interface model to simulate the behavior of mortar joints between masonry units as well as the behavior of frame to panel interface, and a smeared crack finite element formulation has been used to model concrete in the RC frame and masonry units in the infill panels. These models have been implemented in simulating the failure mechanisms exhibited by infilled frames including the crushing and cracking of the concrete frames and masonry panels, and the sliding and separation of the mortar joints.

Seah (1998) suggested an analytical technique, in which the steel frame was modeled using elastic beam-column elements connected with nonlinear rotational, shear, and normal springs. The masonry wall was represented by a series of elastic plane stress elements connected together by a series of springs representing the mortar joints as shown in Fig. 3.7. The suggested analytical technique gave very good results up to
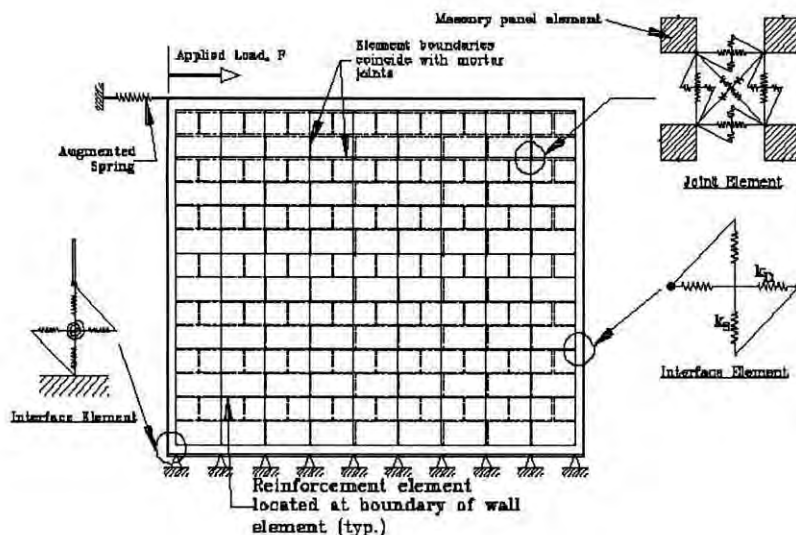
Fig. 3.7. The infilled Frame Model proposed by Seah (1998)

failure as shown in Fig. 3.8, when it was used to model the specimens of the aforementioned testing program conducted in the University of New Brunswick. The model was sophisticated enough to account for the variation in contact lengths and the failure of mortar joints due to shear, tension or compression.

Ghosh and Amde (2002) verified the design of infilled frames to resist lateral loads on buildings in terms of their failure modes, failure loads and initial stiffness using procedures proposed by Riddington (1984) and Pook and Dawe (1986). This verification is made by comparing the results of the analytical procedures of the previous authors with those of a new finite element model for installed frames, which are verified using experimental results. A non-associated interface model has been formulated to model the interface between frame and infill and the mortar joints surrounding the blocks of masonry using the available test data on masonry joints. The failure criteria for masonry include the von Mises criterion for the plane stress condition for uncracked masonry and a smeared crack model. The finite element model provided more insights into the failure mechanisms of the infilled frames.
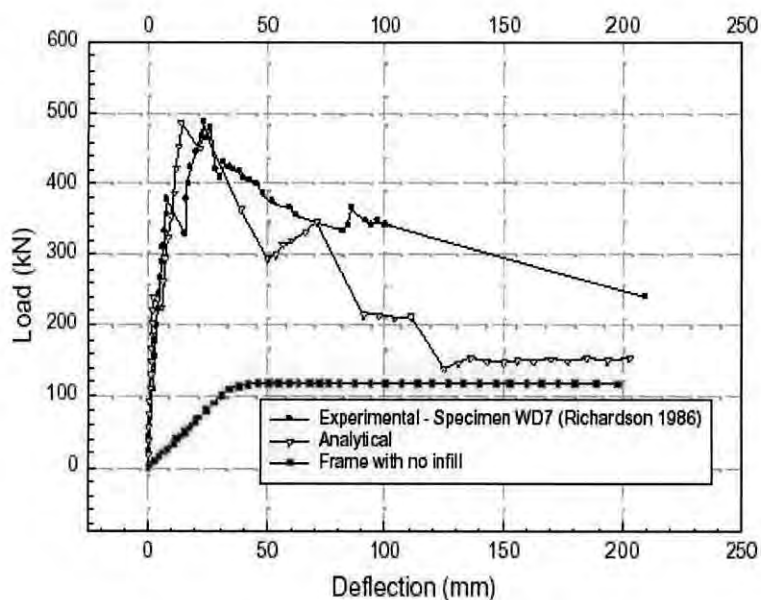
Fig. 3.8. Load Deflection Behavior of a Specimen Modeled by Seah (1998)

3.3 REMARKS

This chapter summarizes the theoretical and experimental research work conducted in the area of infilled frames. It is well and widely recognized now a days that masonry infill walls used for cladding and/or partition in buildings, significantly alter their seismic response, and their effect in changing the stiffness, the ultimate lateral load capacity as well as the ductility supply of the building system should be accounted for in the analysis and design.

Due to the complexity of the contact problem between frame and infill, the sophisticated composite action of them, and the incomplete understanding of the infill role, as well as the numerous uncertainties involved in modeling the effect of infills; design aids such as manuals and software as well as related code provisions hardly include any detailed guidance to take into account the effect of the infills. On the other hand, the contribution of the infill is taken into consideration in the case of structural evaluation or retrofitting, where the overlooked infills are considered to be of most importance and actually the first line of defense.

The objective of this research work is to investigate the effect of ferrocement laminates to URM infill walls confined in reinforced concrete frames as a retrofitting scheme in order to improve the structural performance of these widely used building systems.

Chapter 4

DEVELOPMENT OF FINITE ELEMENT MESH

4.1 INTRODUCTION

This chapter describes the finite element meshing of reinforced concrete frame, infill panel and also the ferrocement. Selection of element type of modeling frames including beam, column and nonlinear contact element is also described. The nonlinear contact element is used to simulate the behavior of infill wall-frame interaction. Some special features like "Birth and Death" are also described briefly in this part.

4.2 MODELING APPROACH CHOSEN FOR PRESENT STUDY

Although there has been a tremendous progressive work going on all around the globe on numerical methods and material modeling, still then, there are numerous problems concerning the methods themselves and also on computational demands. Typically, model of a real structure or a specimen contains fine and large finite element mesh. For modeling concrete and masonry panel, it is necessary to capture several important phenomena such as plasticity, cracking, crushing, creep, swelling, stress stiffening, large deflection, large strain capabilities and possibly softening. For studying global structural behavior of a frame, the equivalent diagonal strut modeling is more suitable and numerically more efficient. But the problem lies in the fact that this model is theoretically weak. First of all, identifying the equivalent nonlinear stiffness of the infill masonry using diagonal struts is not straightforward, especially when there exist some openings, such as doors or windows in the wall. It is also not possible to predict the damaged area of masonry either. The other method based on continuum modeling is more likely to provide an accurate computational representation of both material properties and the failure mechanisms exhibited by the infill panels including the crushing and cracking of the concrete frames and masonry panels and the sliding and separation of the mortar joints. Continuum approach is good for studying the infill itself, cracks and damages in it. Therefore, in this study infill is considered to model as continuum approach.

Existing continuum approaches are smeared type where masonry and mortar are 'mixed' and assumed to be homogeneous e.g. Liauw and Kwan (1985), Mehrabi and Shing (1997) etc. In order to represent the heterogeneity, appropriate mathematical formulations are done. However, such modeling makes the constitutive relation complicated and the model always remains somewhat approximate. If masonry and mortar are individually modeled then relatively simpler material model may be used for each component. In the present study this approach has been used. Here each individual material – concrete, brick masonry, mortar and steel is modeled separately. Thus the computational model can be said to be very comprehensive.

4.3 DEVELOPMENT OF FE MESH

A number of good finite element analysis computer tools or packages are readily available in the civil engineering field. They vary in degree of complexity, usability and versatility. Such packages are ABAQUAS, DIANA, ANSYS, STRAND, ADINA, FEMSKI, and STAAD etc. Some of these programs are intended for a special type of structure. Of all these, the package ANSYS has been proved to be relatively easy to use considering its detailed documentation, flexibility and vastness of its capabilities. The version of ANSYS that has been used for this research work is ANSYS 5.6.

ANSYS is one of the most powerful and versatile packages available for finite element structural analysis. The term structural implies not only civil engineering structures such as buildings, bridges etc. but also naval, aeronautical and mechanical structures such as ship hulls, aircraft bodies and machine housings, as well as mechanical components such as pistons, machine parts, and various tools. The types of structural analysis available in the ANSYS family of products are as follows:

a) Static analysis

b) Modal analysis

c) Harmonic analysis

d) Transient dynamic analysis

e) Spectrum analysis

f) Buckling analysis

g) Explicit dynamic analysis

The primary unknowns (nodal degrees of freedom) calculated in a structural analysis are displacements. Other parameters, such as stresses, strains and reaction forces are then derived from the nodal displacements. Especially its graphical representations are very distinct. Finally the ANSYS 5.6 package is very user friendly. It has a comprehensive graphical user interface (GUI) that gives user easy, interactive access to program functions, commands, documentations and reference material. An intuitive menu system helps user to navigate through the ANSYS program. User can input data using a mouse, a keyboard or a combination of both.

4.3.1 2D FE MODELING OF INFILLED FRAME

4.3.1.1 FE Modeling of Bare Frame

Reinforced concrete frame is a composite type of structure. Reinforced cement concrete, speaking in very common sense, is a mass of hardened concrete with steel reinforcement embedded within it. In this arrangement concrete has higher compressive strength compared to its tensile strength and reinforcement have both high tensile and compressive strength. Two types of elements are chosen, one for concrete and the other for reinforcement. The bare frame consists of a base beam extended beyond the frame boundary, two columns and the upper beam. Here concrete is assumed as a homogeneous and isotropic material. Since plane frames are typically two-dimensional, in this study the RC frame has been modeled by using two

Load applied at the wedge

Column

Base Beam

All D.O.F.s constrained at the extended portion of Base Beam
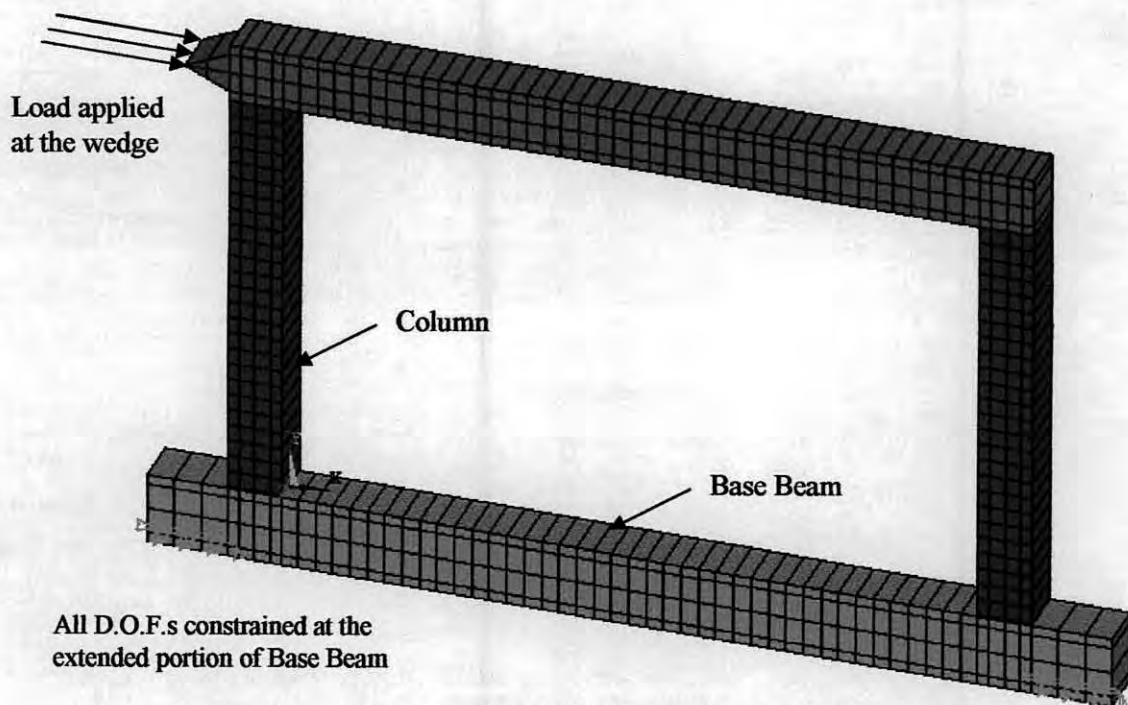
Fig. 4.1. Isometric view of the 2D finite element model of bare frame
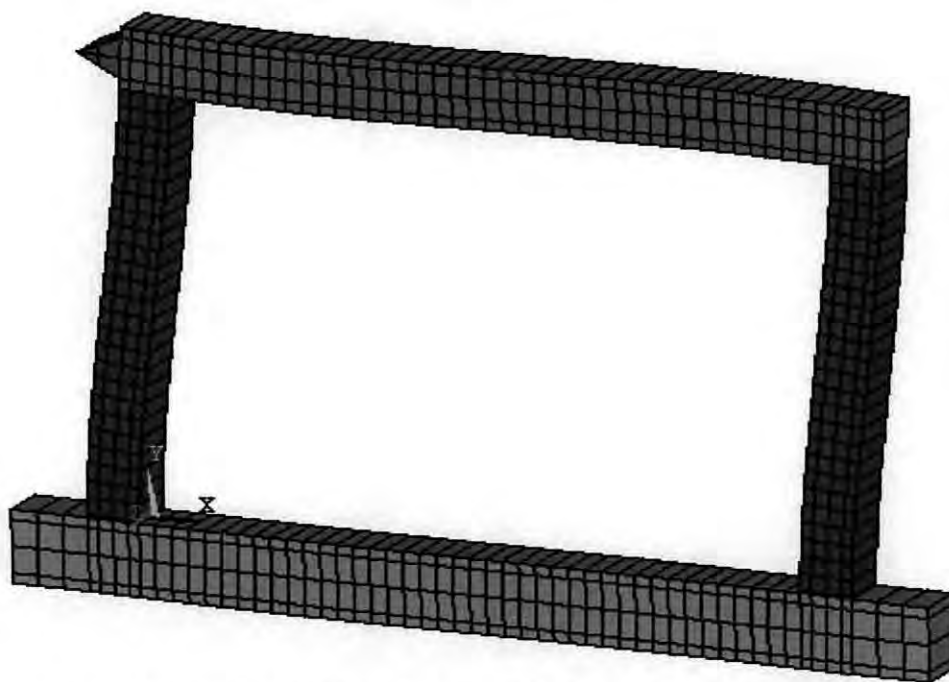
Fig. 4.2. Typical deflected shape of 2D FE model of bare frame

dimensional plane stress elements, which is named as Plane42 in ANSYS program. These elements are basically four noded isoparametric elements. Here simple Drucker-Prager yield criterion is used for concrete modeling. The reinforcements are modeled using simple two dimensional truss elements known as Link1 in ANSYS program. These are two noded elements. All the beams and columns are rectangular in shape. Fig. 4.1 shows the finite element model of bare frame (isometric view) and Fig. 4.2 shows its typical deflected shape.

PLANE42 — 2-D Structural Solid

PLANE42 is used for 2-D modeling of solid structures. The element can be used either as a plane element (plane stress or plane strain) or as an axisymmetric element. The element is defined by four nodes having two degrees of freedom at each node, i.e. translations in the nodal x and y directions. The element has plasticity, creep, swelling, stress stiffening, large deflection, and large strain capabilities. Fig. 4.3 shows a typical shape, geometry, node locations, and the coordinate system of PLANE42 2-D structural solid element.
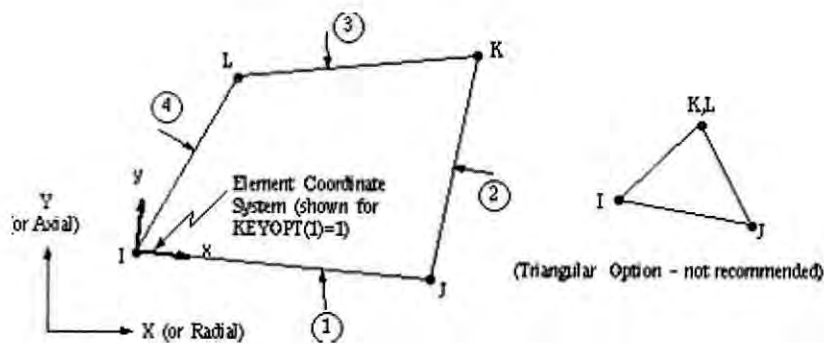
Fig.4.3. Plane42 – 2-D Structural Solid Element

LINK1 — 2-D Spar

LINK1 can be used in a variety of engineering applications. Depending upon the application, the element can be thought as a truss, a link, a spring, etc. The two-dimensional spar element is a uniaxial tension-compression element with two degrees of freedom at each node: translations in the nodal x and y directions. As in a pin-jointed structure, no bending of the element is considered. The special features of this element are plasticity, creep, swelling, stress stiffening, large deflection and birth and death. The typical shape, geometry, node locations, and the coordinate system of a LINK1 element is shown in Fig. 4.4.
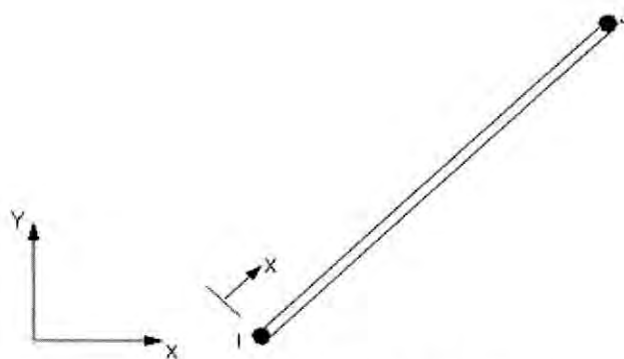
Fig.4.4. LINK1 – 2D-Spar Element

4.3.1.2 FE Modeling of Infill Panel

Masonry is a two-phase material with regular distribution of mortar joints and bricks. The discrete element method is the most commonly used simplification method in simulating the behavior of joints and bricks. Since only in-plane load is considered in this study the infill is modeled by 2 dimensional elements. For the infill, mortars and

bricks are modeled individually and both are modeled by 2-D four noded plane stress elements. A single brick is composed of three individual 2-D four noded plane stress elements. The brick arrangements in the infill wall are shown in Fig. 4.5. The gaps within the bricks are filled with mortar. The FE infill panel is modeled exactly like a real masonry wall. First a mortar course is placed on the base beam then a bricklayer
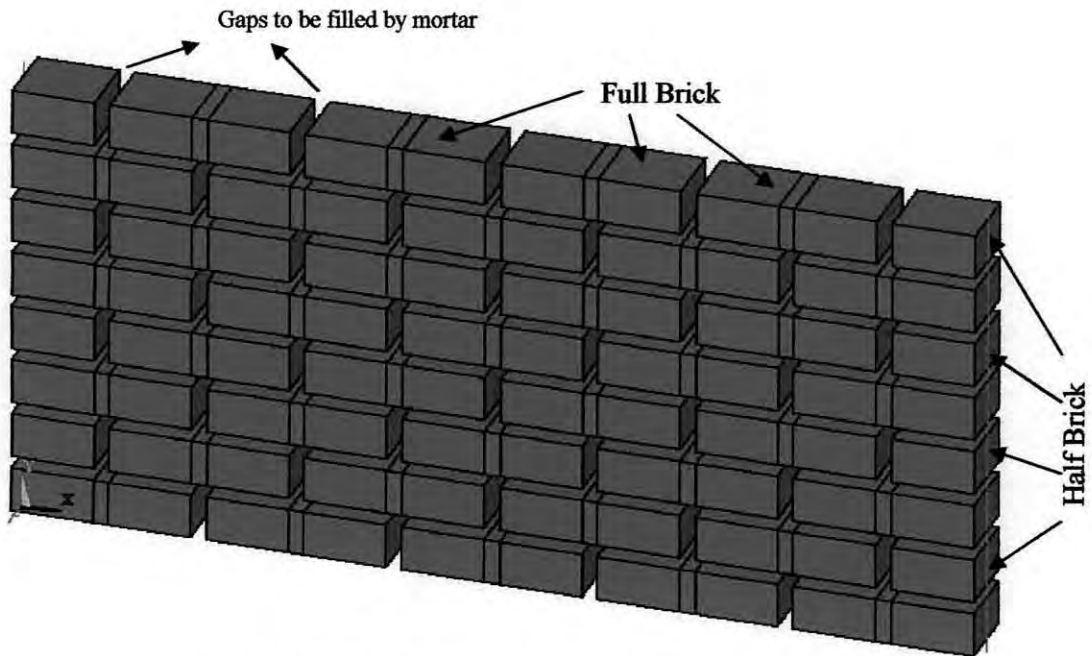
Fig. 4.5. Brick arrangements in the infill wall
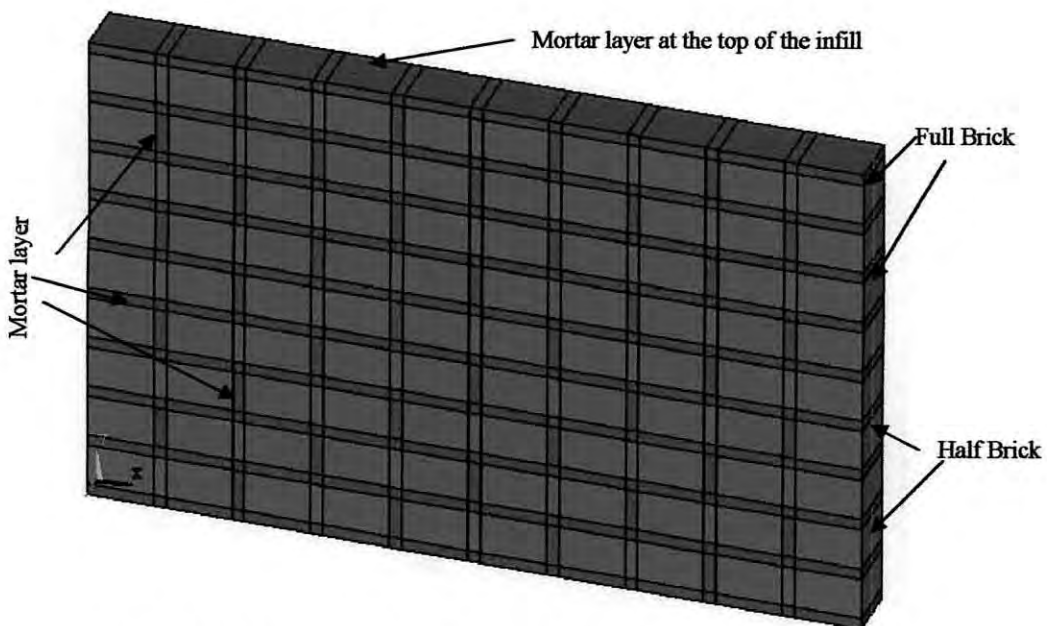
Fig. 4.6. Modeling of masonry infill in staggered way

is laid on the mortar course. Then another mortar layer is laid over the bricklayer then again a bricklayer is placed over the mortar layer. Thus the whole infill is the repetition of these arrangements. If a bricklayer starts with a full brick in one layer, then the next layer will start with a half brick as shown in Fig. 4.5 and at the top of the infill it ends with a layer of mortar as shown in Fig. 4.6.
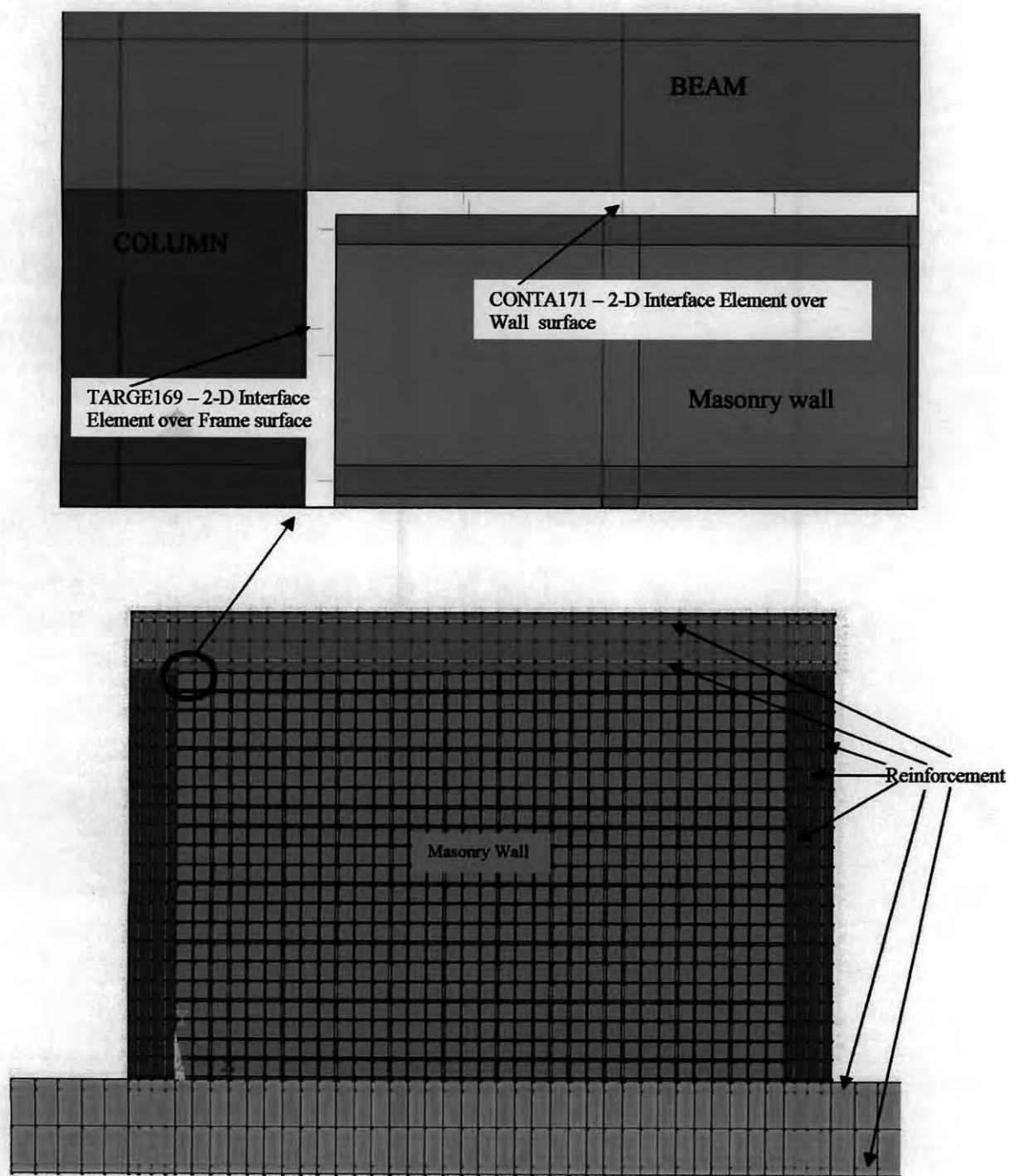
Fig. 4.7. 2D FE model of Masonry infilled frame with close up
view of the interface elements.
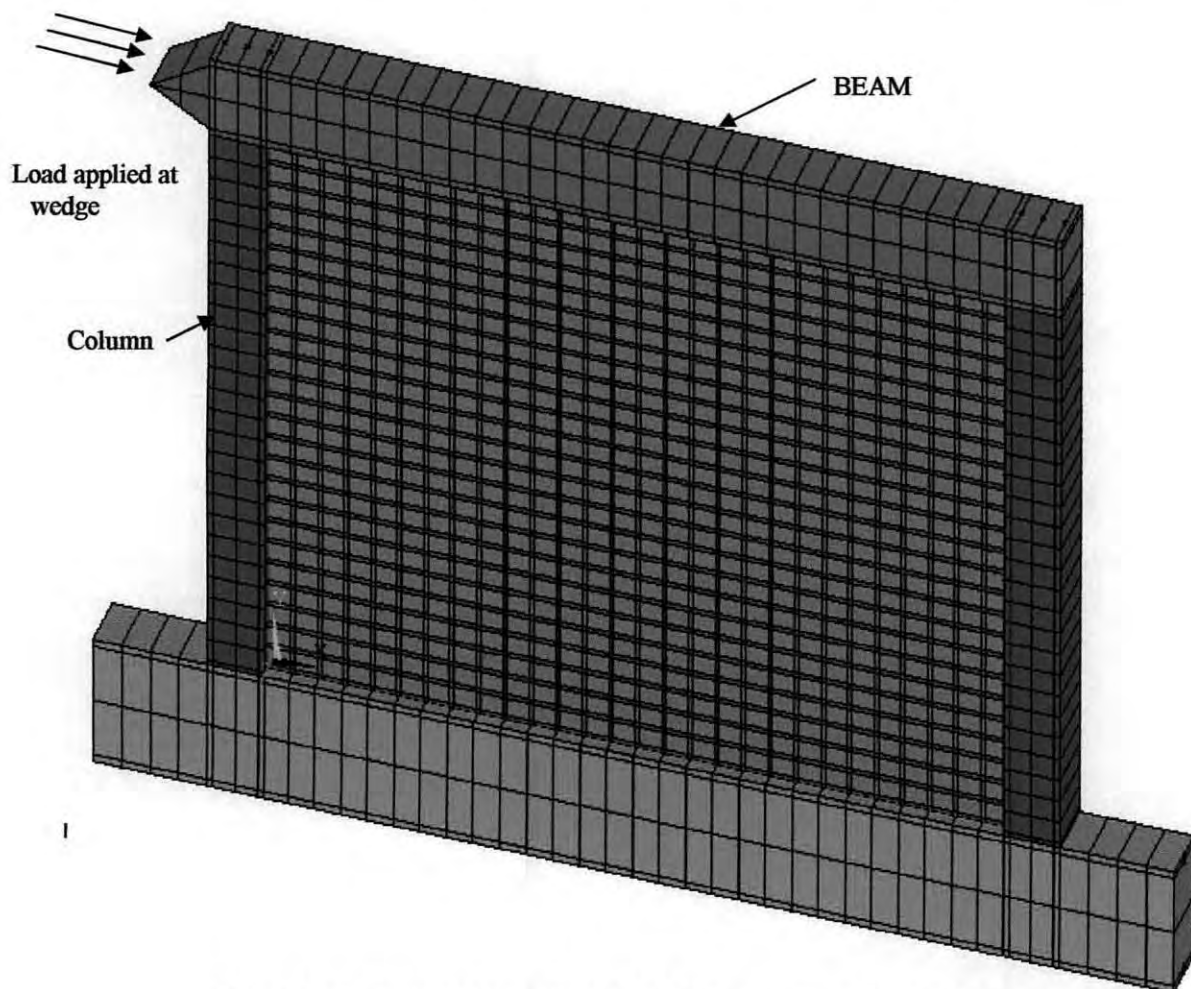
Fig. 4.8. Isometric view of the 2-D FE masonry infilled RC frame
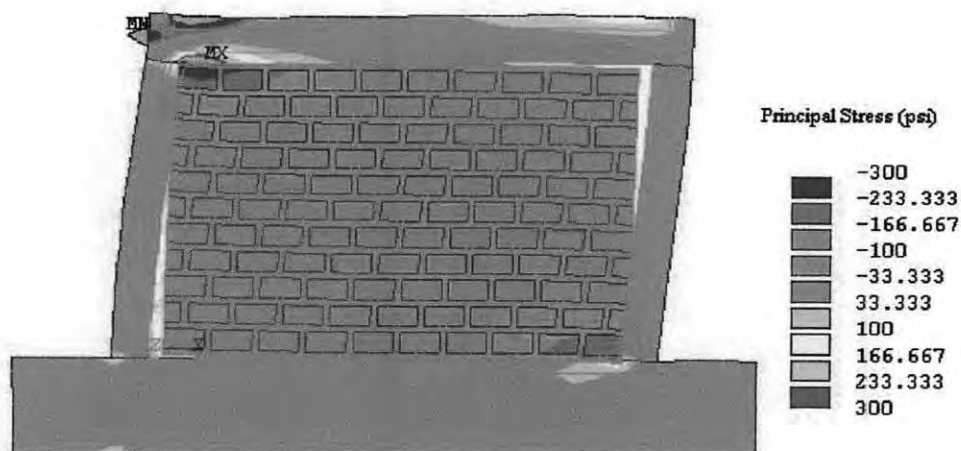
Fig. 4.9. Typical deflected shape and stress contour diagram of
2-D FE model of masonry infilled RC frame.

The interaction between the frame and the infill due to applied load plays the most important role in the behavior of the infilled frames. In most applications, the infill is

connected to the frame by mortar. The interaction between the frame and the infill through this mortar joint is modeled by an interface element capable of transferring shear and normal forces in the elastic and inelastic ranges of loading. Interface elements have been used in the past to model joints and discontinuities, e.g., masonry with mortar joints, rock with faults, and cracked concrete. In the finite element modeling of the infilled frame here, the modeling of the interface between the infill and the frame has been emphasized. In this study the interface elements are modeled considering the contact problem between the wall and the frame as a rigid-to-flexible contact, which means that the bodies are not equally deformable and have stiffness different from each other.

To model a contact problem, like this in ANSYS program, it is important to identify the parts to be analyzed for their possible interaction. The possible contact between these two will be surface-to-surface contact. The finite element model recognizes possible contact pairs by the presence of specific contact elements. These contact problems involving contact between two boundaries, one of the boundaries is conventionally established as the "target" surface and the other is the "contact" surface. For rigid-to-flexible contact, the target surface is always the rigid surface and the contact surface is the deformable surface. Since reinforced concrete is much stiffer than masonry wall, here target surface is considered as reinforced concrete frame part, which is modeled with TARGE169 and the contact surface is considered as masonry wall, which is modeled with CONTA171. Fig. 4.7 shows the position and orientation of the interface elements over frame and wall surfaces. Fig. 4.8 shows the isometric view and Fig. 4.9 shows the typical deflected shape and stress contour of the 2D FE model of the masonry infilled RC frame.

A brief description of the key features of the interface elements' formulation is presented here as follows.

TARGE169 – 2-D Target Segment

TARGE169 as shown in Fig. 4.10, is used to represent various 2-D "target" surfaces for the associated contact elements CONTA171. The contact elements themselves overlay the solid elements describing the boundary of a deformable body and are potentially in contact with the target surface, defined by TARGE169. This target

surface is discretized by a set of target segment elements (TARGE169) and is paired with its associated contact surface via a shared real constant set. Any translational or rotational displacement can be imposed on the target segment element. Even forces and moments can also be imposed on target elements. For rigid targets, these elements can easily be modeled for complex target shapes. For flexible targets, these elements will overlay the solid elements describing the boundary of the deformable target body.
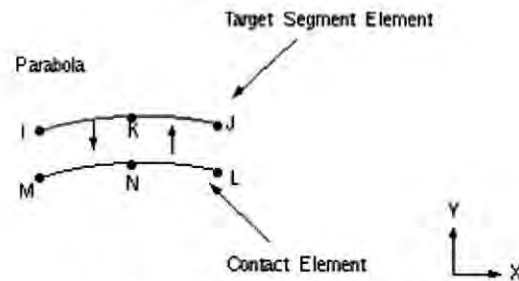
Fig. 4.10. Target surface element of TARGE169

The target surface is modeled through a set of target segments; typically, several target segments comprise one target surface. The target surface can either be rigid or deformable. For modeling rigid-flexible contact, the rigid surface must be represented by a target surface. For flexible-flexible contact, one of the deformable surfaces must be overlaid by a target surface. The target and associated contact surfaces are identified by a shared real constant set. This real constant set includes all real constants for both the target and contact elements. Each target surface can be associated with only one contact surface, and vice-versa.

CONTA171 — 2-D Surface-to-Surface Contact

CONTA171 is used to represent contact and sliding between 2-D "target" surfaces (TARGE169) and a deformable surface, defined by this element. This element has two degrees of freedom at each node: translations in the nodal x and y directions. This element is located on the surfaces of 2-D solid, shell, or beam elements without midside nodes. It has the same geometric characteristics as the solid, shell, or beam element face with which it is connected. Contact occurs when the element surface penetrates one of the target segment elements (TARGE169) on a specified target surface. Coulomb and shear stress friction is allowed.

The geometry and node locations are shown in Fig.4.11. The element is defined by two nodes and the underlying solid, shell, or beam element has no mid-side nodes. The element x-axis is along the I-J line of the element. The correct node ordering of the contact element is critical for proper detection of contact. The nodes must be ordered such that the target must lie to the right side of the contact element when moving from the first contact element node to the second contact element node as in Fig. 4.11. The 2-D contact surface elements are associated with the 2-D target segment elements (TARGE169) via a shared real constant set.
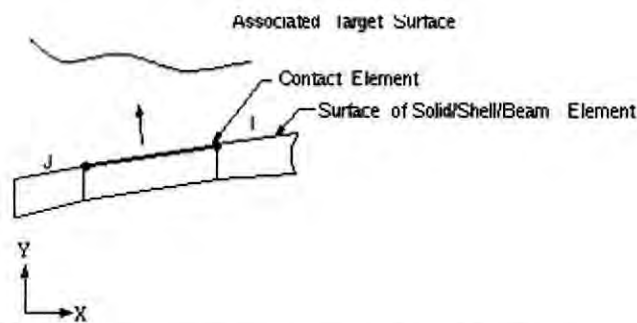
Fig. 4.11. Surface-to-surface contact of CONTA171

4.3.1.3 FE Modeling of Ferrocement Overlay on Infill Panel

In the FE model of the infilled frame, ferrocement is placed over the masonry wall covering the bricks and mortar. Ferrocement overlay is also modeled with four noded 2-dimensional plane stress elements. The FE modeling of masonry infilled frame with ferrocement overlay is shown in Fig. 4.12. To numerically investigate the effectiveness of the proposed repair method it was necessary to add ferrocement overlay on the damaged infill. But after loading and unloading of the infilled frame the whole orientation is changed and all the nodes are displaced from their original location. That's why it is almost impossible to add new elements on the infill panel accurately after loading. But ANSYS program provides a special feature in this regard to serve the purpose alternatively. The element "Birth" and "Death" feature of the ANSYS program is used to add the desired repaired layer to the original models prior to loading and unloading. The repaired layer elements were deactivated "Killed" during the first loading and unloading, subsequently they were activated "Born" in the last load step before reloading the model again.
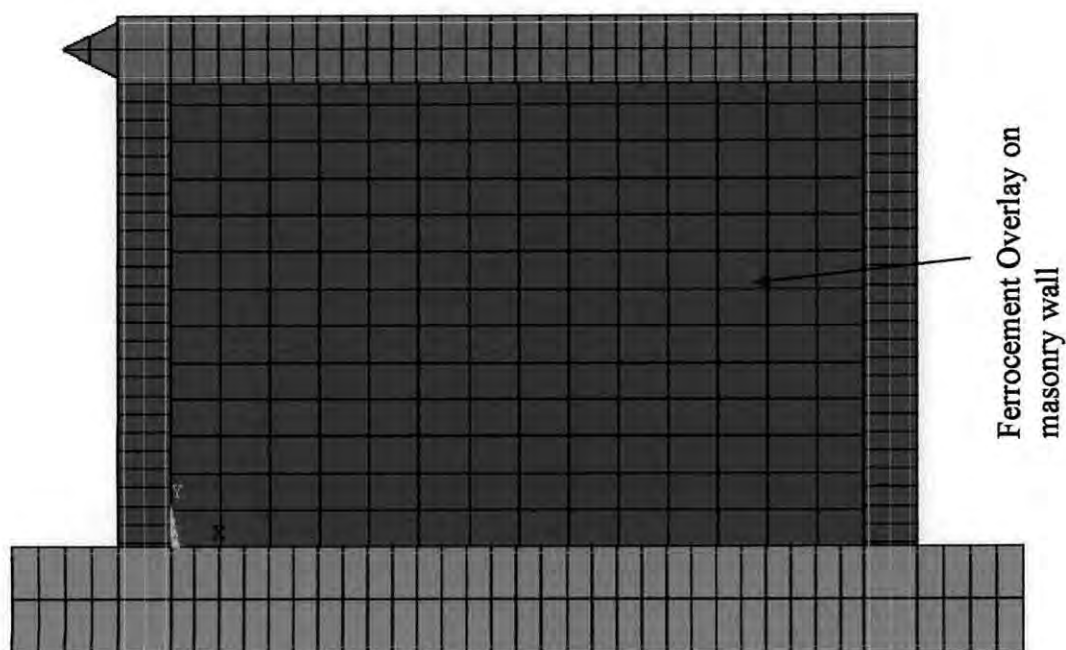
Fig. 4.12. FE modeling of maosonry infilled RC frame with
ferrocement overlay

To achieve the "element death" effect, the ANSYS program does not actually remove
"killed" elements. Instead, it deactivates them by multiplying the tangent modulus by
a severe reduction factor. This factor is set to 1.0E-6 by default, but can be given
other values. Element loads associated with deactivated elements are zeroed out of the
load vector; however, they still appear in element-load lists. Similarly, mass,
damping, specific heat, and other such effects are set to zero for deactivated elements.
The mass and energy of deactivated elements are not included in the summations over
the model. An element's strain is also set to zero as soon as that element is killed.

In like manner, when elements are "born", they are not actually added to the model;
they are simply reactivated. All elements must be created, including those to be born
in later stages of analysis. When an element is reactivated, its stiffness, mass, element
loads, etc. return to their full original values. Elements are reactivated having no
record of strain history. However, initial strain defined as a real constant will not be
affected by birth and death operations. Also, unless large-deformation effects are
turned on, some element types will be reactivated in their originally specified
geometric configuration (large-deformation effects should be included to obtain
meaningful results). Applied strains are then computed for newly activated elements
based on the current load step.

4.3.2 3D FE Modeling of Infilled Frame

4.3.2.1 FE modeling of Bare Frame

3D modeling of infilled frame was rather a difficult task compared to that of 2D modeling. Several other factors had to be considered during modeling of 3D frame. For the modeling of reinforced concrete, concrete is modeled with 8-noded solid element, named as SOLID65 element in the ANSYS program, whereas reinforcement is modeled with simple 3D two noded truss element, known as LINK8 element in the ANSYS program. A single bay portal frame is modeled with these elements where the columns, beam and the base beam are rectangular in shape as shown in Fig. 4.13. Number of nodes and elements in a model vary according to the size of the bay and height of the frame. In the frame additional nodes for columns and beams are defined at the level of mortar to study the infill-frame interaction, which has been discussed in the next section. The typical deflected shape with stress contour diagram of the 3-D finite element reinforced concrete bare frame under lateral load is presented in Fig. 4.14.
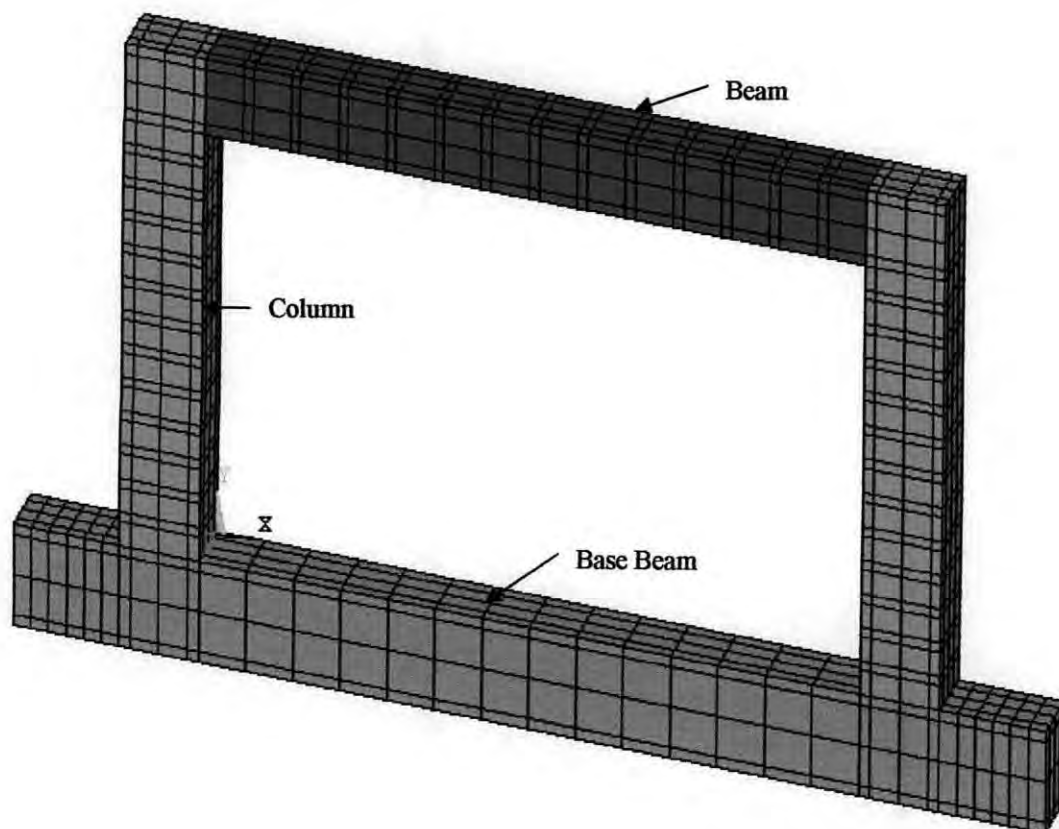
Fig. 4.13. Isometric view of the 3-D FE RC bare frame

Principal Stress (psi)

■	-91.096
■	-72.029
■	-52.962
■	-33.895
■	-14.828
■	4.239
■	23.307
□	42.374
■	61.441
■	80.508
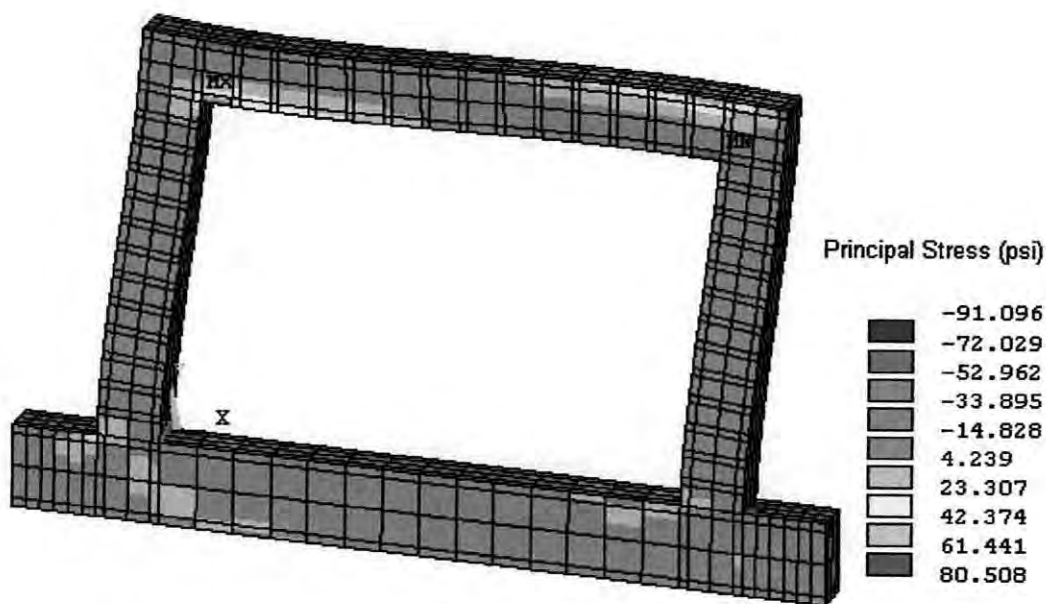
Fig. 4.14. Typical deflected shape with stress contour diagram of
the 3-D FE model of bare RC frame

The base elements of ANSYS used in 3D modeling are discussed in details.

SOLID65 – 3-D Reinforced Concrete Solid

Solid65 element is used for the three-dimensional modeling of solids with or without reinforcing bars (rebar). The solid is capable of cracking in tension and crushing in compression. In concrete applications, for example, the solid capability of the element may be used to model the concrete while the rebar capability is available for modeling reinforcement behavior. The element is defined by eight nodes having three degrees of freedom at each node, translations in the nodal x, y, and z directions. Up to three different rebar specifications may be defined. The special feature of concrete element is special cracking and crushing capabilities. The most important aspect of this element is the treatment of nonlinear material properties. The concrete is capable of cracking (in three orthogonal directions), crushing, plastic deformation, and creep. The rebars are capable of tension and compression, but not shear. They are also capable of plastic deformation and creep. Fig. 4.15 shows a typical shape of SOLID65 – 3-D solid element.
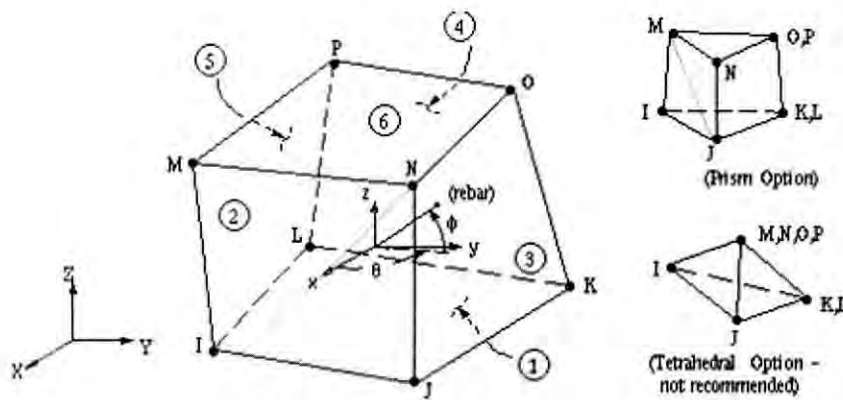
Fig. 4.15. SOLID65 – 3-D reinforced concrete solid element

The geometry, node locations, and the coordinate system for this element are shown in Fig. 4.15. The element is defined by eight nodes and the isotropic material properties. The element has one solid material and up to three rebar materials. Rebar specifications include the material number, the volume ratio, and the orientation angles (θ, φ) as shown in the above figure. The volume ratio is defined as the rebar volume divided by the total element volume. The orientation is defined by two angles (in degrees) from the element coordinate system.

LINK8 — 3-D Spar

Link8 is a spar, which may be used in a variety of engineering applications. This element can be used to model trusses, sagging cables, links, springs, reinforcement in concrete etc. The three-dimensional spar element is a uniaxial tension-compression element with three degrees of freedom at each node: translations in the nodal x, y, and z directions. As in a pin-jointed structure, no bending of the element is considered. Special features include plasticity, creep, swelling, stress stiffening, and large deflection capabilities. The typical shape, geometry, node locations, and the coordinate system of a LINK1 element are shown in Fig. 4.16. The element is defined by two nodes, the cross-sectional area, an initial strain, and the material properties. The element x-axis is oriented along the length of the element from node I toward node J. The initial strain in the element (ISTRN) is given by δ/L, where δ is the difference between the elongated element length, L, (as defined by the I and J node locations) and the zero strain length (initial length).
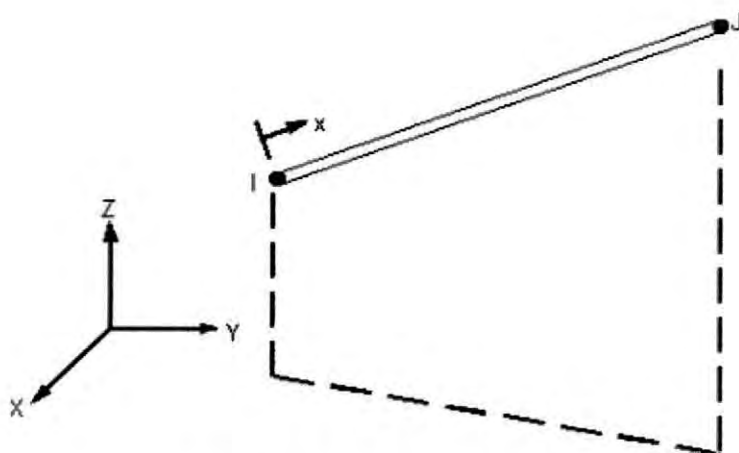
Fig. 4.16. LINK8 – 3D-Spar Element

4.3.2.2 FE Modeling of Infill Panel

Masonry is a two-phase material with regular distribution of mortar course and brick. The discrete element method is the most commonly used simplification method in simulating the behavior of joints and brick. In the FE modeling both bricks and mortars are modeled with 8-noded solid elements known as SOLID45 in ANSYS program. A full brick is modeled with six eight noded solid elements where it is dis-
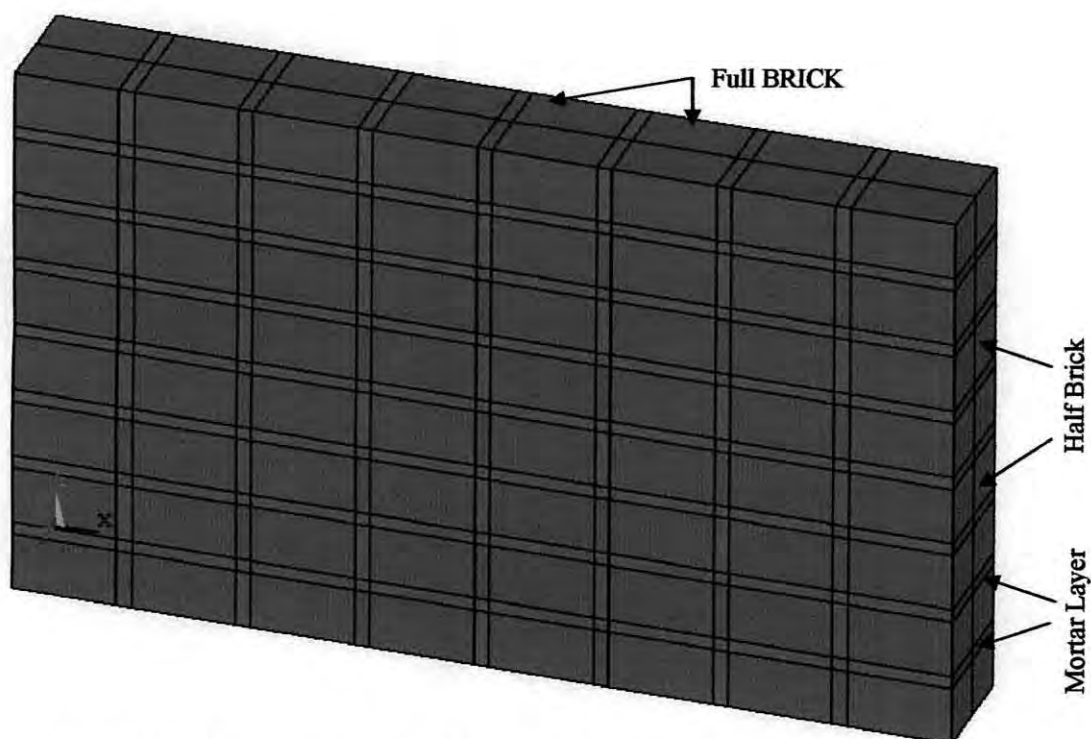
Fig. 4.17. Arrangement of bricks and mortar in the infill wall of FE model of 3-D masonry infilled RC frame
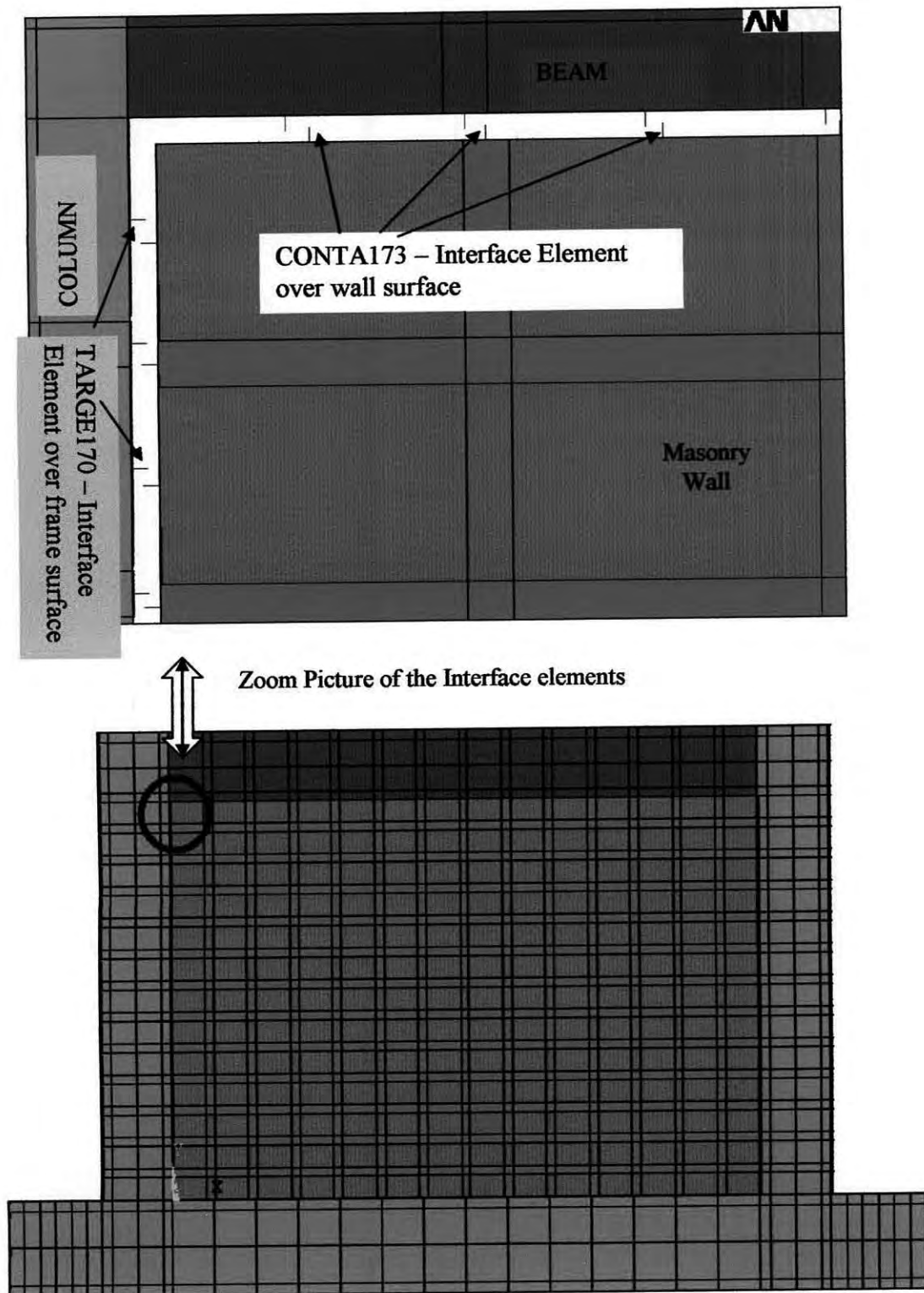
Fig. 4.18. 3D FE model of Masonry infilled frame with close up view of the interface elements.

cretized into three parts along its width and two parts along its longitudinal direction and a half brick is modeled with two 8-noded solid elements divided only along its longitudinal direction. Mortar course in between bricks is divided into two parts

along the direction of width of the brick. Brick and mortar arrangements are shown in Fig. 4.17. The infill is modeled in the same fashion as described in section 4.3.1.2.

The behavior of infilled frame is governed mostly by the interaction between frame and the infill. The infill is connected to the frame by mortar. The interaction between frame and infill through this mortar joint is modeled by a pair of interface elements capable of transferring shear and normal forces in the elastic and inelastic ranges of loading. In such problems involving contact between two boundaries, one of the boundaries is conventionally established as the "target" surface, and the other as the "contact" surface.

Considering the problem as a rigid-flexible contact, the target surface is always the rigid surface, i.e. the surfaces of the RC frame, and the contact surface is the more deformable surface compared to that of target surface, this is the infill wall surface that will be in contact with the frame. The most efficient way to model surface-to-surface contact is asymmetric contact, which is defined as having all contact elements on one surface and all target elements on the other surface. This is sometimes called "one-pass contact."

TARGE170 Interface Element applied over Frame surface

CONTA173 Interface Element applied over Wall surface
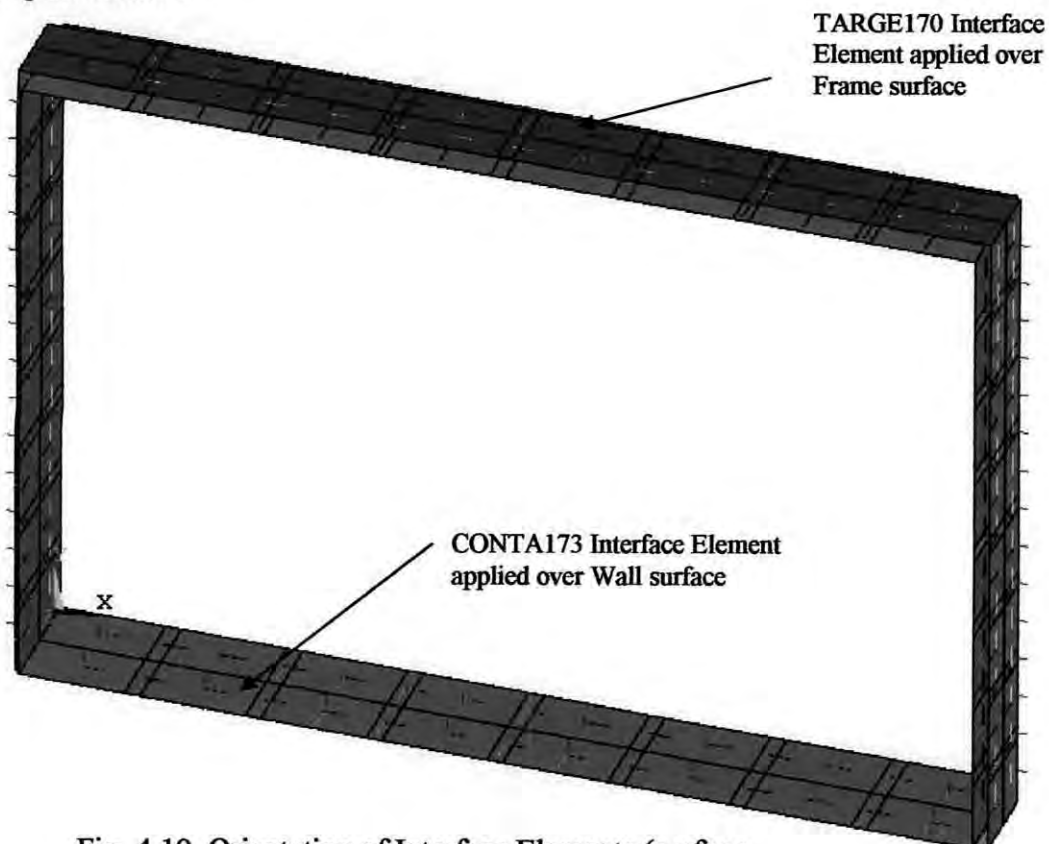
Fig. 4.19. Orientation of Interface Elements (surface-to-surface contact) applied in 3-D FE model of masonry infilled RC frame
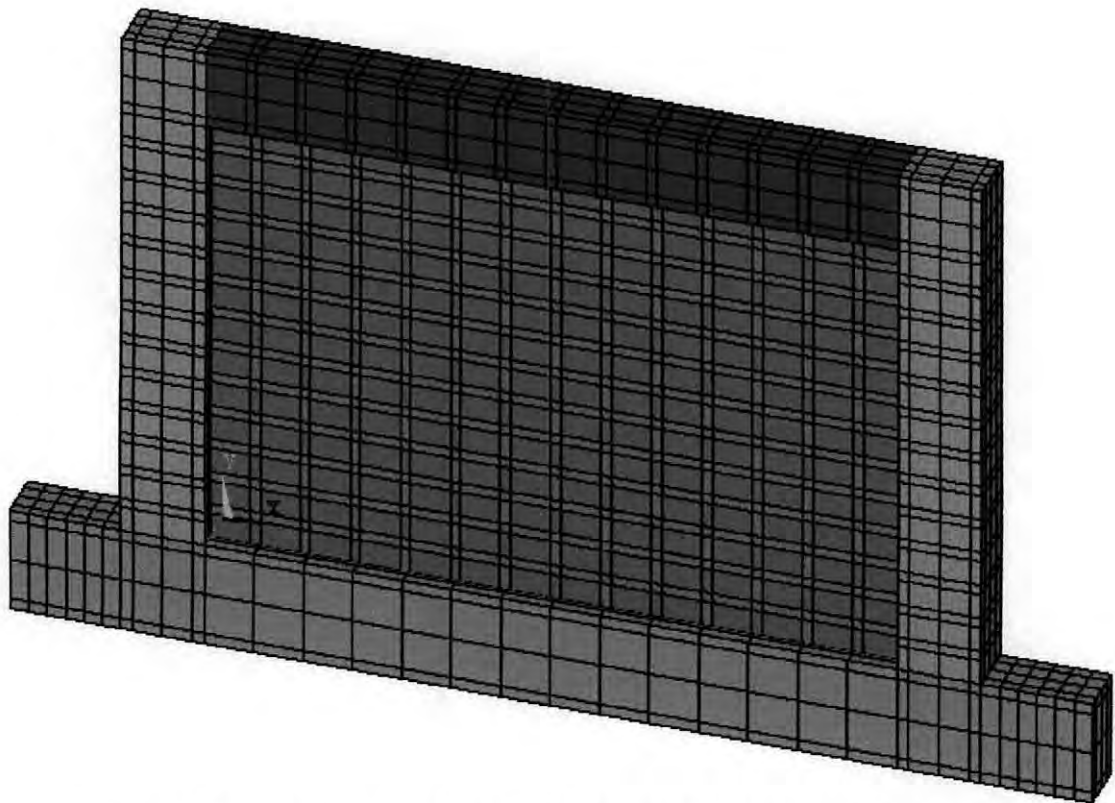
Fig. 4.20. Isometric view of the FE 3-D model of the masonry infilled RC frame

Principal Stress(psi)

■	-150.485
■	-126.386
■	-102.286
■	-78.187
■	-54.088
■	-29.988
□	-5.889
□	18.211
□	42.31
■	66.409

Face Gap
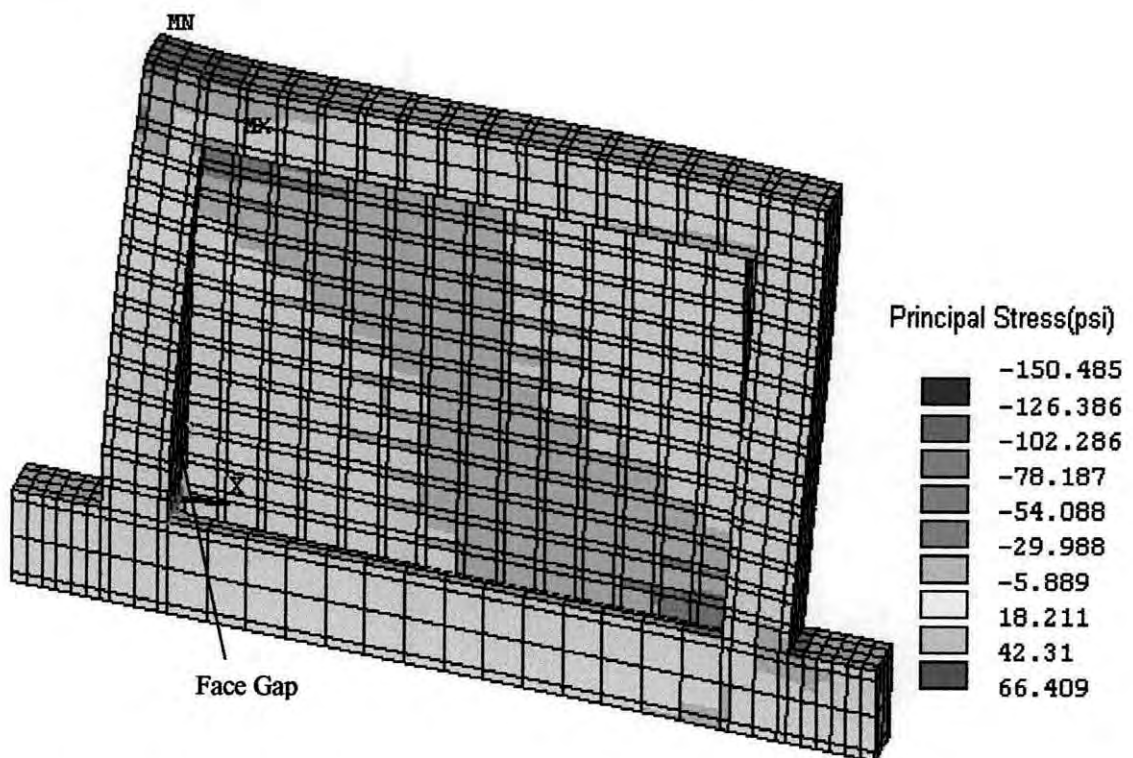
Fig. 4.21. Typical deflected shape with stress contour diagram of the 3-D FE model of masonry infilled RC frame

The surfaces inside the frame that will be in contact with masonry wall are modeled with interface elements defined as TARGE170 in ANSYS program and the outer surfaces of the masonry wall that will be in contact with frame are modeled with 3D interface elements defined as CONTA173. Fig. 4.18 and Fig. 4.19 show the orientation of the interface elements. Fig. 4.20 shows the isometric view and Fig. 4.21 shows the typical deflected shape and stress contour of the 3-D FE model of the masonry infilled RC frame. From the stress contour diagram of Fig. 4.21 it can be observed that incase of masonry infill, high stressed elements are along the diagonal of the infill panels.

The key features of the solid element used for modeling brick and mortar and also the key features of interface elements used for modeling surface-to-surface contact are presented below.

SOLID45 - 3-D Structural Solid

SOLID45 is used for the three-dimensional modeling of solid structures. The element is defined by eight nodes having three degrees of freedom at each node: translations in the nodal x, y, and z directions. The special features of this element are plasticity, creep, swelling, stress stiffening, large deflection, and large strain capabilities.
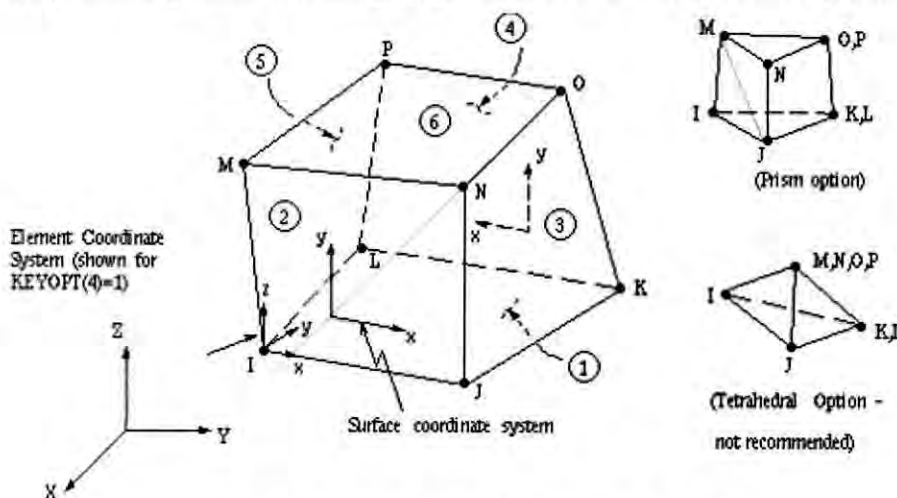
Fig. 4.22. SOLID45 - 3-D Structural Solid

The geometry, node locations, and the coordinate system for this element are shown in Fig. 4.22. The element is defined by eight nodes and the orthotropic material properties. Orthotropic material directions correspond to the element coordinate directions. The element coordinate system orientation is also described in Fig. 4.22.

TARGE170 — 3-D Target Segment

TARGE170 is used to represent various 3-D "target" surfaces for the associated contact elements. The contact elements themselves overlay the solid elements describing the boundary of a deformable body and are potentially in contact with the target surface, defined by TARGE170. This target surface is discretized by a set of target segment elements (TARGE170) and is paired with its associated contact surface via a shared real constant set. Any translational or rotational displacement can be imposed on the target segment element. One can also impose forces and moments on target elements. For rigid target surfaces, these elements can be used to model complex target shapes. For flexible targets, these elements will overlay the solid elements describing the boundary of the deformable target body.
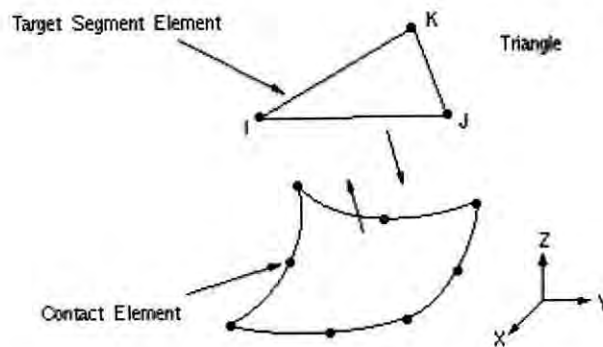
Fig. 4.23. Target surface element of TARGE170

The target surface is modeled through a set of target segments, typically, several target segments comprise one target surface. The target surface can either be rigid or deformable. For modeling rigid-flexible contact, the rigid surface must be represented by a target surface. For flexible-flexible contact, one of the deformable surfaces must be overlayed by a target surface. The target and associated contact surfaces are identified via a shared real constant set. This real constant set includes all real constants for both the target and contact elements. Each target surface can be associated with only one contact surface, and vice-versa.

CONTA173 – 3-D Surface-to-Surface Contact

CONTA173 is used to represent contact and sliding between 3-D "target" surfaces (TARGE170) and a deformable surface, defined by this element. This element has three degrees of freedom at each node: translations in the nodal x, y, and z directions.

This element is located on the surfaces of 3-D solid or shell elements without midside nodes. It has the same geometric characteristics as the solid or shell element face with which it is connected. Contact occurs when the element surface penetrates one of the target segment elements (TARGE170) on a specified target surface. It allows Coulomb and shear stress friction.

The geometry and node locations are shown in Fig. 4.24. The element is defined by four nodes (the underlying solid or shell element has no mid-side nodes). The node ordering is consistent with the node ordering for the underlying solid or shell element. The positive normal is given by the right-hand rule going around the nodes of the element and is identical to the external normal direction of the underlying solid or shell element surface. For shell elements, the same nodal ordering between shell and contact elements defines upper surface contact; otherwise, it represents bottom surface contact. The target surfaces must always be on its outward normal direction.
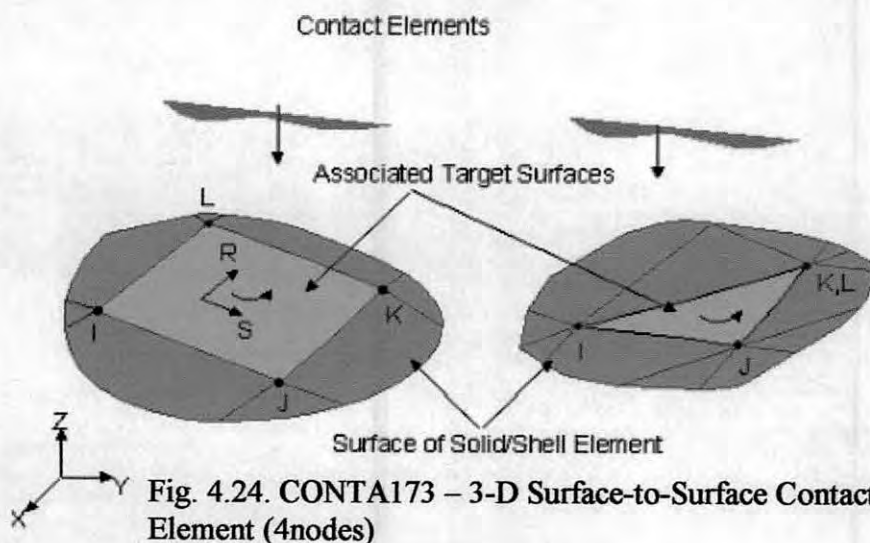
Contact Elements

Fig. 4.24. CONTA173 – 3-D Surface-to-Surface Contact Element (4nodes)

4.4 REMARKS

At the beginning of this study on masonry infilled RC frame, the author first dealt with 3D problems. Although the modeling was precisely done, the only problem that turned the author to think alternatively was the computational time required for solving 3D problems. With a computer of 2.4 GHz speed and 256 MB RAM, it took more than 15 minutes to solve a single iteration of a 3D single bay masonry infilled RC frame under lateral loads without application of contact elements. If contact

elements were applied in the same problem, it took about 2 hours to solve a single iteration. In order to get a full load versus deflection response up to failure of a 3-D masonry infilled RC frame under lateral load it takes as much as 1000 iterations. Therefore it seemed to be next to impossible to deal with 3D problems because it would then require more than 50 days to solve this problem. Modeling the same problem with 2D elements was easier and solution time was much less compared to that of 3D problems. Since only in-plane load is considered in this study, it seemed to be quite logical to work with 2D problems.

This chapter summarizes the experimental and theoretical research work conducted in the area of infilled frames. But it appears that none of these models consider ferrocement as a retrofitting material. It is well established from the previous chapter that ferrocement can be successfully used for the rehabilitation of masonry buildings and a wide variety of structural repairs. Retrofitted infill panels with ferrocement overlay, therefore, require proper investigation both experimentally and numerically to simulate its behavior. This chapter also describes the finite element modeling of RC frame infilled with masonry covered by ferrocement overlay. The model will be used to adequately reflect the effect of ferrocement as a retrofitting material.

Chapter 5

RESULTS AND DISCUSSION

5.1 INTRODUCTION

Numerous experimental and analytical investigations of infilled structures have been conducted over the past fifty years and important advances have been made for both steel and RC frames infilled with masonry. Researches have proved that infilled frames subjected to in plane lateral loading demonstrate substantial strength and stiffness as well as enhanced energy dissipation. Masonry infill itself is a mean of retrofitting or strengthening of existing framed buildings and incorporation of infill is an effective way of reducing lateral drift. Old distressed buildings can regain or improve its strength by repairing its masonry walls. In this respect ferrocement overlay is an effective tool in improving the ductility, rigidity and strength of masonry walls. Extensive experimental and research works [Reinhorn and Prawell (1985); Singh et al. (1988); Irimies and Crainic (1993); Jabarov et al. (1985); Kahn (1984); Alcocer et al. (1996); Ehsani and Saadatmanesh (1996); Oliveria (2001); Fahmy et al. (1997); Fahmy et al. (1999); Alam (2003)] have been carried out to observe the behavior of masonry walls, beams and columns with ferrocement overlay. Although there have been a number of experimental investigations conducted but there is no established numerical model available to study the behavior of damaged infill panels repaired with ferrocement. In this present chapter numerical modeling is verified for bare frame, infilled frame and also for the damaged infill panel retrofitted with ferrocement overlay. The results obtained from the numerical methods, nonlinear finite element analysis using ANSYS package, are presented here and compared with the experimental results available. This comparison will serve as verification for the validity of the adopted FE methodology. The findings have also been discussed to highlight the important observations.

5.2 VERIFICATION OF BARE-FRAME MODEL WITH THE EXPERIMENTAL DATA

In order to investigate the behavior of masonry infilled frame, first of all it is important to verify the adopted FE analysis methodology without masonry infill. Although there are a

number of research works on the performance of RC frames, most of the published works are deficient in one or other data relating to the properties of materials used in the investigation and also the reinforcement arrangements. This has seriously restricted the experimental data available for use in verifying the numerical method. Based on the availability of basic data for the analysis of the bare RC frame the works of Mehrabi et al. (1996) have been found to be very extensive and exact and have been selected for comparison with the finite element method.

The experimental study carried out by the above author varies in the configuration of the RC frames in the reinforcement arrangement and material properties. Two types of frames were considered with respect to lateral loadings. The frames were designed in accordance with the provisions of *ACI 318-89* (1989). The test specimens were chosen to be half-scale frame models and twelve single bay and two two-bay specimens were tested. For the purpose of this present topic only bare frame specimen has been taken into consideration. The bare frame, with design details shown in Fig. 5.1, is a weak frame as described by specimen 1, which was subjected to a monotonically increasing lateral load. This exhibited a fairly flexible and ductile behavior. The load deflection curve is shown in Fig. 5.2. Material tests were also conducted on the reinforcing steel, and concrete samples for each specimen. The material properties for the bare frame (specimen 1) are summarized in Table 5.1 and 5.2.

Section A-A

Section B-B
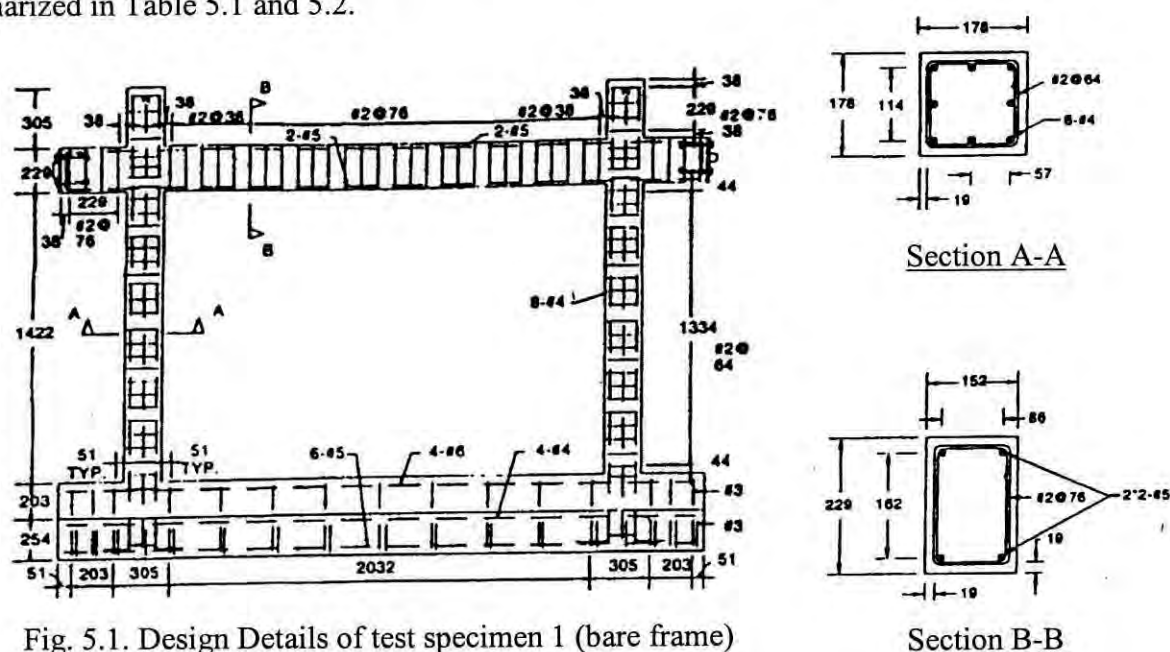
Fig. 5.1. Design Details of test specimen 1 (bare frame) and 8 (infilled frame) by Mehrabi et al. (1996) (units:mm)

Table: 5.1. Average Strengths of Concrete Materials for bare-frame, specimen no. 1 by Mehrabi et al. (1996). (1MPa = 0.145 ksi)

Secant Modulus (MPa)	21930
Compressive Strength (MPa)	30.9
Strain at peak stress	0.0018
Modulus of Rupture (MPa)	6.76
Tensile Strength (split cylinder tests) (MPa)	3.29

Table: 5.2. Average tensile strengths of reinforcing steel by Mehrabi et al. (1996). (1MPa = 0.145 ksi)

Bar Size	Nominal diameter (mm)	Yield Strength (MPa)	Ultimate Strength (MPa)	Grade
no. 2	6.35	367.6	449.6	50
no. 4	12.7	420.7	662.1	60
no. 5	15.9	413.8	662.1	60
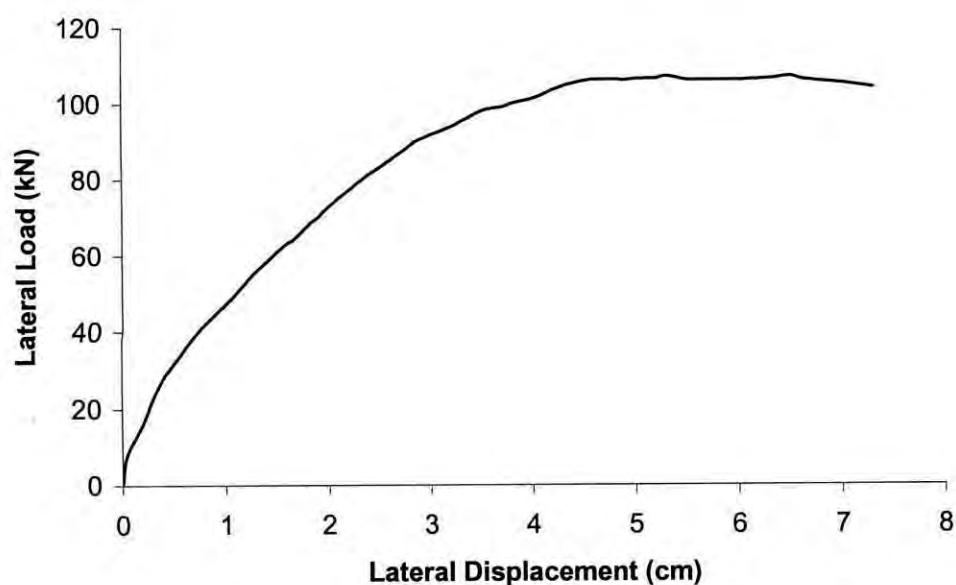
Fig. 5.2. Lateral load-lateral displacement curve for bare-frame (test specimen 1) by Mehrabi et al. (1996).

5.2.1 Finite Element Analysis of Bare Frame Model

To examine the capability of the adopted FE model and for simulating the behavior of the bare-frame test specimen 1, the model was subjected to increased lateral loading up to the ultimate load. The material models for the reinforced concrete frame have been calibrated with the results of the material tests reported in Table 5.1 and 5.2. However, some of these parameters have to be adjusted to obtain a better match with the experimental results as well as to overcome the convergence problems in the numerical solution.

5.2.2 Numerical Results

The adopted FE model has been analyzed using finite element package ANSYS. Fig. 5.3 illustrates the lateral load-lateral displacement curves obtained from the analysis along with the experimental response by Mehrabi et al. (1996). The initial stiffness of both numerical and experimental models is close, but gradually the difference tends to increase, then it varied widely with the increase in loading.
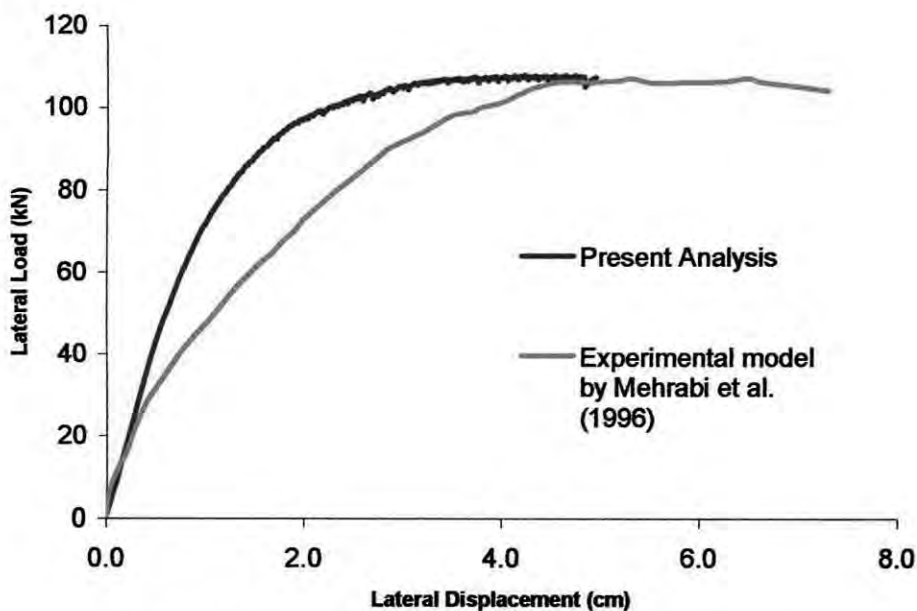
Fig. 5.3. Comparison of lateral load-lateral displacement curves of bare frame (specimen 1) between the adopted numerical model and experimental results by Mehrabi et al. (1996).

A smeared crack finite element model was used by Mehrabi and Shing (1997) to simulate the behavior of concrete in the RC frames. The concrete frames had been modeled with nine noded quadrilateral smeared crack elements and the longitudinal bars in the frame had been modeled with two noded elastic-hardening plastic bar elements. The analysis of the bare frame (specimen 1) had been conducted under monotonically increasing lateral loads. Fig. 5.4 shows the lateral load-displacement results of the bare-frame model by Mehrabi and Singh (1997) along with experimental results and present analysis.
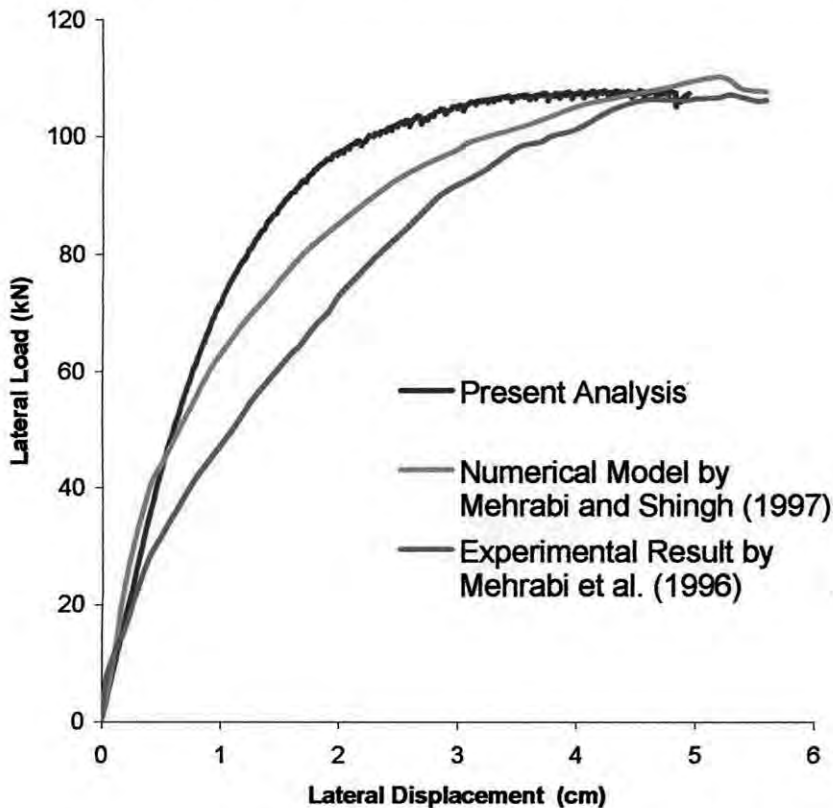
Fig. 5.4. Lateral load-lateral displacement curves for bare frame model by Mehrabi et al. (1996, 1997) along with the present analysis.

The above figure clearly shows that both the numerical models are fairly accurate in calculating the ultimate load capacity of the bare frame structure. The bar diagram in Fig. 5.5 shows the closeness of load carrying capacity of the frame predicted by these two adopted numerical models with the experimental one. The analysis reveals that the initial stiffness of the numerical model proposed by Mehrabi et al. (1997) is very close to the initial stiffness of the adopted FE model.
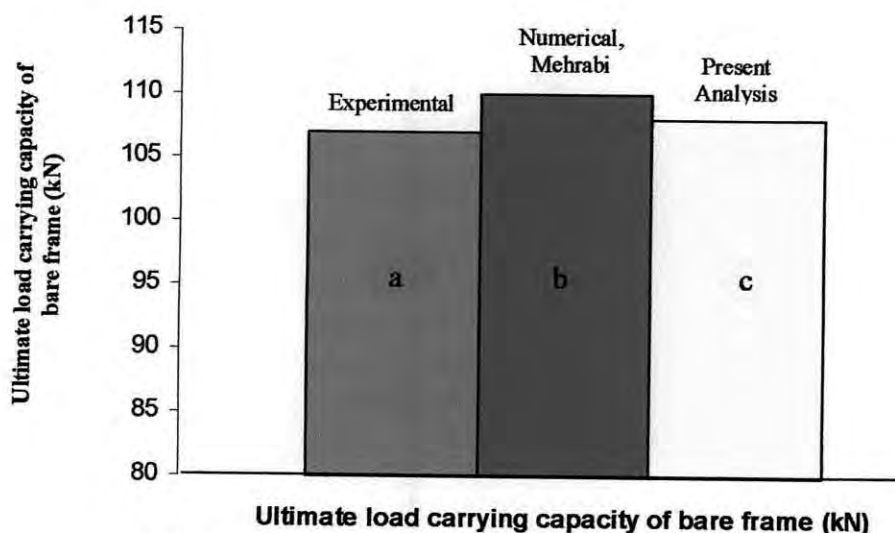
Fig. 5.5. Ultimate load carrying capacity of bare frame a) from the experiment by Mehrabi et al. (1996), b) numerical model by Mehrabi and Shing (1997), and c) the adopted numerical model by the present author.

The variation in stiffness at the intermediate loadings is mainly due to the lack of softening effect in the numerical model of concrete elements. The displacement pattern of the bare frame of the adopted FE model is shown in Fig. 5.6. The outer part of the frame is designated by ABCD and inner portion is designated as EFGH. When the frame is sub-
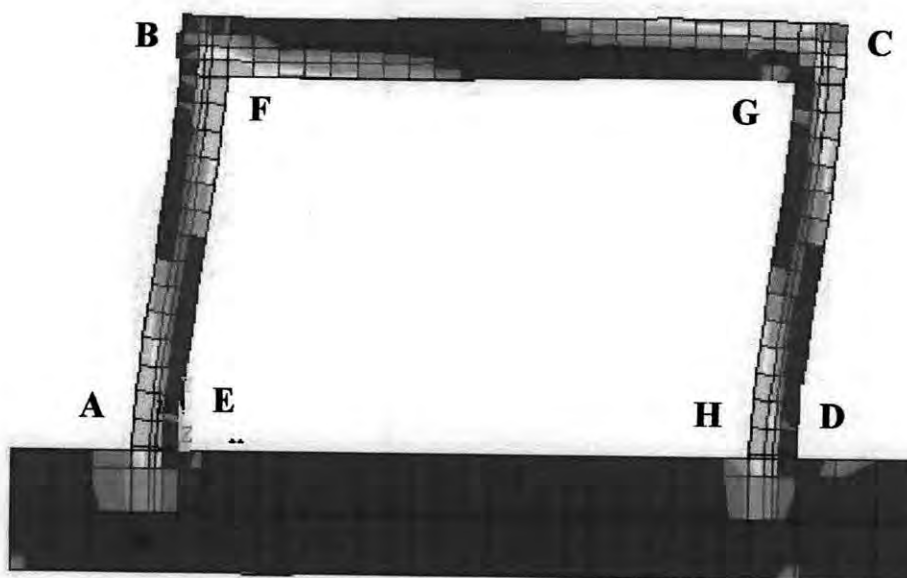
Fig. 5.6. Displacement pattern of the adopted bare-frame FE model

jected to lateral load, tension develops at the outer lower part of the frame on the side where the load is applied i.e. at point A and on the same side at the upper part inside the frame i.e. at point F. Tension also develops on the leeward side where tension develops at the outer upper part i.e. at point C and inner lower part i.e. point H as shown in Fig. 5.6. In the real structure as concrete is weak in tension compared to its compressive strength, tensile cracks develop in concrete when the stress exceeds the modulus of rupture. When cracks develop in the concrete, those parts become ineffective and do not contribute to the strength and stiffness of the frame. But incase of the adopted FE analysis methodology this phenomenon has not been incorporated in the model due to limitations of analysis program. That is why although the elements at the locations of A, F, C and D in Fig. 5.6 were under high tensile stress and beyond their tensile strength, they were not deactivated and even contributed sufficient strength and rigidity to the structure. And this is the reason for the relatively high stiffness of the bare frame at intermediate loading conditions.

5.3 VERIFICATION OF INFILLED FRAME MODEL

After verifying the RC bare-frame in the previous section, this section deals with the verification of infilled frame model with the experimental results. The behavior of masonry infilled frames has been extensively studied by various researchers. Among all of the research works this section will verify the results obtained from the adopted FE model with the experimental and as well as numerical models of Mehrabi et al. (1996 and 1997); and also the experimental results of Alam (2003).

Extensive experimental and analytical studies have been carried out by Mehrabi et al. (1996 and 1997) to investigate the performance of masonry infilled RC frames under in-plane lateral loadings. Several infilled frame specimens were tested in his research. The design details of different RC frame structures have already been discussed in section 5.2. Among the various specimens, specimen no. 8 has been selected to simulate its behavior with the adopted FE model. The geometry and design of RC frame for specimen no. 8 is a weak frame as shown in Fig. 5.1, infilled with weak infill panel composed of solid bricks. The material properties for the RC frame and masonry units are presented in

Table 5.3. Average tensile strengths of reinforcing steel are the same as presented in Table 5.2.

Table: 5.3. Average Strengths of Concrete Materials and Masonry units for infilled frame, specimen no. 8 by Mehrabi et al. (1996). (1Mpa = 0.145 ksi)

1. Frame Concrete	
Secant Modulus (MPa)	17240
Compressive Strength (MPa)	26.8
Strain at peak stress	0.0027
Modulus of Rupture (MPa)	4.86
Tensile Strength (split cylinder tests) (MPa)	2.77
2. Three Course Masonry Prisms	
Secant Modulus (MPa)	5100
Compressive Strength (MPa)	9.52
Strain at peak stress	0.0027
3. Compressive Strength of Masonry units (MPa)	16.48
4. Compressive Strength of Mortar Cylinders (MPa)	15.52
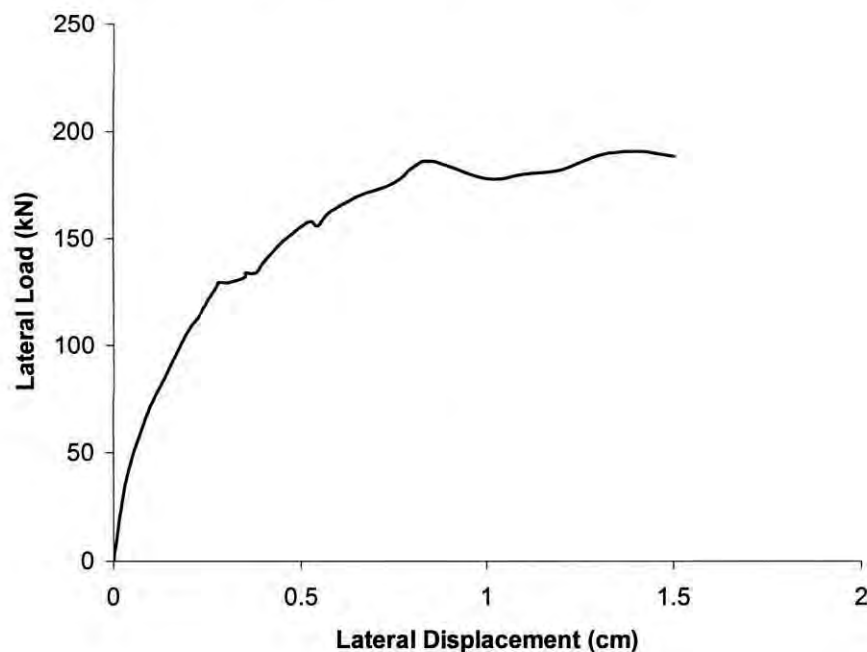
Fig. 5.7. Lateral load-lateral displacement curve for infilled-frame (test specimen 8) by Mehrabi et al. (1996)

5.3.1 Finite Element Analysis of Infilled Frame Model

In regard to the highly brittle, heterogeneous, and inelastic response of masonry, along with the complexities of crack initiation and trajectory, stress concentrations, and the interactive effects between concrete and its reinforcement, it is a difficult task to simulate the exact behavior of masonry infilled RC frames. Using a nonlinear finite element approach for this type of problem is not without its limitations. Despite the afore mentioned restrictions, FE software package ANSYS is used to estimate the ultimate load carrying capacity as well as the load-deformation behavior to test the validity of use for peak load prediction. To examine the capability of the adopted FE model and for simulating the behavior of the infilled-frame test specimen 8 by Mehrabi et al. (1996), the model was subjected to increased lateral loading up to its peak load. The material models for the masonry and reinforced concrete frame have been calibrated with the results of the material tests reported in Table 5.3. However, some of these parameters have to be adjusted to obtain a better match with the experimental results as well as to overcome the convergence problems in the numerical solution.

5.3.2 Numerical Results (Adopted FE Model vs. Mehrabi's (1996, 1997) Model)

After analyzing the numerical model of infilled-frame using FE package, Fig. 5.8 divulges that finite element analysis predicted the peak load quite accurately, which is
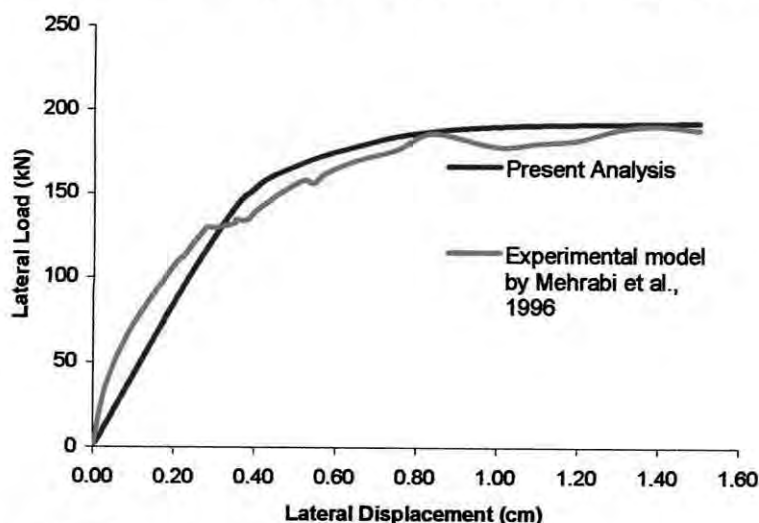
Fig. 5.8. Comparison of lateral load-lateral displacement curves of infilled-frame (test specimen 8) between the adopted numerical model and the experimental results by Mehrabi et al. (1996).

within one percent. Fig. 5.8 illustrates the lateral load-lateral displacement curves of infilled-frame obtained from FE analysis along with the experimental response (Fig.5.7) by Mehrabi et al. (1996). The initial stiffness of the infilled-frame got from the experimental results is relatively high compared to that of the adopted FE model. But gradually the stiffness of both the experimental and numerical models get closer as the load increases.

Mehrabi and Shing (1996) used a smeared crack finite element formulation developed by Lofti and Shing (1991) to model concrete in the RC frames and masonry units in the infill panels. In this formulation a J_2-plasticity model with an isotropic strain-hardening /softening law was utilized to model an uncracked material. The plasticity model is combined with the Rankine tension-cutoff criterion to signal the onset of cracking. After cracks have occurred, the material behavior is modeled by a nonlinear orthotropic model with a coaxial rotating crack formulation. A constitutive model was used to model the behavior of mortar joints between masonry units as well as the joints at the infill-frame interfaces, which considered compressive hardening behavior of interfaces, reversal of shear dilatancy in case of cyclic loading, and the normal contraction of an interface under shear sliding. The lateral load-lateral displacement curve obtained from this constitutive model of Mehrabi et al. (1997) is presented along with the adopted FE model in Fig. 5.9.
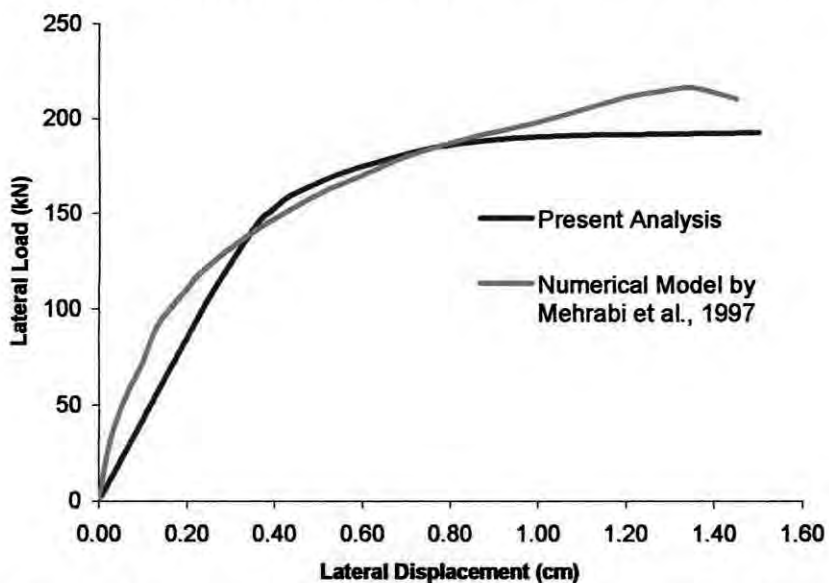
Fig.5.9. Lateral load-lateral displacement curves for infilled-frame numerical model by Mehrabi et al., 1997 and the present analysis

Both the numerical models are in good agreement in predicting the ultimate load carrying capacity of RC frame infilled with masonry panels. The bar diagram in Fig. 5.10 shows how closely the two numerical models can estimate beforehand the ultimate load of infilled-frames compared to that of the experimental results. Ultimate load prediction by the numerical model of Mehrabi et al. (1997) varied 13 percent where as by the adopted model it varied just below one percent.
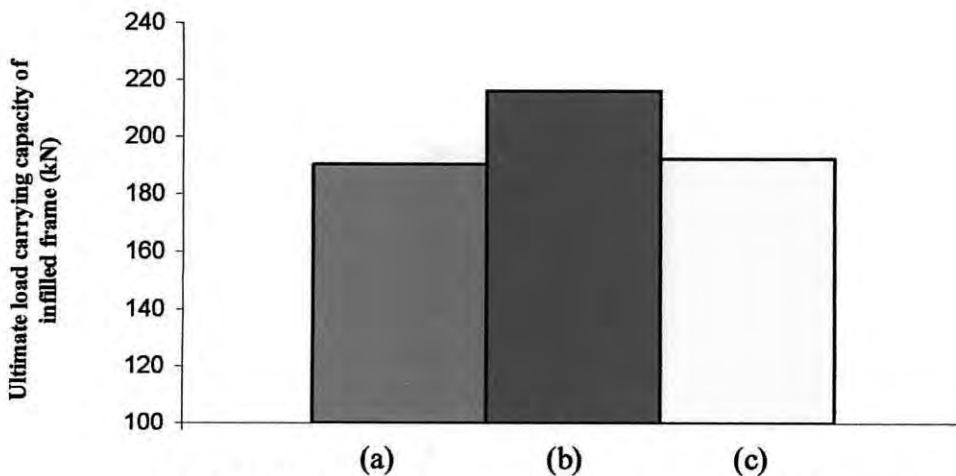
Fig. 5.10. Ultimate load carrying capacity of infilled frame got from the results of a) experiment by Mehrabi et al., 1996, b) numerical model by Mehrabi et al., 1997 and c) the present analysis.
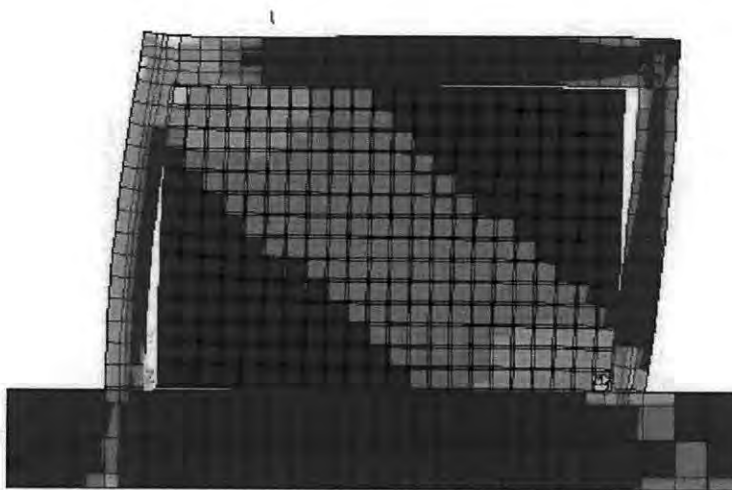
Fig. 5.11. Displacement pattern of the adopted FE model of masonry-infilled RC frame

For the case of infilled frames, three types of failure mechanisms were observed by Mehrabi et al. (1996). In the case of a strong infill and a weak frame, the ultimate resistance and failure were very much dominated by the diagonal and horizontal cracks in the infill and the shear failure of the windward column. In the case of a strong infill and a strong frame, the ultimate resistance was governed by corner crushing in the infill. But as for the case of a weak frame with a weak panel (test specimen 8), the lateral resistance is mainly governed by the sliding of the bed joints often occurring over the entire panel. This has also been proved by the displacement pattern of the infilled-frame by the adopted FE model as shown in Fig. 5.11. The figure clearly demonstrates the diagonal strut action of an infilled-frame structure by observing the high stressed elements along the diagonal of the masonry infill panel.

5.3.3 Numerical Results of Adopted FE Model vs. Alam's (2003) Expt. Results

As discussed earlier, an experimental study was performed by Alam (2003) to investigate the in-plane strength of masonry infilled RC frame. A FE model was developed for the masonry infilled RC frame where the geometry and design of the frame was according to the detailing shown in Fig. 2.4 and 2.5. The material properties for the RC frame and
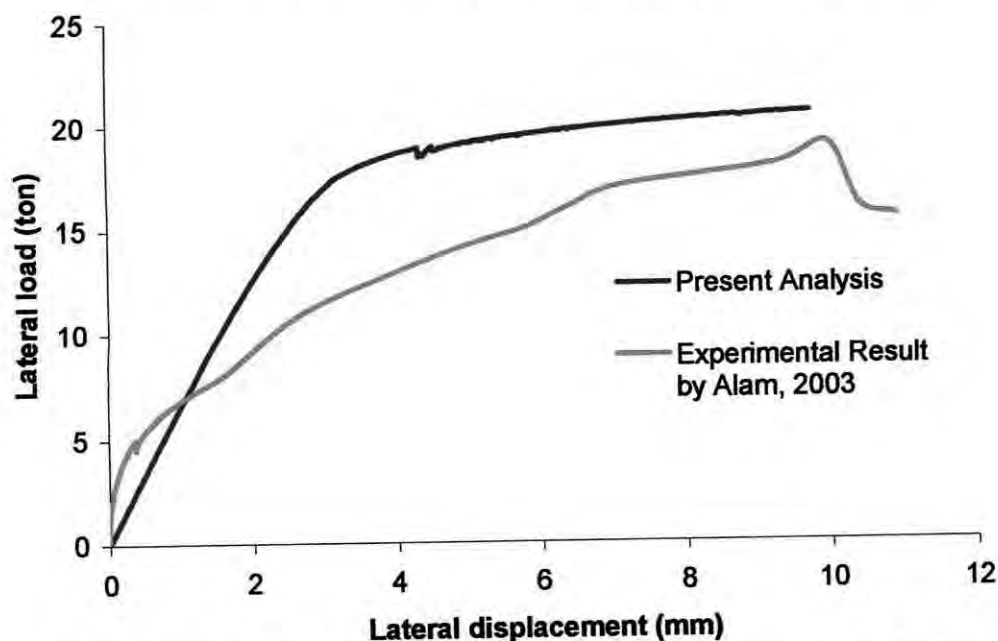
Fig. 5.12. Comparison of lateral load-lateral displacement curves of infilled-frame between the adopted numerical model and the experimental results by Alam, 2003

masonry units are presented in Table 2.1 and 2.3. Average tensile strength of reinforcing steel is the same as presented in Table 2.2. Fig. 5.12 illustrates the lateral load-lateral displacement curves of infilled-frame obtained from FE analysis along with the experimental response by Alam (2003).

In this case although the FE model overestimates the peak load by only 8%, still then the acceptability of the FE model in predicting ultimate load carrying capacity of the infilled frame is quite obvious in the sense that it is in good agreement with the experimental results of both by Mehrabi et al. (1996) as well as by Alam (2003). The bar diagram in Fig. 5.13 shows how closely the FE model approximates the ultimate load carrying capacity of the infilled frame.
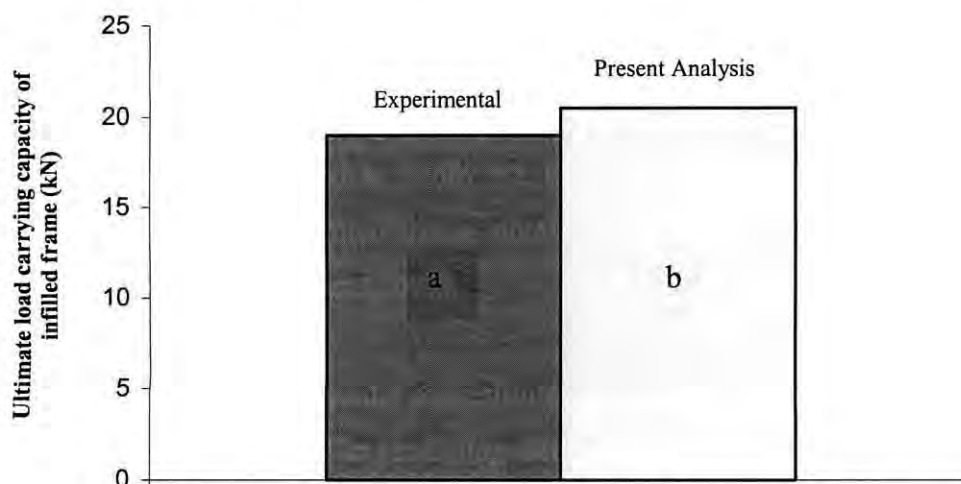
Fig. 5.13. Ultimate load carrying capacity of infilled frame obtained from the results of a) experiment by Alam, 2003 and b) the adopted numerical model by the present author.

5.3.4 BARE FRAME VS. INFILLED FRAME

If masonry infill panel is incorporated with bare frame, it greatly increases the in-plane lateral load resisting capacity. Fig. 5.14 shows the experimental lateral load deflection response of the bare frame and also the infilled frame along with the present FE analysis. The ultimate lateral load resisting capacity of the bare frame was experimentally found as 107 kN (Mehrabi et al., 1996). With the same material properties and the same design of the bare frame, when it was infilled with masonry panel, its ultimate load resisting

capacity of the bare frame was found to be 190.5 kN (Mehrabi et al., 1996), which is almost double than that of bare frame
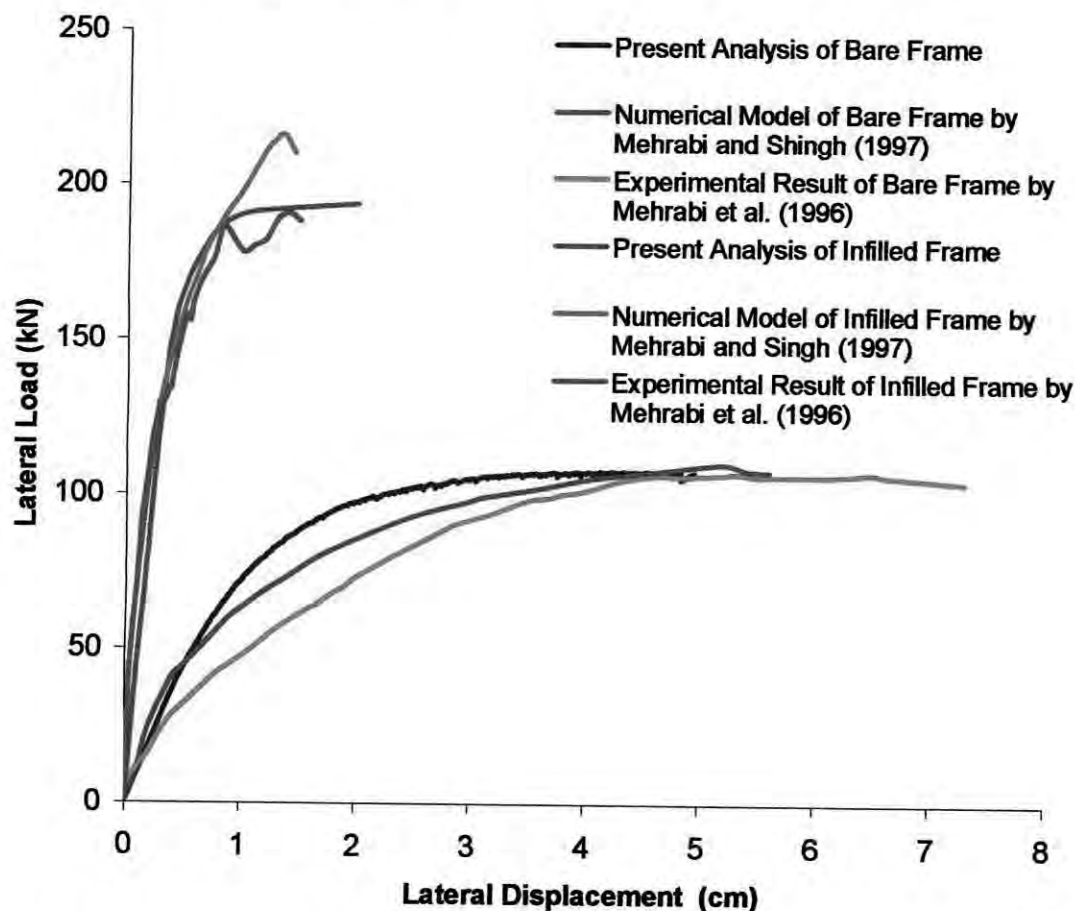
Fig. 5.14. Comparison of lateral load- displacement curves of bare frame versus infilled frame as obtained from experiments and present analysis.

5.4 VERIFICATION OF THE RETROFITTED MODEL

After analyzing the masonry infilled RC frame, the distressed frame was repaired with ferrocement overlay. Then the retrofitted infilled RC frame was again subjected under monotonically increased loading. The properties of mortar used for ferrocement is shown in Table 2.4. The behavior of the retrofitted frame is discussed in the earlier chapter. The same FE model is used to simulate the behavior of retrofitted infilled frame with simple modifications. Only ferrocement is incorporated with the existing model under distressed condition. Then the model was again analyzed under monotonically increased loading.

Fig. 5.15 illustrates the lateral load-lateral displacement curves of infilled-frame obtained after loading and unloading (without ferrocement overlay) and reloading of the retrofitted infilled frame with ferrocement overlay obtained from FE analysis along with the experimental response by Alam (2003).
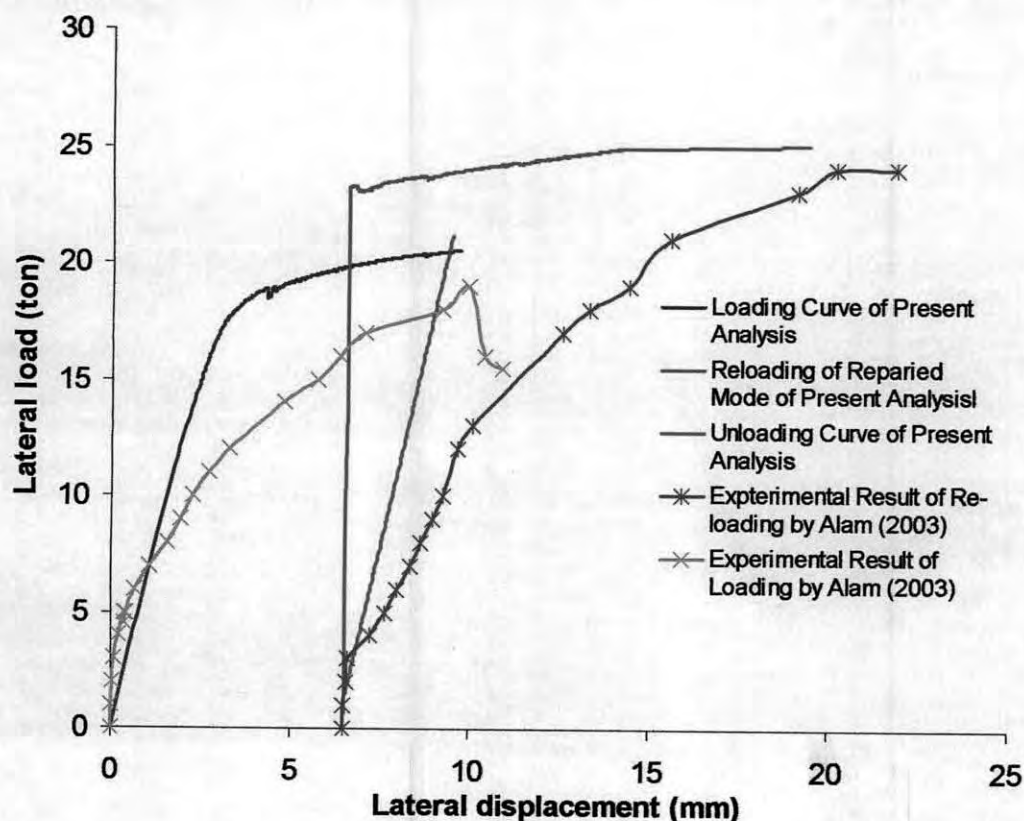
Fig. 5.15. Comparison of Lateral load-displacement curves of the results obtained from present analysis and experiment by Alam (2003).

The above figure clearly shows the capability of the adopted FE model in predicting the ultimate load carrying capacity of the retrofitted masonry infilled RC frame as well. Another observation of the retrofitted numerical model is that the peak load was achieved almost at the same lateral displacement as that of the real frame. Fig. 5.16 depicts the closeness of the numerical model in estimating beforehand the peak load of the retrofitted infilled-frames with ferrocement overlay with that of the experimental results. Ultimate load prediction by the adopted finite element model varied below 4 percent, which seems to be fairly accurate.
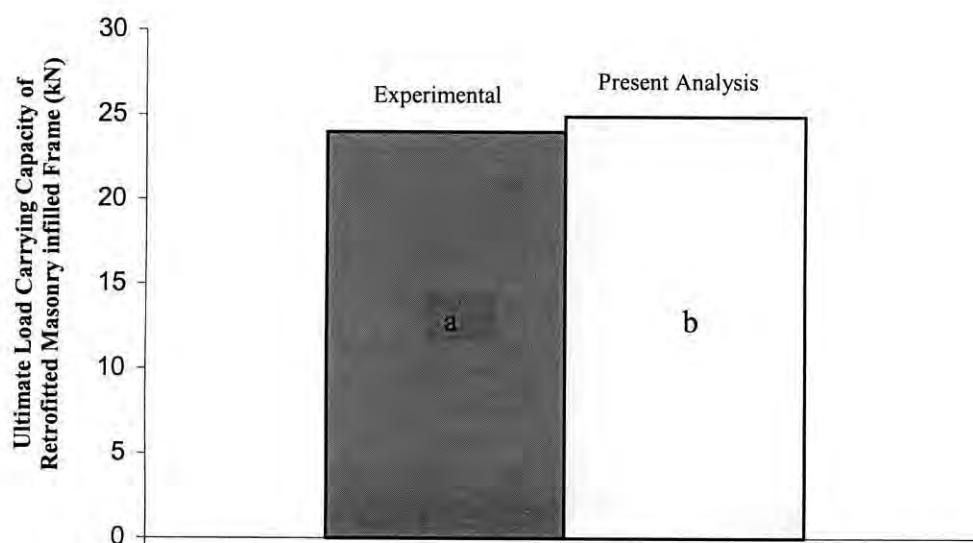
Fig. 5.16. Ultimate load carrying capacity of retrofitted masonry infilled frame obtained from the results of a) experiment by Alam (2003) and b) the present analysis.

The FE model of the infilled frame was assembled with the ferrocement overlays altogether. While the load is applied in the infilled frame, the ferrocement elements were deactivated/killed. Killed elements do not contribute to the stiffness of the frame as their components are multiplied by numbers close to zero value. When the load is reached at the peak then the FE model was unloaded. After unloading the frame did not get back to its original position as it had already reached beyond its elastic limit during loading. And in the plastic state the frame had some residual strain, which has been shown in Fig. 5.15.

After unloading the infilled frame, the ferrocement elements were activated/made alive to simulate the effect of retrofitting with ferrocement overlays. Then the repaired frame was loaded again in the form of displacement. But as soon as the displacement was applied the load without showing gradual increment, just jumped up to a certain value, which has been shown in Fig. 5.16. The main reason behind this is the presence of ferrocement elements prior to loading. Although they had no contribution to the stiffness or rigidity to the structure, but as they were present with the masonry infill panels, they were subjected to the applied strain during loading and unloading. Therefore after unloading when ferrocement elements were activated, certain amount of strain that was present in the

ferrocement was applied instantaneously. And this caused the sudden jump and marked increase in the load during reloading.

5.5 REMARKS

The adopted FE analysis methodology predicts the lateral stiffness up to failure, and the ultimate load carrying capacity of the bare frame, masonry infilled RC frame and the retrofitted masonry infilled RC frame to an acceptable degree of accuracy. The technique accounts for the nonlinear behavior that occurs in both the reinforced concrete frame and in the masonry wall. It is observed that incorporation of infill panel in the RC frame increases the stiffness, strength and load carrying capacity and reduces the lateral drift of the frames. It is also noted that retrofitted techniques with ferrocement overlays considerably enhances the strength and stiffness of the infilled frames even more than the original infilled frame.

Chapter 6

CONCLUSIONS AND RECOMMENDATIONS

6.1 CONCLUSIONS

Masonry infill walls in frame structures have long been known to affect strength, stiffness and post-peak behavior of the infilled frame structures. Seismic areas, ignoring the composite action of infill panel and frame is not always on the safe side, since the interaction between the wall and the frame under lateral loads dramatically changes the overall characteristics of the composite structure and hence its response to seismic loads creates a major source of hazard during seismic events.

The study conducted herein focuses on the investigation of the retrofitting effect of masonry- infilled reinforced concrete frames subjected to in-plane lateral loads using ferrocement overlays bonded to the exterior faces of the infill walls. Chapter 2 summarizes the experimental and theoretical research work conducted in the area of infilled frames. It is now widely recognized that masonry infill walls used for cladding and/or partition in buildings, significantly alter their performance, and their effect in changing the stiffness, the ultimate lateral load carrying capacity as well as the ductility of the building system should be accounted for in analysis and design.

Chapter 3 discusses the computational model available on masonry infilled frame. Chapter 4 describes the development of the finite element (FE) model of the bare frame and the masonry infilled frame with and without ferrocement coating. Assumptions and expressions used for the development of numerical model are also presented here. Chapter 5 presents the results obtained from the analysis of the FE models showing the load-deflection relationship of the RC frame with infill panels, original and the retrofitted one following step-by-step logical approximations based on and supported by experimental observations.

The following conclusions may be drawn from the current investigation.

1. It is possible to develop a comprehensive FE model to analyze an infilled frame considering each individual component like concrete, steel, mortar, brick, infill-frame interface in a discrete manner.

2. The macro-models developed in this study contain all the variables possible considering various dimensions and material properties, which can be used effectively in investigating various effects of different parameters.

3. The developed model can successfully simulate the experimental results and can predict the failure load with reasonable accuracy.

4. The numerical model can be used to estimate the load carrying capacity of the existing structures.

5. The numerical model can also be used to estimate the amount of strengthening that can be achieved by ferrocement overlaying of an existing structure.

6.2 RECOMMENDATIONS

The numerical modeling of the effect of retrofitting infilled frames using ferrocement laminates is far from complete. The main constraint was lack of sufficient experimental data of repaired infill panels with ferrocement overlay confined within RC frames. It is believed, however, that this research provides a milestone in the effort to utilize ferrocement for structural strengthening of the masonry infill walls. The following recommendations for future work are suggested:

1. Further improvement of the numerical model can be brought by refining the load-displacement curve in the inelastic region by varying the modulus of elasticity of concrete or by deactivating the high stressed tensile elements gradually.

2. Further experimental investigations are required to study the effect of ferrocement overlay upon infill panels and then verify the proposed model with the corresponding experimental results.

3. Investigate the retrofitting of multi-story and/or multi-bay infilled frames using ferrocement laminates.

4. The proposed numerical model uses finite element method in which the RC frame and the infill panel have been discretized as a series of plane stress elements. Analyzing such models require huge time. Therefore, it is important to form an alternative technique, which will be applicable even in multi-bay frame structure in shorter time.

5. A diagonal strut approach may be adequate to model the retrofitted system. The retrofitting effect will be accounted for incorporating design parameters to account for the stiffness, strength and ductility increase.

6. Provide design guidelines of the ferrocement-masonry composite walls in order to optimize the selection of the composite materials to retrofit URM infilled frames. This possibly entails further assemblage testing in order to study the effect of various laminates accompanied with a microscopic level of FE modeling to investigate the different failure mechanisms for symmetrical and unsymmetrical retrofit where the laminates are placed on one side only, etc.

7. Effect of dynamic loading on the behavior of retrofitted masonry-infilled RC frames may be investigated.

REFERENCES

ACI Committee 549. "Guide for Design, Construction, and Repair of Ferrocement (ACI 549. 1R-93)", American Concrete Institute, Farmington Hills, Mich., 1993, 30 pp.

Ahmed, T. et al. "Experimental Study of Ferrocement as a Retrofit Material for Masonry Columns." Fifth Int. Symposium on Ferrocement, Manchester, 1994, pp. 269-276.

Alam, M. M. M. "Experimental Evaluation of the Lateral Strength of Masonry Infilled Reinforced Concrete Frame Retrofitted with Ferrocement." M.Engg. thesis, 2003, Dept. of Civil Engg., Bangladesh Uni. of Engg. and Tech., Dhaka.

Al-Chaar, G., Issa, M., and Sweeney, S. "Behavior of Masonry-Infilled Nonductile Reinforced Concrete Frames". J. Struct. Engg., Vol. 128, No.8, 2002, pp. 1055-1063.

Alcocer, S. M. et al. "Retrofitting of Confined Masonry Walls with Welded Wire Mesh." Proceedings of the Eleventh World Conference on Earthquake Engineering, 1996, Acapulco, Mexico.

Amos, K. A. "The Shear Strength of Masonry Infilled **Steel** Frames." M.Sc. thesis, 1986. Dept. of Civil Engineering, University of New Brunswick, Fredericton.

Andrews, G. and Sharma, A. K. "Repaired Reinforced Concrete Beams." Concrete International, Vol. 10, No. 4, 1988, pp. 47-51.

ANSYS®5.6. 1996, ANSYS® Inc. 201 Johnson Road, Houston, PA, 15342-1300.

Anwar, A.W., Nimityongskul, P., Pama, R. P. and Robles-Austriaco, L. "Method of Rehabilitation of Structural Beam Elements Using Ferrocement", Journal of Ferrocement, Vol. 21, No.3, 1991, pp.229-234.

Barau, H. K., and Mallick, S. K. "Behavior of Mortar Infilled Steel Frames Under Lateral Load" Building and Environment, Pergamon Press, UK. Vol 12, 1977, pp. 263-272.

Bertero, V. V., and Brokken, S. "Infills in Seismic Resistant Building". J. Struct. Engg., ASCE, Vol. 109, No. 6, 1983, 1337-1361.

Chen W. F. "Plasticity in Reinforced Concrete" McGraw-Hill, 1982, New York, NY,

Colombo, A., Negro, P. and Verzeletti, G. "Improving Ductility and Energy Dissipation Capacity by Means of Polymeric Nets", Proceedings of the 12th World Conference on Earthquake Engineering, 2000, #1910 on CD-ROM, New Zealand.

Comite Euro-International Du Beton. "RC Frames Under Earthquake Loading" State of the art report, 1996. Tomas Telford Services Ltd, 1 Heron Quay, London E14 4JD.

Dawe, J. L., and Charalambous, P. D. "Finite Element Analysis for Wall-Frame Interaction" Proceedings, Eight International Loadbearing Brickwork Symposium, 1983. British Ceramic Society, Stoke-on-Trent. UK.

Dawe, J. L., and Seah, C. K. "Behavior of Masonry Infilled Steel Frames" Canadian Journal of Civil Engineering, Vol. 16, No. 6, 1989, pp. 865-876.

Decanini, L.D., Gavarini, C. and Mollaioli, F. "Strengthening of Frame Buildings with infill Masonry" Proceedings of the Italian-French symposium on strengthening and repair of structures in seismic area, 1994, Nice, France.

Dey, P.K. "Sway characteristics of RC frame under lateral load in presence of brick masonry". B.Sc. thesis, 2000, Dept. of Civil Engg., BUET.

Dhanasekar, M., and Page, A.W. "The Influence of Brick Masonry Infill Properties on the Behavior of Infilled Frames" Proc., Int. Conf. of Civil Engrs., U.K., Part 2, 81(Dec.), 1986, pp. 593-605.

Durrani, A.J. and Luo, Y.H. "Seismic Retrofit of Flat Slab Buildings with Masonry Infills", Proceedings of the 10th World Conference on Earthquake Engineering, 1992.

Dymiotis, C., Kappos, A. J., and Chryssanthopoulos, M. K. "Seismic Reliability of Masonry-Infilled RC frames". Journal of Structural Engineering, Vol. 127, No. 3, 2001, pp. 296-305.

Ehsani, M. R., Saadatmanesh, H., and Velazquez-Dimas, J. L. "Behavior of retrofitted URM Walls under Simulated Earthquake Loading" Journal of Composites for Construction, ASCE, Vol. 3, No. 3, 1999, pp. 134–142.

Ehsani, M. R., Saadatmanesh, H. and Al-Saidy, A. "Shear Behavior of URM Retrofitted with FRP Overlays," Journal of Composites for Construction, ASCE, Vol. 1, No. 1, February, 1997, pp. 17-25.

Ehsani, M. R. and Saadatmanesh, H. "Seismic Retrofitting of URM Walls with Fiber Composites." Masonry Society Journal, 1996.

El-Dakhakhni, W. W. "Experimental and Analytical Seismic Evaluation of Concrete Masonry-Infilled Steel Frames Retrofitted using GFRP Laminates", Ph.D. thesis, 2002, Civil and Architectural Engineering Department, Drexel University, Philadelphia.

El-Dakhakhni, W. W., Elgaaly, M., and Hamid, A.A. "Finite Element Modeling of Concrete Masonry-Infilled Steel Frame," 9th Canadian Masonry Symposium, 2001, The University of New Brunswick, Canada.

Eldakhakhni, W. W. "Non-Linear Finite Element Modeling of Concrete Masonry-Infilled Steel Frame," M.Sc. thesis, 2000, Civil and Architectural Engineering Department, Drexel University, Philadelphia.

Fahmy, E. H., Shaheen, Y. B. I., and Korany, Y. S. "Repairing Reiforced Concrete Columns Using Ferrocement Laminates." Journal of Ferrocement, Vol. 29, No. 2, 1997, pp. 115-124.

Fahmy, E. H., Shaheen, Y. B. I., and Korany, Y. S. "Repairing Reiforced Concrete Beams by Ferrocement." Journal of Ferrocement, Vol. 27, No. 1, 1997, pp. 19-32.

Fiorato, A. E., Sozen, M. A., and Gamble, W.L. "An Investigation of the Interaction of Reinforced Concrete Frames with Masonry Filler Walls", Civil Eng. Studies, Structural Research Series Report No. 370, 1970, Univ. of Illinois, Urbana, III.

Flanagan, R. D., Bennett, R. M., and Barclay, G. A. "In-plane Behavior of Structural Clay Tile Infilled Frames", Journal of Structural Engineering, ASCE, Vol. 125, No. 6, 1999, pp. 590-599.

Ghosh, A. K., Amde, A. M. "Finite Element Analysis of Infilled Frames", Journal of Structural Engineering, Vo. 128, No. 7, 2002, pp. 88-889.

Hakam, Z, H. R. "Retrofit of Hollow Concrete Masonry Infilled Steel Frames Using Glass Fiber Reinforced Plastic Laminates" Ph.D. thesis, 2000, Civil and Architectural Engineering Department, Drexel University, Philadelphia.

Hamid, A. A., Ziab, G., and El Nawawy, O. "Modulus of Elasticity of Concrete Masonry" Fourth North American Masonry Conference, 1987. University of California at Los Angeles, Paper 7.

Haque, M.E. "Effect of randomly distributed infills on the vibration characteristics of reinforced concrete frames". M.Sc. thesis, 2002, Dept. of Civil Engineering, BUET.

Haroun, M. A., Ghoneam, E. H. and Salama, A. E. "Seismic Strengthening of Masonry-Infilled Frames by Fiber Composites" 1st Middle East workshop on structural composites, 1996, Sharm El-Shiekh, Egypt.

Holmes, M. "Steel Frames with Brickwork and Concrete Infilling" Proceedings of the Institution of Civil Engineers, Vol. 19, 1961, pp. 473-478.

Holmes, M. "Combined Loading on Infilled Frames" Proceedings of the Institution of Civil Engineers, Vol. 25, 1963, pp. 31-38.

Humayun, I. A., and Robbles-Austriaco, L. "State of the Art on Rehabilitation and Re-strengthening of Structures using Ferrocement". Journal of Ferrocement, Vol. 21, No. 3, 1991, pp. 243-258.

Iorns, M.E. "Laminitated ferrocement for better repairs". Concrete International 9(9), 1987, pp. 875-889.

Irimies, M., and Crainic, L. "Behavior of Repair/Strengthened Unreinforced Masonry Shear Walls." Proceedings of the Sixth North American Masonry Conference, 1993, Drexel University, pp. 555-563.

Islam, M. S., Kim, H. I. and Maniar, F. "Seismic Retrofit of Two Historic Steel Buildings with Unreinforced masonry Infill Walls" Proceedings of the 5th national conference on earthquake engineering, 1994, Oakland, CA, USA.

Jabarov, M. et al. "Strengthening of Damaged Masonry by Reinforced Mortar Layers." Proceedings of the Seventh World Conference on Earthquake Engineering, 1985, 15(3), pp. 73-80.

Kadir, M. R. A., Samad, A. A. A., Muda, Z. C. and Ali, A. A. A. "Flexural Behaviour of Composite Beam with Ferrocement Permanent Formwork", Journal of Ferrocemtnt, Vil. 27, No.3, July 1997, pp. 209-213.

Kadir, M. R. A. "The Structural Behavior of Masonry Infilled Panels in Framed Structures" Ph.D. thesis, 1974, Department of Civil Engineering, University of Edinburgh.

Kahn, L. F. "Shotcrete Retrofit for Unreinforced Brick Masonry." Proceedings of the Eighth World Conference on Earthquake Engineering, 1984, San Francisco, pp. 583-590.

Kahn, L.F., and Hanson, R.D. "Infilled walls for earthquake strengthening." Journal of Structural Engineering, ASCE, Vol. 105, No. 2, 1979, pp. 283-296.

Kappos, A. J., Stylianidis, K.C., and Michailidis, C.N. "Analytical Models of Brick Masonry Infilled R/C Frames under Lateral Loading", Journal of Earthquake Engineering, Vol. 2, No. 1, 1998b, pp. 59-87.

Kappos, A. J., Penelis, G. G., and Drakopoulos, C. G. " Evaluation of Simplified Models for Lateral Load Analysis of Unreinforced Masonry Buildings", Journal of Structural Engineering, Vol. 128, No. 7, 2002, pp. 890-897.

Kaushik, S. K. and Dubey, A. K. "Performance Evaluation of RC Ferrocement Composite Beams." Proceeding of Fifth International Symposium on Ferrocement, UMIST, Manchester, September 1994, pp. 241-255.

Klingner, R. E., and Bertero, V. V. "Earthquake Resistance of Infilled Frames." Journal of Structural Engineering, ASCE, Vol. 104, No. 6, 1978

Kolsch, H. "Carbon Fiber Cement Matrix (CFCM) Overlay System for Masonry Strengthening." Journal of Composites for Construction, ASCE, Vol. 2, No. 2, 1998, pp. 105-109.

Laursen P. T., Seible F., Hegemier G. A., and Innamorato D. "Seismic Retrofit and Repair of Masonry Walls with Carbon Overlays" Non-Metallic (FRP) Reinforcement for Concrete Structures, edited by L. Taerwe, RILEM, 1995, pp. 616-627.

Liauw, T. C. and Kwan, K. H. Unified plastic analysis for infilled frames. J. Struct. Engg., ASCE, Vol. 120, No.9, 1985, pp. 1861-1876.

Liauw, T. C., and Kwan, K. H. "Plastic Theory of Non-Integral Infilled Frames." Proceedings of the Institution of Civil Engineers, Part 2, Vol. 75, 1983, pp. 379-396.

Liauw, T. C., and Lo, C.Q. "Multi-bay Infilled Frames without Shear Connectors." ACI Structural Journal, July-August 1988, pp. 423-428.

Lub, K. B., and Van Wanroij, M. C. G. "Strengthening of Reinforced Concrete Beams with Shotecret Ferrocement." Proceedings of Third International Conference on Ferrocement, Roorkee, University of Roorkee, 1988, pp. 477-485.

Madan, A., Reinhorn, A. M., Mander, J. B., and Valles, R.E. "Modeling of Masonry Infill Panels for Structural Analysis." ASCE Journal of Structural Division, Vol. 123, No. ST10, pp. 1295-1302.

Mainstone, R. J. "On the Stiffness and Strengths of Infilled Frames." Proceedings of the Institution of Civil Engineers, Supplement IV, 1971, pp 57-90.

Mainstone, R.J., and Weeks, G.A. "The Influence of Bounding Frame on the Racking Stiffness and Strength of Brick Walls." Proceedings of the 2nd Int. Brick Masonry Conf., 1970, Stoke-on-Trent, England, pp. 165-171.

Mallick, D. V., and Severn, R. T. "The Behavior of Infilled Frames under Static Loading." Proceedings of the Institution of Civil Engineers, 1967, Vol. 38, pp. 639-656.

Mander, J.B., and Nair, B. "Seismic Resistance of Brick-Infilled Steel Frames with and without Retrofit." TMS journal February 1994, pp. 24-37.

Manos, C. J., Thaumpta, J., and Bilal, Y. "Influence of Masonry Infills on the Earthquake Response of Multi-Story RC Structures" Proceedings of the 12th World Conference on Earthquake Engineering, 2000, #112 on CD-ROM, New Zealand.

McBride, R. T. "The Behavior of Masonry Infilled Steel Frames Subjected to Racking", M.Sc. thesis, 1984, Dept. of Civil Engineering, University of New Brunswick, Fredericton, NB, Canada.

Mehrabi, A. B., Shing, P. B. " Finite Element Modeling of Masonry-Infilled RC Frames." ASCE Journal of Structural Division, 1997, Vol.123, No. ST05, pp. 604-613.

Mehrabi, A. B., Shing, P. B., Schuller, M., and Noland, J. "Experimental Evaluation of Masonry-Infilled RC Frames." Journal of Structural Engineering, ASCE, Vol. 122, No. 3, 1996, pp. 228-237.

Mehrabi, A. B., Shing, P. B., Schuller, M., and Noland, J. "Performance of Masonry-Infilled RC Frames under In-plane Lateral Loads." Report CU/SR-94-6, 1994, Dept. of Civ., Envir., and Arch. Engg., Univ. of Colorado, Boulder, Colo.

Mosalam, K.M., Ayala, G., White, R.N., and Roth, C. "Seismic Reliability of LRC Frames with and without Masonry Infill Walls." Journal of Earthquake Engineering, Vol. 1, No. 4, 1997, pp. 693-720.

Murty, C.R.V. and Jain, S.K. "Beneficial Influence of Masonry Infill Walls on Seismic Performance of Reinforced Concrete Frame Buildings", Proceedings of the 12th World Conference on Earthquake Engineering, 2000, #1790 on CD-ROM, New Zealand.

Nedwell, P. J. et al. "Investigation into the repair of Short Square Columns using Ferrocement." Fifth Int. Symposium on Ferrocement, 1994, Manchester, pp. 277-285.

Oliveira, F. L. "Rehabilitation of Masonry Walls by Application of Ferrocement Coatings." Ph.D. thesis, 2001, University of Sao Paulo. Sao Carlos, SP. Portuguese.

Paulay, T. and Priestley, M. J. N. "Seismic Design of Reinforced Concrete and Masonry Buildings." John Wiley & Sons, Inc., 1992, New York, NY, USA.

Pincheira, J. A. "Rehabilitation of Reinforced Concrete Structures - The Intregation of Experimental Results and Analytical Models." ACI Special Publication, Vol.162, August 1996.

Pincheira, J.A. and Jirsa, J. O. "Seismic Response of RC Frames Retrofitted with Steel Braces or Walls". ASCE Structural Journal, Vol.121, No.8, August 1995.

Pook, L. L., and Dawe, J. L. "Effects on Interface Conditions Between a Masonry Shear Panel and Surrounding Steel Frame." Proc., 4th Canadian Masonry Symposium, 1986, Univ. of New Brunswick Press, Frederiction, N.B., Canada, pp. 910-921.

Rahman, A.K.M. Habibur. "Strengthening of distressed RC slabs by using ferrocement overlay", M.Engg. thesis, Department of Civil Engineering, BUET, Dhaka, August, 2002, pp.7-21.

Reinhorn, A. M., Prawel, S. P. and Jia, Z. H. "Experimental Study on External Ferrocement Coating for Masonry Walls." Journal of Ferrocement, Vol. 15, No. 3, 1985.

Reinhorn, A. M., and Prawel, S. P. "Ferrocement for Seismic Retrofit of Structures." Second Int. Symposium on Ferrocement, 1985, Roorkee, pp. 157-172.

"Report on Seismic Risk of Five Selected Cities of Bangladesh", Department of Civil Engineering and Bureau of Research, Testing and Consultation of Bangladesh University of Engineering and Technology in association with CARE-Bangladesh. September 2002.

Richardson, J. "The Behavior of Masonry Infilled Steel Frames." M.Sc. thesis, 1986, Dept. of Civil Engineering, University of New Brunswick, Fredericton, NB, Canada.

Riddington, J. R. "The Influence of Initial Gaps on Infilled Frame Behavior." Proceedings of the Institution of Civil Engineers, 1984, London, England.

Riddington, J. R., and Smith, B. S. "Analysis of Infilled Frames Subjected to Racking with Design Recommendations." The Structural Engineer, Vol. 55, No. 6, 1977, pp. 263-268.

Romualdi, J. P. "Ferrocement for Infrastructure Rehabilitation." Concrete International, 9(9), 1987, pp. 34-38.

Sachanski, S. "Analysis of the Earthquake Resistance of Frame Buildings Taking into Consideration the Carrying Capacity of the Filling Masonry" Proceedings of the Second World Conference on Earthquake Engineering, Vol. 3, Tokyo, 1960, pp. 2127-2141.

Saneinejad A., and Hobbs, B. "Inelastic Design of Infilled Frames." Journal of Structural Division, ASCE, Vol. 121, No. ST4, 1995, pp. 634-650.

Sharma, S. P.; Sharma, P.C: Singh, K.P.; and Bhatia, S.S. "Ferrocement treatment for repairing a 50,000 gallon overhead water tank." Journal of Ferrocement, Vol. 14, No. 3, 1984, pp. 241-248.

Seah, C. K. "A Universal Approach for the Analysis and Design of Masonry Infilled Frame Structures." Ph.D. thesis, 1998. The University of New Brunswick, Canada.

Singh, K. K. et al. "Strengthening of Brick Masonry Columns by Ferrocement." Third Int. Symposium on Ferrocement, 1988, Roorkee, pp. 306-313.

Smith, B. S. "Lateral Stiffness of Infilled Frames." ASCE Journal of Structural Division, Vol. 88, No. ST6, 1962, pp. 183-199.

Smith, B. S. "Behavior of Square Infilled Frames." ASCE Journal of the Structural Division, Vol. 92, No. ST1, 1966, pp. 381-403.

Smith, B. S., and Carter, C. "A Method of Analysis for Infilled Frames." Proceedings of the Inst. of Civil Engineers, 1969, Vol. 44, pp. 31-48.

Waset, A. "Sway characteristics of brick infilled reinforced concrete building frame under lateral load." M.Engg. thesis, 2002, Dept. of Civil Engineering, BUET.

Taghdi M., Bruneau M., and Saatcioglu M. "Seismic Retrofitting of Low-Rise Masonry and Concrete Walls using Steel Strip." ASCE Journal of Structural Engineering, September 2000, pp. 1017-1025.

Takiguchi, K., and Abdullah. "Shear Strengthening of Reinforced Concrete Columns Using Ferrocement Jacket." ACI Structural Journal, Vol. 98, No. 5, pp. 696-704.

Takiguchi, K., and Abdullah. "Ferrocement as an Alternative Material to Enhance Seismic Performance of R/C Columns." Journal of Ferrocement, Vol. 30, No. 2, 2000, pp. 177-189.

Thomas, F. G. "The Strength of Brickwork." The Structural Engineer, Part 2, Vol. 36, 1953, pp. 35-41.

Trikha, D.N.; Sharma, P.C.; and Johnson, S. "Rehabilitation of Corrosion-Damaged Steel Tanks by Ferrocement Treatment at University of Roorkee." In proceeding of 3rd International Conference on Ferrocement, Roorkee, University of Roorkee, 1988, pp. 207-215.

Tso, W. K., Rutenberg, A. "Seismic Spectral Response of Coupled Shear Walls." ASCE Journal of the Structural Division, Vol. 103, No. ST1, pp. 181-196.

Weeks, J., Seible, F., Hegemier, G. and Priestly, M. J. N. "The U.S.-TCCMAR Full-scale Five-story Research Building Test, Part V- Repair and Retest" Report No. 9.4-5, Department of Applied Mechanics and Engineering Sciences, University of California, San Diego, January 1994.

Wood, R. H. "The Stability of Tall Buildings." Proceedings of the Institution of Civil Engineers, 1958, Vol. 11, pp. 69-102.

Yong, T. C. "Shear Strength of Masonry Panels in Steel Frames" M.Sc. thesis, 1984, Department of Civil Engineering, University of New Brunswick, Canada.

Zarnic, R. "Masonry-infilled Reinforced Concrete Frames as Subassemblies of Earthquake-Resistant Buildings." Earthquake Damage Evaluation and Vulnerability Analysis of Building Structures, A. Koridze, ed., 1990, OMEGA Scientific, Wallingford, Oxon, U.K., 79-100.

Zarnic, R. and Tomazevic, M. "Behavior of repaired masonry infilled RC frames." Rep. To U.S.-Yugoslav Joint Board of Scientific and Tech. Cooperation, Inst. For Testing and Res. In Mat. And Struct., 1990, Ljubljana, Yugoslavia.

APPENDIX A

```
! ----------------------------------------------------------------------------------------
! Author:
!                         M. Shahria Alam
!                         Lecturer
!                         Dept. of Civil Engineering
!                         BUET, Dhaka-10000.
!----------------------------------------------------------------------------------------
! As a part of the thesis work "Numerical Modeling of Masonry Infill Panels Retrofitted with Ferro-
! cement" for the partial fulfillment of M.Sc. in Civil Engineering (Structural).
!****************************************************************************************
```

! The model is generated from data, obtained from "Finite Element Modeling of Masonry-Infilled
! Frames" By Armin B. Mehrabi, P. Benson Shing, ASCE Structural Journal, MAY 1997, Vol. No.
! ST05, pp. 604-613.

! Here the lateral load displacement curve obtained by analyzing the macro model will be used for
! verification of numerical model against experimental results of Masonry-Infilled frame (Specimen 8)
```
!****************************************************************************************
```

```
/PREP7                  ! Post Processor 7
ANTYPE,STATIC                  ! Analysis type
```

```
!*****************PARAMETER******************
```

```
H=65/12                 ! ft ( colm height) f/f distance
B=92/12                 ! ft ( beam length) c/c distance
B_EXT=1.5               ! in ft Base Beam Extended upto B-EXT
B_BM_DX=6               ! in inches Base Beam Extended size/Division = 6"
WWZ=3.6                 ! in (wall thickness)

CTX=7                   ! in (colm thickness along span length)
CTZ=7                   ! in (colm thinckness _|_ to span length also _|_ to the computer screen)
BDY=9                   ! in (beam depth)
BTZ=6                   ! in (Beam width)
B_BDY=18                ! in (BASE Beam depth)
B_BTZ=10                ! in (BASE Beam width)
COVR=2.5                ! in ( cover = clear cover + 1/2 dia of the bar)
FACE_GAP=0.02           ! in ( Gap between frame and wall consider 0.5mm)

WLX=B*12-CTX            ! Colm-Colm clear distance
WHY=H*12-BDY            ! Colm clear height

WLX_GAP=B*12-CTX-2*FACE_GAP      ! Wall length considering Gap
WHY_GAP=H*12-BDY-2*FACE_GAP      ! Wall Height Considering Gap
```

```
!****BRICK and MORTAR SIZE******
```

```
BRKl=7.5                ! in (Brick length)
BRKw=WWZ                ! in (Brick Width)
BRKh=3.6                ! in (Brick height)
MRTR=1.25               ! in (Mortar height)
```

```
!*******INFILL ARRANGEMENT******
```

```
NoBrkX=NINT((WLX_GAP+MRTR)/(BRKl+MRTR))
! No of bricks in one layer

NoBrkY=NINT((WHY_GAP-MRTR)/(BRKh+MRTR))
```

! No of brick layers in the infill

!*******RESIZING OF BRICKS*********   ! Using NoBrkX and NoBrkY

BRKl=(WLX_GAP-(NoBrkX-1)*MRTR)/NoBrkX
BRKh=(WHY_GAP-(NoBrkY+1)*MRTR)/NoBrkY

!*********************************
! Material Property of Concrete
!*********************************

fc=3900   !psi (fc' of concrete)
NUc=0.15   ! poission's ratio of conc.
Cdens=150/(12**3)   ! #/in^3 (density of conc.)
EXc=2.5E6   !psi (Modulus of Elasticity of Conc.)
Gc=EXc/(2*(1+NUc))   !psi (Shearing Modulus of Elasticity of Conc.)
AREAc=CTX*CTZ   !in^2 (Colm area)
MUc=0.35   !Coefficient of friction
WEDGE_TK=CTZ   !in Wedge Thickness

!***********************************
! Material Property of Mild Steel
!***********************************

EXr=29E6   ! psi (Modulus of Elasticity of Mild Steel)
Rdens=0.29334   ! lb/in^3 (Density of Mild Steel)
NUr=0.3
Gr=EXr/(2*(1+NUr))   !psi (Shearing Modulus of Elasticity of Conc.)
AREAr=0.59   ! in^2 (Area of barS)
PLT_TK=CTZ   ! in Plate Thickness

!*********************
!BASE BEAM
!*********************
Ar_B_BM=1.8

!*********************
!COLUMN
!*********************
Ar_COLM=AREAr

!*********************
!BEAM
!*********************
Ar_BM=0.31

!*********************************
! Material Property of Brick
!*********************************

NUb=0.141   ! poission's ratio of Brick
fb=1380   ! psi Compressive Strength of Masonry
EXb=7.4E5   ! psi Modulus of Masonry
Gb=EXb/(2*(1+NUb))   ! psi (Shearing Modulus of Elasticity of)
Bdens=0.0695   ! lb/in^3 (Density of Mild Steel)
AREAb=1.8   ! in^2 (Area of barS)

```
!********************************
! Material Property of Mortar
!********************************

fm=1750                         ! psi Compressive Strength of Mortar
EXm=4.74e5                      ! psi  Modulus of Elasticity of mortar
NUm=0.202
Gm=EXm/(2*(1+NUm))             !psi Shearing Modulus of Elasticity of
Mdens=0.0895                    ! lb/in^3 ( Density of Mild Steel)
AREAm=1.8                       ! in^2 ( Area of barS)


!*****************CALCULATION***************

IZZc=CTZ*(CTX**3)/12           ! in^4 ( Moment of Inertia of Colm about Z axis)
IYYc=CTX*(CTZ**3)/12           ! in^4 ( Moment of Inertia of Colm about X axis)
IXXc=IZZc+IYYc
AREAb=BDY*BTZ                   ! in^2 (Beam area)
IZZb=BTZ*(BDY**3)/12           ! in^4 ( Moment of Inertia of Beam about Z axis)
IYYb=BDY*(BTZ**3)/12           ! in^4 ( Moment of Inertia of Beam about Y axis)
IXXb=IZZb+IYYb


!*************DIVISION***************
DIVCX=4                         ! Column is divided into 4 segments along X axis
DIVBY=4                         ! Beam is divided into 4 segments along Y axis
B_DIVBY=4                       ! Base Beam Extended portion is divided into 4 segments along Y axis

B_DIVEBX=NINT(B_EXT*12/B_BM_DX)
! Base Beam Extended portion is divided into B_DIVEBX segments along Y axis

BRK_DIV=3                       ! Brick is divided into 3 parts



!********************
!ELEMENT
!********************
ET,1,PLANE42,,,3                ! Plane Stress with thickness input  KEYOPT(3)=3
ET,2,LINK1                      ! 2D Spar Element
ET,3,TARGE169                   ! Target Element for Interfacing  between wall and frame
ET,4,CONTA171                   ! Contact Element for Interfacing  between wall and frame

!**********************
!REAL CONSTANT
!**********************

R,1,B_BTZ                       ! Base Beam thickness
R,2,CTZ                         ! Column thickness
R,3,BTZ                         ! Beam thickness
R,4,BRKw                        ! Infill thickness(Brick)
R,5,WWZ                         ! Mortar thickness=infill thickness
R,6,Ar_B_BM                     ! Area of a Single bar of Base Beam
R,7,Ar_COLM                     ! Area of a Single bar of Column
R,8,Ar_BM                       ! Area of a Single bar of Beam
R,9,0,WWZ,1, ,0.001, ,
RMORE, , ,,FACE_GAP, , ,        ! Real Constant for Interface Element
RMORE, ,
R,10,PLT_TK                     ! Plate thickness
R,11,WEDGE_TK                   ! Wedge thickness

!***************MATERIAL PROPERTY********************
```

```
! Material Property of Base Beam
MP,DENS,1,Cdens
MP,EX,1,EXc
MP,PRXY,1,NUc
MP,GXY,1,Gc
MP,MU,1,MUc

! Material Property of Column
MP,DENS,2,Cdens
MP,EX,2,EXc
MP,PRXY,2,NUc
MP,GXY,2,Gc
MP,MU,2,MUc

! Material Property of Beam
MP,DENS,3,Cdens
MP,EX,3,EXc
MP,PRXY,3,NUc
MP,GXY,3,Gc
MP,MU,3,MUc


! Material Property of Bricks
MP,DENS,4,Bdens
MP,EX,4,EXb
MP,PRXY,4,NUb
MP,GXY,4,Gb
MP,MU,4,MUc

! Material Property of Mortar
MP,DENS,5,Mdens
MP,EX,5,EXm
MP,PRXY,5,NUm
MP,GXY,5,Gm
MP,MU,5,MUc

! Material Property of Reinforcement
MP,DENS,6,Rdens
MP,EX,6,EXr

! Material Property of Steel Plate
MP,DENS,7,Rdens
MP,EX,7,EXr
MP,PRXY,7,NUr
MP,GXY,7,Gr

! Material Property of Concrete Wedge
MP,DENS,8,Cdens
MP,EX,8,EXc
MP,PRXY,8,NUc
MP,GXY,8,Gc
MP,MU,8,MUc

!***************************
!Defining Concrete Properties
!***************************

C_COHSN=1132
B_COHSN=200
M_COHSN=100
```

!TB, Lab, MAT, NTEMP, NPTS, TBOPT — Activates a data table for
!nonlinear material properties or special element input.

!TBDATA, STLOC, C1, C2, C3, C4, C5, C6 — Defines data for the data !table

```
TB,DP,1,,
TBDATA,,C_COHSN,30,0

TB,DP,2,,
TBDATA,,C_COHSN,30,0

TB,DP,3,,
TBDATA,,C_COHSN,30,0

TB,DP,4,,
TBDATA,,B_COHSN,30,0

TB,DP,5,,
TBDATA,,M_COHSN,30,0
```

!*************************
!Defining Steel Properties
!*************************

```
TB,BISO,6,1,
TBDATA,,59500,
```

!***************BASEBEAM*********************

! Node Generation

```
*DO,I,1,B_DIVEBX
I=I-1
N,I+1,(-B_EXT*12 + I*B_BM_DX-CTX),-B_BDY
! Node Generation for Extended portion of Base Beam
*END DO                              ! Left Portion
```

```
N,,-CTX,-B_BDY                       ! Node at the bottom of Base Beam at a Location of 1st
Node of Left Column
N,,COVR-CTX,-B_BDY                   ! Position of reinforcement
N,,-CTX/2,-B_BDY                     ! Location of Middle Node of Colm
N,,-COVR,-B_BDY                      ! Position of reinforcement
N,,,-B_BDY                           ! Last Node of Left Colm Location
```

```
*GET,N_B_LCL1,NODE,0,NUM,MAX         ! N_B_LCL1=Node No. at the bottom of
                                     ! Base Beam at a Location of Last Node of Left Colm
N_B_WN1=N_B_LCL1+1                    ! N_B_WN1=Node No. at the bottom of Base
                                     ! Beam at a Location of middle of 1st Brick
N,N_B_WN1,BRKl/2+FACE_GAP,-B_BDY
NSEL,,NODE,,N_B_WN1,N_B_WN1                        ! Nodes are just at the position of
                                                  !middle of Bricks
NGEN,(NoBrkX*2-1),1,ALL,,,(BRKl/2+MRTR/2)         ! Generating nodes of the Base
                                     ! Beam at the position of the bricks
N,,WLX,-B_BDY                                      ! Node at the bottom of Base Beam at a
                                     ! Location of 1st Node of Right Column
N,,WLX+COVR,-B_BDY                   ! Position of reinforcement
N,,WLX+CTX/2,-B_BDY                  ! Location of Middle Node of Colm
N,,WLX-COVR+CTX,-B_BDY               ! Position of reinforcement
```

```
N,,WLX+CTX,-B_BDY                              ! Last Node of Left Colm Location

*DO,I,1,B_DIVEBX
N,,(WLX+CTX+ I*B_BM_DX),-B_BDY                 ! Node Generation for Extended portion
                                               ! of Base Beam
*END DO                                        ! Right Portion

*GET,T_B_1L,NODE,0,NUM,MAX                     ! T_B_1L=Total number of Nodes at
                                               ! the bottom of the Base Beam
NSEL,S,NODE,,1,T_B_1L                          ! Selecting all the nodes at the ground
                                               ! level of Base Beam
NGEN,2, T_B_1L, ALL,,,,COVR                    ! Generating Nodes at the reinforcment
                                               ! level of Beam Base
NSEL,S,NODE,,1,T_B_1L                          ! Selecting all the nodes at the ground
                                               ! level of Base Beam
NGEN,2, T_B_1L*2, ALL,,,,B_BDY/2               ! Generating Nodes at the mid-level
                                               !of Beam Base
NSEL,S,NODE,,1,T_B_1L                          ! Selecting all the nodes at the
                                               !ground level of Base Beam
NGEN,2, T_B_1L*3, ALL,,,,B_BDY-COVR            ! Generating Nodes at the
                                               ! reinforcement level of Beam Base
NSEL,S,NODE,,1,T_B_1L                          ! Selecting all the nodes at the
                                               !ground level of Base Beam
NGEN,2, T_B_1L*4, ALL,,,,B_BDY                 ! Generating Nodes at the
                                               ! reinforcement level of Beam Base
*GET,T_B_BN,NODE,0,NUM,MAX                     ! T_B_BN=Total number of
                                               ! Nodes used in the Base Beam

!****************************************
!ELEMENT GENERATION OF BASE BEAM
!****************************************

TYPE,1
MAT,1
REAL,1

I=1
J=I+1
K=T_B_1L+2
L=K-1
E,I,J,K,L                                      ! Creating 1st Base Beam Element at the Ground
EGEN,T_B_1L-1,1,ALL                            ! Creating 1st Layer of Base Beam Element
EGEN,B_DIVBY,T_B_1L,ALL                        ! Creating all the Base Beam Elements

!****************************
! LEFT COLUMN
! ************************

N1LCOLM=T_B_BN+1
N,,-CTX                                        ! 1st Node at the upper left corner of left column
                                               ! over X axis CTX unit left from origin
N,,COVR-CTX                                    ! Position of reinforcement
N,,-CTX/2
N,,-COVR                                       ! Position of reinforcement
N,                                             ! So far 5 nodes are declared for left Colm of the base.

NSEL,S,NODE,,N1LCOLM,N1LCOLM+DIVCX             ! Selecting Base Column Nodes
NGEN,2,(DIVCX+1),ALL,,,,(FACE_GAP+MRTR)        ! Generating Nodes at the
                                               !height of Interface Gap
NSEL,S,NODE,,N1LCOLM+(DIVCX+1),N1LCOLM+(DIVCX+1)*2-1
! Selecting Column Nodes at Base Brick Level
```

```
NGEN,NoBrkY,(DIVCX+1),ALL,,,,BRKh+MRTR
! Generating all the nodes upto 2nd Last Mortar Level

NSEL,S,LOC,Y,WHY-BRKh-MRTR-FACE_GAP,WHY
NGEN,2,(DIVCX+1),ALL,,,,FACE_GAP+MRTR+BRKh

*GET,N_LCOLM,NODE,0,NUM,MAX                          ! N_LCOLM= Last Node No. of
                                                     ! the Left Column

! ELEMENT GENERATION OF LEFT COLUMN

TYPE,1
MAT,2
REAL,2

I=N1LCOLM
J=I+1
K=N1LCOLM+(DIVCX+1)+1
L=K-1
E,I,J,K,L

ESEL,S,MAT,,2
EGEN,DIVCX,1,ALL
EGEN,(NoBrkY+1),(DIVCX+1),ALL

!*****************************************************
!RIGHT COLUMN
!*****************************************************

T_N_COLM=1-N1LCOLM+N_LCOLM              ! Total No. of Nodes of a Column

NSEL,S,NODE,,N1LCOLM,N_LCOLM
NGEN,2,T_N_COLM,ALL,,,B*12
! Generating nodes of 2nd Column at a distance of B*12 inch

ESEL,S,MAT,,2
EGEN,2,T_N_COLM,ALL

*GET,N_RCOLM,NODE,0,NUM,MAX
! N_RCOLM= Last Node No. of the Right Column

!**********************************************************
!BEAM GENERATION
!**********************************************************

!NODE GENERATION

N1BEAM=N_RCOLM+1  ! 1st Node at the upper left corner of the BEAM
N,,-CTX,WHY              ! 1st Node at the upper left corner of the BEAM
N,,COVR-CTX,WHY                 ! Position of reinforcement
N,,-CTX/2,WHY
N,,-COVR,WHY           ! Position of reinforcement
N,,,WHY                         ! So far 5 nodes are declared for left Colm of the base.

*GET,N_BMLCL1,NODE,0,NUM,MAX               ! N_BMLCL1=Node No. at the bottom of Beam
                                           ! at a Location of Last Node of Left Column

N_BMWN1=N_BMLCL1+1
! N_BMWN1=Node No. at the bottom of Beam at a Location of middle of 1st Brick
```

```
N,N_BMWN1,BRKl/2+FACE_GAP,WHY
NSEL,,NODE,,N_BMWN1,N_BMWN1
NGEN,(NoBrkX*2-1),1,ALL,,,(BRKl/2+MRTR/2)
! Generating nodes of the Beam at the position of the bricks

N,,WLX,WHY                  ! Node at the bottom of Beam at a location of 1st Node of Right Column
N,,WLX+COVR,WHY             ! Position of reinforcement
N,,WLX+CTX/2,WHY            ! Location of Middle Node of Colm
N,,WLX-COVR+CTX,WHY  ! Position of reinforcement
N,,WLX+CTX,WHY                                          ! Last Node of Right Colm Location
*GET,N_BM1L,NODE,0,NUM,MAX                              ! N_BM1L=Node No. at the end
                                                       ! of 1st layer of the Beam
TN_BM_1L=1-N1BEAM+N_BM1L                                ! TN_BM_1L=Total No. of
                                                       ! Nodes in the 1st layer of Beam
NSEL,S,NODE,,N1BEAM,N_BM1L                              ! Selecting all the nodes at the 1st
                                                       ! layer of Beam
NGEN,2, TN_BM_1L, ALL,,,,COVR                           ! Generating Nodes at the
                                                       ! reinforcement level of Beam
NSEL,S,NODE,,N1BEAM,N_BM1L                              ! Selecting all the nodes at the 1st
                                                       ! layer of Beam
NGEN,2, TN_BM_1L*2, ALL,,,,BDY/2                        ! Generating Nodes at the mid-
                                                       ! level of Beam
NSEL,S,NODE,,N1BEAM,N_BM1L                              ! Selecting all the nodes at the 1st
                                                       ! layer of Beam
NGEN,2, TN_BM_1L*3, ALL,,,,BDY-COVR                     ! Generating Nodes at the
                                                       ! reinforcement level of Beam
NSEL,S,NODE,,N1BEAM,N_BM1L                              ! Selecting all the nodes at the 1st
                                                       ! layer of Beam
NGEN,2, TN_BM_1L*4, ALL,,,,BDY                          ! Generating Nodes at the top
                                                       ! level of Beam
*GET,L_BM_N,NODE,0,NUM,MAX                              ! L_BM_N=Last Node of the
                                                       ! Beam at the top layer


!ELEMENT GENERATION

TYPE,1
MAT,3
REAL,3

I=N1BEAM
J=I+1
K=J+TN_BM_1L
L=K-1
E,I,J,K,L

ESEL,S,MAT,,3
EGEN,TN_BM_1L-1,1,ALL
EGEN,DIVBY,TN_BM_1L,ALL

!********************************************************
!INFILL NODE GENERATION
!********************************************************

N1_MRTR=L_BM_N+1                        ! 1st Node of INFILL (Mortar Element)
N,,FACE_GAP,FACE_GAP                     ! 1st Node of INFILL
N,,FACE_GAP+BRKl/2-MRTR/2,FACE_GAP

NSEL,S,NODE,,N1_MRTR,N1_MRTR+1
NGEN,NoBrkX*2,2,ALL,,,BRKl/2+MRTR/2
NGEN,2,NoBrkX*2*2,ALL,,,,MRTR
```

NGEN,NoBrkY+1,NoBrkX*2*2*2,ALL,,,,BRKh+MRTR

```
!***********************************************************
!INFILL ARRANGEMENT
!***********************************************************
! First there is one course of MRTR on the Base-Beam then a Brick Layer is Layer
! The infill is the repetition of these arrangements 1layer Mortar then 1layer Brick
! At the top of the infill it ends with a layer of MRTR

! Now defining a brick with a 4 noded Plane42 (plane stress) element
! Brick layer is composed in this way ----  |____| |____|M|____| |____|M|____  ----
! M means mortar

! In the vertical direction, in one layer it starts with one full brick then in the latter
! layer it starts with a 1/2 brick, Thus the alternate arrangement continues
! In this way      Starts with Full Brick->  |_____|M|_____|M|_____| -------------! Starts with Half
Brick->|__|M|_____|M|_____|M|_____|  ------------

! If BRICK Layers are odd number (Say 5 Layers) then no. of Layers start with a Full
! size will be of  NINT((5+.5)/2)=3 Layers
! AND If BRICK Layers are even number (Say 4 Layers) then no. of Layers start with
! Half size will be of  NINT((4+.5)/2)=2 Layers

NoLFLBRK= NINT((NoBrkY+0.5)/2)          ! NoLFLBRK= No. of BRICK Layers
                                        !starting with Full Brick
                                        ! L=Layer, FL=Full Size Brick
NoLHFBRK= NoBrkY-NoLFLBRK               ! NoLHFBRK= No. of BRICK Layers
                                        !starting with Half Brick
                                        ! L=Layer, HF=Half Size Brick

! BRICK, Definition : A Full Brick is composed of 3 Plane Stress elements.
! Each element is a 4 noded Plane42 element, Brick Length is divided into 3 segments

!***********************************************************
!BRICK ELEMENT GENERATION
!***********************************************************

TYPE,1
MAT,4
REAL,4

N1BRK=N1_MRTR+NoBrkX*2*2                 ! Node no. of 1st Brick Position
I=N1BRK
J=I+1
K=I+NoBrkX*2*2+1
L=K-1
E,I,J,K,L

*GET,E1FLBRK1,ELEM,,NUM,MAX
! E1FLBRK1= Element Number of 1st part of a Full BRICK in the 1st Layer

ESEL,S,MAT,,4
EGEN,BRK_DIV,1,ALL                       ! 1st Full Brick is Generated
EGEN,NoBrkX,BRK_DIV+1,ALL                ! Generating 1st Brick Layer
EGEN,NoLFLBRK,(NoBrkX*2*2)*4,ALL
! Generating all the brick layers starting with Full Size BRICKs

!2ND BRICK LAYER
! Generating alternate layer or the next layer
```

```
I=N1_MRTR+(NoBrkX*2*2)*3    ! Node no. of 1st Half Brick Position
J=I+1
K=I+NoBrkX*2*2+1
L=K-1
E,I,J,K,L                    ! Generating 1st Half Brick

*GET,E1HFBRK2,ELEM,,NUM,MAX
! E1HFBRK2= Element Number of 1st Half BRICK in the 2nd Layer
! E1HFBRK2, Here 1HF = 1st Half Brick, 2 = 2nd Layer

I=I+2
J=J+2
K=K+2
L=L+2
E,I,J,K,L                              ! Generating 1st part of 2nd Brick in the 2nd Layer

*GET,E2FLBRK2,ELEM,,NUM,MAX
! E2FLBRK2= Element Number of 1st part of a Full BRICK in the 2nd Layer
! E2FLBRK2, Here 2= 2nd brick, FL = part of a Full Brick, 2 = 2nd Layer


ESEL,S,ELEM,,E2FLBRK2          ! Selecting the 1st part of Full BRICK in the 2nd Layer
EGEN,BRK_DIV,1,ALL              ! 1st Full Brick is Generated in the 2nd Layer
EGEN,NoBrkX-1,BRK_DIV+1,ALL           ! Generating 2nd Brick Layer except last Half Brick

ESEL,S,ELEM,,E1HFBRK2,E1HFBRK2    ! Selecting the 1st  Half BRICK  in the 2nd Layer
EGEN,2,(NoBrkX*2-1)*2,ALL     ! Creating the last brick of the 2nd Layer which is a Half BRICK
*GET,ELSTBRK2,ELEM,,NUM,MAX       ! ELSTBRK2= Element Number of last
                                  ! Half BRICK in the 2nd Layer

! There are "NoLHFBRK" No. of BRICK Layers starting with Half Brick

ESEL,S,ELEM,,E1HFBRK2,ELSTBRK2    ! Selecting all the bricks in the 2nd layer
EGEN,NoLHFBRK,(NoBrkX*2*2)*4,ALL          ! Generating all the brick layers
                                          ! starting with Full Size BRICKs
! Creating Mortar Layer in between Brick Layers

TYPE,1
MAT,5
REAL,5

I=N1_MRTR
J=I+1
K=I+NoBrkX*2*2+1
L=K-1
E,I,J,K,L                 ! Generating 1st part of Mortar
ESEL,S,MAT,,5
EGEN,NoBrkX*2*2-1,1,ALL
EGEN,NoBrkY+1,(NoBrkX*2*2)*2,ALL

!****************************************************************
!Generating Mortar Elements in between Bricks in 1st,3rd,,,,,layers
!****************************************************************
! Generating Mortar Elements in Brick Layers starting with Full Brick

I=N1BRK+BRK_DIV
J=I+1
K=I+NoBrkX*2*2+1
L=K-1
E,I,J,K,L                                 ! Generating 1st part of Mortar in betn Bricks
```

```
*GET,E1BMRTR1,ELEM,,NUM,MAX        ! E1BMRTR1= Element Number of
                                   ! 1st part of MORTAR in betn Bricks
ESEL,S,ELEM,,E1BMRTR1              ! Selecting 1st part of 1st MORTAR element
                                   ! of 1st row of BRICK Layers
EGEN,NoBrkX-1,1+BRK_DIV,ALL        ! Generating All the MORTAR elements in
                                   ! the 1st BRICK Layers, starting with a Full BRICK
EGEN,NoLFLBRK,(NoBrkX*2*2)*4,ALL   ! Generating All the MORTAR elements
! in all the BRICK Layers, starting with a Full BRICK
!*****************************************************************
!Generating Mortar Elements in between Bricks in 2nd,4th,,,,,layers
!*****************************************************************
!Generating MORTAR elements in BRICK layers starting with a Half Brick

I=N1BRK+(NoBrkX*2*2)*2+1
J=I+1
K=I+NoBrkX*2*2+1
L=K-1
E,I,J,K,L                          ! Generating 1st part of Mortar in between Bricks

*GET,E1BMRTR2,ELEM,,NUM,MAX        ! E1BMRTR2= Element Number of 1st
! MORTAR in the 2nd BRICK Layer starting with a Half Brick

ESEL,S,ELEM,, E1BMRTR2             ! Selecting 1st MORTAR element of 2nd
                                   ! row of BRICK Layers starting with a Half Brick

EGEN,NoBrkX,1+BRK_DIV,ALL ! Generating All the MORTAR elements in the
! 2nd BRICK Layers, starting with a Half BRICK

EGEN,NoLHFBRK,(NoBrkX*2*2)*4,ALL ! Generating All the MORTAR elements
! in the BRICK Layers, starting with a Half BRICK

!*********************************
!Reinforcing Base Beam
!*********************************

TYPE,2
MAT,6
REAL,6

N1FR_BBM=1+T_B_1L  !1st Node of 1st Layer of Reinforcement of Base Beam
N1MR_BBM=N1FR_BBM+T_B_1L           !1st Node of Middle Layer of Reinforce-
                                   !ment of Base Beam
N1LR_BBM=N1MR_BBM+T_B_1L           !1st Node of Last Layer of Reinforce-
                                   !ment of Base Beam
*DO,I,1,T_B_1L-1
I=I-1
E,N1FR_BBM+I,N1FR_BBM+I+1! Reinforcement in Bottom Layer of BaseBeam
*ENDDO

*DO,I,1,T_B_1L-1
I=I-1
E,N1LR_BBM+I,N1LR_BBM+I+1          ! Reinforcement in Top Layer of BaseBeam
*ENDDO

ESEL,S,MAT,,6

!*********************************
!REINFORCING 2 COLUMNS
!*********************************
```

```
REAL,7

!Reinforcing LEFT COLUMN
No_NCOLM=N_LCOLM-N1LCOLM+1      ! No. of Nodes in a Column
LR_NCOLM=No_NCOLM/(DIVCX+1)      ! No. of Nodal Layers in a Column

!Reinforcing Left Side of Left Column
*DO,NUM,1,LR_NCOLM-1
NUM=NUM-1
I=N1LCOLM+NUM*(DIVCX+1)+1
J=I+(DIVCX+1)
E,I,J
*END DO

!Reinforcing Middle of Left Column
*DO,NUM,1,LR_NCOLM-1
NUM=NUM-1
I=N1LCOLM+NUM*(DIVCX+1)+(DIVCX/2)      ! DIVCX=EVEN
J=I+(DIVCX+1)
E,I,J
*END DO
!Reinforcing Right Side of Left Column
*DO,NUM,1,LR_NCOLM-1
NUM=NUM-1
I=N1LCOLM+NUM*(DIVCX+1)+DIVCX-1
J=I+(DIVCX+1)
E,I,J
*END DO

*GET,LENo_RC1,ELEM,,NUM,MAX
! LENo_RC1= Last Element Number of Reinforcement in Left Column1


! Extending COLUMN Reinforcement into the Base Beam

*DO,NUM,1,B_DIVBY
I=B_DIVEBX+2+T_B_1L*(NUM-1)
J=I+T_B_1L
E,I,J
*END DO

*DO,NUM,1,B_DIVBY
I=B_DIVEBX+1+DIVCX/2+T_B_1L*(NUM-1)
J=I+T_B_1L
E,I,J
*END DO

*DO,NUM,1,B_DIVBY
I=B_DIVEBX+DIVCX+T_B_1L*(NUM-1)
J=I+T_B_1L
E,I,J
*END DO


! EXTENDING COLUMN REINFORCEMENT INTO THE TOP BEAM

*DO,NUM,1,DIVBY
I=N1BEAM+1+TN_BM_1L*(NUM-1)
J=I+TN_BM_1L
```

```
E,I,J
*END DO

*DO,NUM,1,DIVBY
I=N1BEAM+DIVCX/2+TN_BM_1L*(NUM-1)
J=I+TN_BM_1L
E,I,J
*END DO

*DO,NUM,1,DIVBY
I=N1BEAM+DIVCX-1+TN_BM_1L*(NUM-1)
J=I+TN_BM_1L
E,I,J
*END DO

*GET,E_L_R_C,ELEM,,NUM,MAX          ! E_L_R_C= Element Number of Last
                                    !Reinforcement Extending from Column into Beam


!*******************************
!Reinforcing RIGHT COLUMN
!*******************************

REAL,7

ESEL,S,ELEM,,(LENo_RC1-(LR_NCOLM-1)*3+1),LENo_RC1
EGEN,2,No_NCOLM,ALL

! Extending Reinforcement from Right Column into Base Beam and Top Beam

ESEL,S,ELEM,,E_L_R_C-(DIVBY+B_DIVBY)*3+1,E_L_R_C-DIVBY*3
! Selecting the extended reinforcement of Left Column into Base Beam

EGEN,2,NoBrkX*2+DIVCX,ALL
! Extending Reinforcement into Base Beam

ESEL,S,ELEM,,E_L_R_C-DIVBY*3+1,E_L_R_C
! Selecting the extended reinforcement of Left Column into Top Beam

EGEN,2,NoBrkX*2+DIVCX,ALL
! Extending Reinforcement into Top Beam

!*********************************
!Reinforcing Beam
!*********************************

REAL,8

! N1BEAM=1st Node of the Beam
! L_BM_N=Last Node of the Beam at the top layer
! TN_BM_1L=Total No. of Nodes in the 1st layer of Beam

! Reinforcing Bottom Layer of Reinforcment in Beam
*DO,NUM,1,TN_BM_1L-1
I=N1BEAM+TN_BM_1L+NUM-1
J=I+1
E,I,J
*END DO

! Reinforcing Top Layer of Reinforcment in Beam
*DO,NUM,1,TN_BM_1L-1
```

```
I=N1BEAM+TN_BM_1L*(DIVBY-1)+NUM-1
J=I+1
E,I,J
*END DO




!***************************
!INTERFACE ELEMENT
!***************************
! APPLYING TARGET ELEMENT
!***************************

TYPE,3
REAL,9

! Defining Interface Element Between Base Beam & Infill
! TARGET Element on Base Beam
MAT,1
*DO,NUM,1,(NoBrkX*2)
I=B_DIVEBX+DIVCX+T_B_1L*B_DIVBY+(NUM+1)
J=B_DIVEBX+DIVCX+T_B_1L*B_DIVBY+NUM
E,I,J
*END DO

! Defining Interface Element Between Left Column & Infill
! TARGET Element on Left Column
MAT,2
*DO,NUM,1,NoBrkY+1
I=N1LCOLM+DIVCX+(DIVCX+1)*(NUM-1)
J=N1LCOLM+DIVCX+(DIVCX+1)*NUM
E,I,J
*END DO


! Defining Interface Element Between Right Column & Infill
! TARGET Element on Right Column
MAT,2
*DO,NUM,1,NoBrkY+1
I=N1LCOLM+T_N_COLM+(DIVCX+1)*NUM
J=N1LCOLM+T_N_COLM+(DIVCX+1)*(NUM-1)
E,I,J
*END DO

! Defining Interface Element Between Top Beam & Infill
! TARGET Element on Beam
MAT,3
*DO,NUM,1,(NoBrkX*2)
I=N1BEAM+DIVCX+NUM-1
J=N1BEAM+DIVCX+NUM
E,I,J
*END DO


!**********************!
!APPLYING CONTACT ELEMENT
!**********************!
```

```
TYPE,4
REAL,9

! Defining Interface Element Between Base Beam & Infill(over INFILL)
! Applying CONTACT ELEMENT below MORTAR
MAT,5
*DO,NUM,1,(NoBrkX*2*2-1)
I=N1_MRTR+NUM-1
J=N1_MRTR+NUM
E,I,J
*END DO

! Defining Interface Element Between Left Column & Infill
! Applying CONTACT ELEMENT at the left side of INFILL over BRICK
MAT,4
*DO,NUM,1,NoBrkY*2+1
I=N1BRK+NoBrkX*2*2*(NUM-1)
J=N1BRK+NoBrkX*2*2*(NUM-2)
E,I,J
*END DO

! Defining Interface Element Between Right Column & Infill
! Applying CONTACT ELEMENT at the right side of INFILL over BRICK
MAT,4
*DO,NUM,1,NoBrkY*2+1
I=N1BRK+NoBrkX*2*2*(NUM-1)-1
J=N1BRK+NoBrkX*2*2*NUM-1
E,I,J
*END DO

! Defining Interface Element Between Top Beam & Infill
! Applying CONTACT ELEMENT at the top of INFILL over MORTAR
MAT,5
*DO,NUM,1,(NoBrkX*2*2-1)
I=N1_MRTR+(NoBrkY*2+1)*NoBrkX*2*2+NUM
J=N1_MRTR+(NoBrkY*2+1)*NoBrkX*2*2+NUM-1
E,I,J
*END DO



!************************************************
!CREATING A WEDGE AT THE LEFT OF LEFT COLUMN
!************************************************

*GET,LASTNODE,NODE,,NUM,MAX

N1WEDGE=LASTNODE+1

!NODE GENERATION
N,,-CTX-(BDY-2*COVR)/2,WHY+COVR+(BDY-2*COVR)/4          !N1WEDGE
N,,-CTX-(BDY-2*COVR)/2,WHY+BDY/2
N,,-CTX-(BDY-2*COVR)/2,WHY+BDY-COVR-(BDY-2*COVR)/4
N,,-CTX-(BDY-2*COVR),WHY+BDY/2

!ELEMENT GENERATION
N_1LBEAM=(DIVBY+1)*2+NoBrkX*2-1

TYPE,1
REAL,11
```

MAT,8

I=N1BEAM+N_1LBEAM
J=I+N_1LBEAM
K=N1WEDGE+1
L=N1WEDGE
E,I,J,K,L

I=N1BEAM+N_1LBEAM*2
J=I+N_1LBEAM
K=N1WEDGE+2
L=N1WEDGE+1
E,I,J,K,L

TYPE,1
REAL,10
MAT,8

I=N1WEDGE
J=N1WEDGE+1
K=N1WEDGE+3
L=N1WEDGE+3
E,I,J,K,L

I=N1WEDGE+1
J=N1WEDGE+2
K=N1WEDGE+3
L=N1WEDGE+3
E,I,J,K,L

!***************************
!MERGE
!***************************
ALLSEL
NUMMRG,NODE
NUMMRG,ELEM
NUMCMP,NODE
NUMCMP,ELEM

!***
!SUPPORT CONDITIONS
!***

NSEL,S,LOC,X,-CTX,-(B_EXT*12+CTX)
NSEL,R,LOC,Y,-B_BDY,-B_BDY
D,ALL,ALL

NSEL,S,LOC,X,B*12,B_EXT*12+B*12
NSEL,R,LOC,Y,-B_BDY,-B_BDY
D,ALL,ALL

!***
! NUMBERING MATERIAL NUMBERS BY COLORS ONLY
!***

ALLSEL
/NUM,1
/PNUM,MAT,1
/REPLOT

```
GPLOT
! GRAPHICS DISPLAY OF ALL FORCES AND BOUNDARY CONDITIONS
/PBC,ALL,,1
/PBC,NFOR,,0
/PBC,NMOM,,0
/PBC,RFOR,,0
/PBC,RMOM,,0
/PBC,PATH,,0
/REP
!**************************************************************
!Nonlinear Control and Displacement Steps
!**************************************************************

/SOLU
ANTYPE,STATIC
NROPT,AUTO
EQSLV,SPARSE
CNVTOL,F,,0.1,,1
CNVTOL,U,,0.0025
NEQIT,100
AUTOTS,ON

DEF_STEP=45

*DO,I,1,DEF_STEP

! Now selecting the nodes (except top and bottom) at the face of the
! column, which intersects with beam.

NSEL,S,LOC,X,-CTX-(BDY-2*COVR)
NSEL,R,LOC,Y,WHY+BDY/2

*IF,I,LE,8,THEN

D,ALL,UX,I*0.01            !***APPLYING DISPLACEMENTS****
ALLSEL
NSUBST,4,20,2

*ELSEIF,I,LE,15,THEN
D,ALL,UX,0.08+(I-8)*0.005      !***APPLYING DISPLACEMENTS****
ALLSEL
NSUBST,(I-6)*2,40,(I-6)

*ELSEIF,I,LE,25,THEN
D,ALL,UX,0.115+(I-15)*0.0025   !***APPLYING DISPLACEMENTS****
ALLSEL
NSUBST,(I-6)*2,50,(I-10)

*ELSEIF,I,LE,35
D,ALL,UX,0.14+(I-25)*0.0025    !***APPLYING DISPLACEMENTS****
ALLSEL
NSUBST,(I-6)*2,75,(I-15)

*ELSE
D,ALL,UX,0.165+(I-35)*0.0025   !***APPLYING DISPLACEMENTS****
ALLSEL
NSUBST,(I-6)*2,90,(I-15)

*ENDIF
```

```
OUTRES,ALL,ALL
LSWRITE,I

*END DO

LSSOLVE,1,DEF_STEP,1

SAVE
FINISH

!************************
!DEFORMED SHAPE
!************************

/POST1
PLDISP,0                    ! DEFORMED SHAPE
FINISH

!************************
! GET RESULTS
!************************

/POST26
FORCE,TOTAL                 ! Force Result
SHELL,TOP
LAYERP26,0
ESOL,2,1677,1394,F,X,fx1            ! Element Solution
FORCE,TOTAL
SHELL,TOP
LAYERP26,0
ESOL,3,1676,1394,F,X,fx2
NSOL,4,1394,U,X,N1394UX
NSOL,5,1390,U,X,MrtrUX
NSOL,6,1350,U,X,BrkUX
PRVAR,1,2,3,4,5,6,
SAVE
```

APPENDIX B

```
! -----------------------------------------------------------------------------------------------------------
! Author:
!                                      M. Shahria Alam
!                                      Lecturer
!                                      Dept. of Civil Engineering
!                                      BUET, Dhaka-10000.
!------------------------------------------------------------------------------------------------------------
! As a part of the thesis work "Numerical Modeling of Masonry Infill Panels Retrofitted with Ferro-
! cement" for the partial fulfillment of M.Sc. in Civil Engineering (Structural).
!***************************************************************************************
! The model is generated from M.Sc Thesis "Experimental Evaluation of Lateral Strength of Masonry-
! Infilled RC Frame Retrofitted with Ferrocement" by Miah Md. Maksudul Alam (2003)
! Here the experimental results obtained by Alam (2003) will be used to VERIFY the numerical model
! by Lateral load Displacement Curves
! Here no Contact Element is used, but a special feature named "birth and death" feature has been
! incorporated in this model


!***************************************************************************************


/PREP7                    ! Post Processor 7
ANTYPE,STATIC             ! Analysis type


!******************PARAMETER*******************


H=65/12           ! ft ( colm height) f/f distance
B=65/12           ! ft ( beam length) c/c distance
B_EXT=2           ! in ft Base Beam Extended upto B-EXT
B_BM_DX=6         ! in inches Base Beam Extended size/Division = 6"
WWZ=2.75          ! in (wall thickness)
CTX=6             ! in (colm thickness along span length)
CTZ=6             ! in (colm thinckness _|_ to span length also _|_ to the computer screen)
BDY=6             ! in (beam depth)
BTZ=6             ! in (Beam width)
B_BDY=18          ! in (BASE Beam depth)
B_BTZ=12          ! in (BASE Beam width)
COVR=1.3          ! in ( cover = clear cover + 1/2 dia of the bar)
FACE_GAP=0        ! in ( Gap between frame and wall consider 0.5mm)


WLX=B*12-CTX                      ! Colm-Colm clear distance
WHY=H*12-BDY                      ! Colm clear height
WLX_GAP=B*12-CTX-2*FACE_GAP       ! Wall length considering Gap
WHY_GAP=H*12-BDY-2*FACE_GAP       ! Wall Height Considering Gap


!****BRICK and MORTAR SIZE******
BRKl=4.4                  ! in (Brick length)
BRKw=WWZ                  ! in (Brick Width)
BRKh=1.4                  ! in (Brick height)
MRTR=0.5                  ! in (Mortar height)


!*******INFILL ARRANGEMENT******
NoBrkX=NINT((WLX_GAP+MRTR)/(BRKl+MRTR))
! No of bricks in one layer
NoBrkY=NINT((WHY_GAP-MRTR)/(BRKh+MRTR))
! No of brick layers in the infill


!*******RESIZING OF BRICKS*********          ! Using NoBrkX and NoBrkY
BRKl=(WLX_GAP-(NoBrkX-1)*MRTR)/NoBrkX
BRKh=(WHY_GAP-(NoBrkY+1)*MRTR)/NoBrkY
```

```
!********************************
! Material Property of Concrete
!********************************
fc=2378                         !psi (fc' of concrete)
NUc=0.15                        ! poission's ratio of conc.
Cdens=150/(12**3)              ! #/in^3 (density of conc.)

EXc=2.8E6                       !psi ( Modulus of Elasticity of Conc.)
Gc=EXc/(2*(1+NUc))             !psi (Shearing Modulus of Elasticity of Conc.)
AREAc=CTX*CTZ                   !in^2 (Colm area)
MUc=0.35                        !Coefficient of friction
WEDGE_TK=CTZ                    !in Wedge Thickness


!************************************
! Material Property of Mild Steel
!************************************
EXr=29E6                ! psi ( Modulus of Elasticity of Mild Steel)
Rdens=0.29334           ! lb/in^3 ( Density of Mild Steel)
NUr=0.3
Gr=EXr/(2*(1+NUr))      !psi (Shearing Modulus of Elasticity of Conc.)
AREAr=0.75              ! in^2 ( Area of barS)
PLT_TK=CTZ              ! in Plate Thickness


!*********************
!BASE BEAM
!*********************
Ar_B_BM=2


!*********************
!COLUMN
!*********************
Ar_COLM=AREAr


!*********************
!BEAM
!*********************
Ar_BM=0.6


!********************************
! Material Property of Brick
!********************************
NUb=0.141               ! poission's ratio of Brick
fb=2300                 ! psi Compressive Strength of Masonry
EXb=7.4E5               ! psi  Modulus of Masonry
Gb=EXb/(2*(1+NUb))      ! psi (Shearing Modulus of Elasticity of )
Bdens=0.0695            ! lb/in^3 ( Density of Mild Steel)


!********************************
! Material Property of Mortar
!********************************
fm=1750                 ! psi Compressive Strength of Mortar
EXm=4.74e5              ! psi  Modulus of Elasticity of mortar
NUm=0.202
Gm=EXm/(2*(1+NUm))      !psi Shearing Modulus of Elasticity of
Mdens=0.0895            ! lb/in^3 ( Density of Mild Steel)
AREAm=1.8               ! in^2 ( Area of barS)


!********************************
! Material Property of Ferrocement
!********************************
```

```
EXf=3.75e6                    ! psi  Modulus of Elasticity of Ferrocement
NUf=0.202                     !
Gf=EXf/(2*(1+NUf))            ! psi Shearing Modulus of Elasticity of
Fdens=0.1                     ! lb/in^3 ( Density of Mild Steel)
FEROCMNT=1.5                  ! in Ferrocement thickness


!*****************CALCULATION***************
IZZc=CTZ*(CTX**3)/12 ! in^4 ( Moment of Inertia of Colm about Z axis)
IYYc=CTX*(CTZ**3)/12 ! in^4 ( Moment of Inertia of Colm about X axis)
IXXc=IZZc+IYYc
AREAb=BDY*BTZ  ! in^2 (Beam area)
IZZb=BTZ*(BDY**3)/12 ! in^4 ( Moment of Inertia of Beam about Z axis)
IYYb=BDY*(BTZ**3)/12 ! in^4 ( Moment of Inertia of Beam about Y axis)
IXXb=IZZb+IYYb


!*************DIVISION****************
DIVCX=4               ! Column is divided into 4 segments along X axis
DIVBY=4               ! Beam is divided into 4 segments along Y axis
B_DIVBY=4             ! Base Beam Extended portion is divided into 4 segments along Y axis
B_DIVEBX=NINT(B_EXT*12/B_BM_DX)
! Base Beam Extended portion is divided into B_DIVEBX segments along Y axis


BRK_DIV=3     ! Brick is divided into 3 parts


!****************
ELEMENT
!****************
ET,1,PLANE42,,,3         ! Plane Stress with thickness input  KEYOPT(3)=3
ET,2,LINK1


!**********************
!REAL CONSTANT
!**********************
R,1,B_BTZ             ! Base Beam thickness
R,2,CTZ          ! Column thickness
R,3,BTZ          ! Beam thickness
R,4,BRKw             ! Infill thickness(Brick)
R,5,WWZ              ! Mortar thickness=infill thickness
R,6,Ar_B_BM          ! Area of a Single bar of Base Beam
R,7,Ar_COLM   ! Area of a Single bar of Column
R,8,Ar_BM            ! Area of a Single bar of Beam
R,9,PLT_TK           ! Plate Thickness
R,10,WEDGE_TK        ! Wedge Thickness
R,11,FEROCMNT        ! Ferrocement Thickness


!***************MATERIAL PROPERTY*******************
! Material Property of Base Beam
MP,DENS,1,Cdens
MP,EX,1,EXc
MP,PRXY,1,NUc
MP,GXY,1,Gc
MP,MU,1,MUc

! Material Property of Column
MP,DENS,2,Cdens
MP,EX,2,EXc
MP,PRXY,2,NUc
MP,GXY,2,Gc
MP,MU,2,MUc
```

```
! Material Property of Beam
MP,DENS,3,Cdens
MP,EX,3,EXc
MP,PRXY,3,NUc
MP,GXY,3,Gc
MP,MU,3,MUc
! Material Property of Bricks
MP,DENS,4,Bdens
MP,EX,4,EXb
MP,PRXY,4,NUb
MP,GXY,4,Gb
MP,MU,4,MUc

! Material Property of Mortar
MP,DENS,5,Mdens
MP,EX,5,EXm
MP,PRXY,5,NUm
MP,GXY,5,Gm
MP,MU,5,MUc

! Material Property of Reinforcement for Base Beam
MP,DENS,6,Rdens
MP,EX,6,EXr

! Material Property of Steel Plate
MP,DENS,7,Rdens
MP,EX,7,EXr
MP,PRXY,7,NUr
MP,GXY,7,Gr

! Material Property of Concrete Wedge
MP,DENS,8,Cdens
MP,EX,8,EXc
MP,PRXY,8,NUc
MP,GXY,8,Gc
MP,MU,8,MUc

! Material Property of Reinforcement for Column and Beam
MP,DENS,9,Rdens
MP,EX,9,EXr

! Material Property of FerroCement
MP,DENS,10,Fdens
MP,EX,10,EXf
MP,PRXY,10,NUf
MP,GXY,10,Gf
MP,MU,10,MUc

!***************************
!Defining Concrete Properties
!***************************
C_COHSN=500
B_COHSN=400
M_COHSN=700
F_COHSN=750

!TB, Lab, MAT, NTEMP, NPTS, TBOPT — Activates a data table for
!nonlinear material properties or special element input.
```

!TBDATA, STLOC, C1, C2, C3, C4, C5, C6 — Defines data for the data table

```
TB,DP,1,,
TBDATA,,C_COHSN,30,0

TB,DP,2,,
TBDATA,,C_COHSN,30,0
TB,DP,3,,
TBDATA,,C_COHSN,30,0

TB,DP,4,,
TBDATA,,B_COHSN,30,0

TB,DP,5,,
TBDATA,,M_COHSN,30,0

!*************************
!Defining Steel Properties
!*************************
! For Base Beam
TB,BISO,6,1,
TBDATA,,63000,

! For Column and Beam
TB,BISO,9,1,
TBDATA,,46000,

TB,DP,10,,
TBDATA,,F_COHSN,30,0

!***************BASEBEAM*********************
```

```
! Node Generation
*DO,I,1,B_DIVEBX
I=I-1
N,I+1,(-B_EXT*12 + I*B_BM_DX-CTX),-B_BDY    ! Node Generation for Extended
                                            ! portion of Base Beam
*END DO                                     ! Left Portion

N,,-CTX,-B_BDY                              ! Node at the bottom of Base Beam at a Location of 1st
Node of Left Column
N,,COVR-CTX,-B_BDY                          ! Position of reinforcement
N,,-CTX/2,-B_BDY                            ! Location of Middle Node of Colm
N,,-COVR,-B_BDY                             ! Position of reinforcement
N,,,-B_BDY                                  ! Last Node of Left Colm Location

*GET,N_B_LCL1,NODE,0,NUM,MAX               ! N_B_LCL1=Node No. at the
! bottom of Base Beam at a Location of  Last Node of Left Colm

N_B_WN1=N_B_LCL1+1                          ! N_B_WN1=Node No. at the bottom of Base
                                           ! Beam at a Location of middle of 1st Brick
N,N_B_WN1,BRKl/2+FACE_GAP,-B_BDY
NSEL,,NODE,,N_B_WN1,N_B_WN1                 ! Nodes are just at the position of
                                           ! middle of Bricks
NGEN,(NoBrkX*2-1),1,ALL,,,(BRKl/2+MRTR/2)  ! Generating nodes of the Base
                                           ! Beam at the position of  the bricks
N,,WLX,-B_BDY                              ! Node at the bottom of Base Beam at a
                                           ! Location of 1st Node of Right Column
N,,WLX+COVR,-B_BDY                         ! Position of reinforcement
N,,WLX+CTX/2,-B_BDY                        ! Location of Middle Node of Colm
```

```
N,,WLX-COVR+CTX,-B_BDY          ! Position of reinforcement
N,,WLX+CTX,-B_BDY               ! Last Node of Left Colm Location


*DO,I,1,B_DIVEBX
N,,(WLX+CTX+ I*B_BM_DX),-B_BDY   ! Node Generation for Extended portion of Base Beam
*END DO                         ! Right Portion


*GET,T_B_1L,NODE,0,NUM,MAX      ! T_B_1L=Total number of Nodes at the
                                ! bottom of the Base Beam
NSEL,S,NODE,,1,T_B_1L           ! Selecting all the nodes at the ground level of Base Beam
NGEN,2, T_B_1L, ALL,,,,COVR     ! Generating Nodes at the reinforcement level of Beam Base
NSEL,S,NODE,,1,T_B_1L           ! Selecting all the nodes at the ground level of Base Beam
NGEN,2, T_B_1L*2, ALL,,,,B_BDY/2     ! Generating Nodes at the mid-level of Beam Base
NSEL,S,NODE,,1,T_B_1L           ! Selecting all the nodes at the ground level of Base Beam
NGEN,2, T_B_1L*3, ALL,,,,B_BDY-COVR          ! Generating Nodes at the reinforce-
                                             ! ment level of Beam Base
NSEL,S,NODE,,1,T_B_1L           ! Selecting all the nodes at the ground level of Base Beam
NGEN,2, T_B_1L*4, ALL,,,,B_BDY          ! Generating Nodes at reinforcement level of Beam Base
*GET,T_B_BN,NODE,0,NUM,MAX      ! T_B_BN=Total number of Nodes used in the Base Beam

!***************************************
!ELEMENT GENERATION OF BASE BEAM
!***************************************
TYPE,1
MAT,1
REAL,1

I=1
J=I+1
K=T_B_1L+2
L=K-1
E,I,J,K,L                       ! Creating 1st Base Beam Element at the Ground
EGEN,T_B_1L-1,1,ALL             ! Creating 1st Layer of Base Beam Element at the Ground
EGEN,B_DIVBY,T_B_1L,ALL         ! Creating all the Base Beam Elements

!*********************
!LEFT COLUMN
!*********************
N1LCOLM=T_B_BN+1
N,,-CTX                         ! 1st Node at the upper left corner of left column over
                                ! X axis CTX unit left from origin
N,,COVR-CTX                     ! Position of reinforcement
N,,-CTX/2
N,,-COVR                        ! Position of reinforcement
N,                              ! So far 5 nodes are declared for left Colm of the base.

NSEL,S,NODE,,N1LCOLM,N1LCOLM+DIVCX     ! Selecting Base Column Nodes
NGEN,2,(DIVCX+1),ALL,,,,(FACE_GAP+MRTR) ! Generating Nodes at the height of Interface Gap
NSEL,S,NODE,,N1LCOLM+(DIVCX+1),N1LCOLM+(DIVCX+1)*2-1
! Selecting Column Nodes at Base Brick Level

NGEN,NoBrkY,(DIVCX+1),ALL,,,,BRKh+MRTR
! Generating all the nodes upto 2nd Last Mortar Level

NSEL,S,LOC,Y,WHY-BRKh-MRTR-FACE_GAP,WHY
NGEN,2,(DIVCX+1),ALL,,,,FACE_GAP+MRTR+BRKh

*GET,N_LCOLM,NODE,0,NUM,MAX               ! N_LCOLM= Last Node No. of the Left Column
```

```
!**************************************************
!ELEMENT GENERATION OF LEFT COLUMN
!**************************************************
TYPE,1
MAT,2
REAL,2

I=N1LCOLM
J=I+1
K=N1LCOLM+(DIVCX+1)+1
L=K-1
E,I,J,K,L
ESEL,S,MAT,,2
EGEN,DIVCX,1,ALL
EGEN,(NoBrkY+1),(DIVCX+1),ALL


!*********************************************************
!RIGHT COLUMN
!*********************************************************


T_N_COLM=1-N1LCOLM+N_LCOLM                  ! Total No. of Nodes of a Column

NSEL,S,NODE,,N1LCOLM,N_LCOLM
NGEN,2,T_N_COLM,ALL,,,B*12          ! Generating nodes of 2nd Colm. at a distance of B*12 inch
ESEL,S,MAT,,2
EGEN,2,T_N_COLM,ALL

*GET,N_RCOLM,NODE,0,NUM,MAX     ! N_RCOLM= Last Node No. of the Right Column

!*********************************************************
!BEAM GENERATION
!*********************************************************

!NODE GENERATION

N1BEAM=N_RCOLM+1        ! 1st Node at the upper left corner of the BEAM
N,,-CTX,WHY             ! 1st Node at the upper left corner of the BEAM
N,,COVR-CTX,WHY         ! Position of reinforcement
N,,-CTX/2,WHY
N,,-COVR,WHY            ! Position of reinforcement
N,,,WHY                 ! So far 5 nodes are declared for left Colm of the base.

*GET,N_BMLCL1,NODE,0,NUM,MAX             ! N_BMLCL1=Node No. at the
! bottom of Beam at a Location of Last Node of Left Column

N_BMWN1=N_BMLCL1+1              ! N_BMWN1=Node No. at the bottom of Beam
                               ! at a Location of middle of 1st Brick
N,N_BMWN1,BRKl/2+FACE_GAP,WHY
NSEL,,NODE,,N_BMWN1,N_BMWN1
NGEN,(NoBrkX*2-1),1,ALL,,,(BRKl/2+MRTR/2)
! Generating nodes of the Beam at the position of the bricks

N,,WLX,WHY            ! Node at the bottom of Beam at a Location of 1st Node of Right Column
N,,WLX+COVR,WHY      ! Position of reinforcement
N,,WLX+CTX/2,WHY         ! Location of Middle Node of Colm
N,,WLX-COVR+CTX,WHY      ! Position of reinforcement
N,,WLX+CTX,WHY           ! Last Node of Right Colm Location

*GET,N_BM1L,NODE,0,NUM,MAX       ! Node No. at the end of 1st layer of the Beam
```

```
TN_BM_1L=1-N1BEAM+N_BM1L          ! Total No. of Nodes in the 1st layer of Beam

NSEL,S,NODE,,N1BEAM,N_BM1L        ! Selecting all the nodes at the 1st layer of Beam
NGEN,2, TN_BM_1L, ALL,,,,COVR     ! Generating Nodes at the reinforcement level of Beam
NSEL,S,NODE,,N1BEAM,N_BM1L        ! Selecting all the nodes at the 1st layerl of Beam
NGEN,2, TN_BM_1L*2, ALL,,,,BDY/2  ! Generating Nodes at the mid-level of Beam
NSEL,S,NODE,,N1BEAM,N_BM1L                ! Selecting all the nodes at the 1st layer of Beam
NGEN,2, TN_BM_1L*3, ALL,,,,BDY-COVR      ! Generating nodes at reinforcement level of beam
NSEL,S,NODE,,N1BEAM,N_BM1L                ! Selecting all the nodes at the 1st layer of Beam
NGEN,2, TN_BM_1L*4, ALL,,,,BDY    ! Generating Nodes at the top level of Beam
*GET,L_BM_N,NODE,0,NUM,MAX        ! L_BM_N=Last Node of the Beam at the top layer

! ELEMENT GENERATION

TYPE,1
MAT,3
REAL,3

I=N1BEAM
J=I+1
K=J+TN_BM_1L
L=K-1
E,I,J,K,L
ESEL,S,MAT,,3
EGEN,TN_BM_1L-1,1,ALL
EGEN,DIVBY,TN_BM_1L,ALL


!**********************************************************
!INFILL NODE GENERATION
!**********************************************************


N1_MRTR=L_BM_N+1                     ! 1st Node of INFILL(Mortar Element)
N,,FACE_GAP,FACE_GAP                        ! 1st Node of INFILL
N,,FACE_GAP+BRKl/2-MRTR/2,FACE_GAP
NSEL,S,NODE,,N1_MRTR,N1_MRTR+1
NGEN,NoBrkX*2,2,ALL,,,BRKl/2+MRTR/2
NGEN,2,NoBrkX*2*2,ALL,,,,MRTR
NGEN,NoBrkY+1,NoBrkX*2*2*2,ALL,,,,BRKh+MRTR


!**********************************************************
!INFILL ARRANGEMENT
!**********************************************************


NoLFLBRK= NINT((NoBrkY+0.5)/2)
! NoLFLBRK= No. of BRICK Layers starting with Full Brick
! L=Layer, FL=Full Size Brick

NoLHFBRK= NoBrkY-NoLFLBRK
! NoLHFBRK= No. of BRICK Layers starting with Half Brick
! L=Layer, HF=Half Size Brick

! BRICK, Definition : A Full Brick is composed of 3 Plane Stress elements.
! Each element is a 4 noded Plane42 element.
! Brick Length is divided into 3 segments

!**********************************************************
!BRICK ELEMENT GENERATION
!**********************************************************

TYPE,1
```

```
MAT,4
REAL,4

N1BRK=N1_MRTR+NoBrkX*2*2                          ! Node no. of 1st Brick Position

I=N1BRK
J=I+1
K=I+NoBrkX*2*2+1
L=K-1
E,I,J,K,L

*GET,E1FLBRK1,ELEM,,NUM,MAX                       ! E1FLBRK1= Element Number of 1st
                                                  ! part of a Full BRICK in the 1st Layer

ESEL,S,MAT,,4
EGEN,BRK_DIV,1,ALL                                ! 1st Full Brick is Generated
EGEN,NoBrkX,BRK_DIV+1,ALL                         ! Generating 1st Brick Layer
EGEN,NoLFLBRK,(NoBrkX*2*2)*4,ALL                  ! Generating all the brick layers starting
                                                  ! with Full Size BRICKs

!2ND BRICK LAYER
! Generating alternate layer or the next layer

I=N1_MRTR+(NoBrkX*2*2)*3          ! Node no. of 1st Half Brick Position
J=I+1
K=I+NoBrkX*2*2+1
L=K-1
E,I,J,K,L                         ! Generating 1st Half Brick

*GET,E1HFBRK2,ELEM,,NUM,MAX       ! E1HFBRK2= Element Number of 1st
! Half BRICK in the 2nd Layer; E1HFBRK2, Here 1HF = 1st Half Brick, 2 = 2nd Layer

I=I+2
J=J+2
K=K+2
L=L+2
E,I,J,K,L                         ! Generating 1st part of 2nd Brick in the 2nd Layer

*GET,E2FLBRK2,ELEM,,NUM,MAX       ! E2FLBRK2= Element Number of 1st
! part of a Full BRICK in the 2nd Layer
! E2FLBRK2, Here 2= 2nd brick, FL = part of a Full Brick, 2 = 2nd Layer

ESEL,S,ELEM,,E2FLBRK2              ! Selecting the 1st part of Full BRICK in the 2nd Layer
EGEN,BRK_DIV,1,ALL                ! 1st Full Brick is Generated in the 2nd Layer
EGEN,NoBrkX-1,BRK_DIV+1,ALL            ! Generating 2nd Brick Layer except last half Brick
ESEL,S,ELEM,,E1HFBRK2,E1HFBRK2    ! Selecting the 1st  Half BRICK in the 2nd Layer
EGEN,2,(NoBrkX*2-1)*2,ALL     ! Creating the last brick of the 2nd Layer which is a Half BRICK

*GET,ELSTBRK2,ELEM,,NUM,MAX       ! ELSTBRK2= Element Number of last
                                  ! Half BRICK in the 2nd Layer
! There are "NoLHFBRK" No. of BRICK Layers starting with Half Brick
ESEL,S,ELEM,,E1HFBRK2,ELSTBRK2    ! Selecting all the bricks in the 2nd Layer
EGEN,NoLHFBRK,(NoBrkX*2*2)*4,ALL ! Generating all the brick layers starting
                                  ! with Full Size BRICKs
! Creating Mortar Layer in between Brick Layers

TYPE,1
MAT,5
REAL,5

I=N1_MRTR
J=I+1
```

```
K=I+NoBrkX*2*2+1
L=K-1
E,I,J,K,L                              ! Generating 1st part of Mortar
ESEL,S,MAT,,5
EGEN,NoBrkX*2*2-1,1,ALL
EGEN,NoBrkY+1,(NoBrkX*2*2)*2,ALL
!*****************************************************************
!Generating Mortar Elements in between Bricks in 1st,3rd,,,,,layers
!*****************************************************************
! Generating Mortar Elements in Brick Layers starting with Full Brick

I=N1BRK+BRK_DIV
J=I+1
K=I+NoBrkX*2*2+1
L=K-1
E,I,J,K,L                   ! Generating 1st part of Mortar in betn Bricks

*GET,E1BMRTR1,ELEM,,NUM,MAX      ! E1BMRTR1= Element Number of 1st
                                 ! part of MORTAR in betn Bricks
ESEL,S,ELEM,,E1BMRTR1            ! Selecting 1st part of 1st MORTAR
                                 ! element of 1st row of BRICK Layers
EGEN,NoBrkX-1,1+BRK_DIV,ALL      ! Generating All the MORTAR elements
                                 ! in the 1st BRICK Layers, starting with a Full BRICK
EGEN,NoLFLBRK,(NoBrkX*2*2)*4,ALL ! Generating All the MORTAR elements
                                 ! in all the BRICK Layers, starting with a Full BRICK


!*****************************************************************
!Generating Mortar Elements in between Bricks in 2nd,4th,,,,,layers
!*****************************************************************

!Generating MORTAR elements in BRICK layers starting with a Half Brick
I=N1BRK+(NoBrkX*2*2)*2+1
J=I+1
K=I+NoBrkX*2*2+1
L=K-1
E,I,J,K,L                                ! Generating 1st part of Mortar in betn Bricks

*GET,E1BMRTR2,ELEM,,NUM,MAX     ! E1BMRTR2= Element Number of 1st
! MORTAR in the 2nd BRICK Layer starting with a Half Brick

ESEL,S,ELEM,, E1BMRTR2                   ! Selecting 1st MORTAR element of 2nd row of
                                         ! BRICK Layers starting with a Half Brick
EGEN,NoBrkX,1+BRK_DIV,ALL ! Generating All the MORTAR elements in the
! 2nd BRICK Layers, starting with a Half BRICK

EGEN,NoLHFBRK,(NoBrkX*2*2)*4,ALL ! Generating All the MORTAR elements
! in the BRICK Layers, starting with a Half BRICK

!********************************
!Reinforcing Base Beam
!********************************

TYPE,2
MAT,6
REAL,6

N1FR_BBM=1+T_B_1L  !1st Node of 1st Layer of Reinforcement of Base Beam
N1MR_BBM=N1FR_BBM+T_B_1L         !1st Node of Middle Layer of
                                 ! Reinforcement of Base Beam
N1LR_BBM=N1MR_BBM+T_B_1L         !1st Node of Last Layer of
```

```
                                    ! Reinforcement of Base Beam
*DO,I,1,T_B_1L-1

I=I-1
E,N1FR_BBM+I,N1FR_BBM+I+1        ! Reinforcement in Bottom Layer of BaseBeam
*ENDDO
*DO,I,1,T_B_1L-1
I=I-1
E,N1LR_BBM+I,N1LR_BBM+I+1        ! Reinforcement in Top Layer of BaseBeam

*ENDDO

ESEL,S,MAT,,6

!********************************
!REINFORCING 2 COLUMNS
!********************************

TYPE,2
MAT,9
REAL,7

!Reinforcing LEFT COLUMN

No_NCOLM=N_LCOLM-N1LCOLM+1       ! No. of Nodes in a Column
LR_NCOLM=No_NCOLM/(DIVCX+1)      ! No. of Nodal Layers in a Column

!Reinforcing Left Side of Left Column
*DO,NUM,1,LR_NCOLM-1
NUM=NUM-1
I=N1LCOLM+NUM*(DIVCX+1)+1
J=I+(DIVCX+1)
E,I,J
*END DO

!Reinforcing Middle of Left Column
*DO,NUM,1,LR_NCOLM-1
NUM=NUM-1
I=N1LCOLM+NUM*(DIVCX+1)+(DIVCX/2)        ! DIVCX=EVEN
J=I+(DIVCX+1)
E,I,J
*END DO

!Reinforcing Right Side of Left Column
*DO,NUM,1,LR_NCOLM-1
NUM=NUM-1
I=N1LCOLM+NUM*(DIVCX+1)+DIVCX-1
J=I+(DIVCX+1)
E,I,J
*END DO

*GET,LENo_RC1,ELEM,,NUM,MAX
! LENo_RC1= Last Element Number of Reinforcement in Left Column1

! Extending COLUMN Reinforcement into the Base Beam

*DO,NUM,1,B_DIVBY
I=B_DIVEBX+2+T_B_1L*(NUM-1)
J=I+T_B_1L
E,I,J
```

```
*END DO

*DO,NUM,1,B_DIVBY
I=B_DIVEBX+1+DIVCX/2+T_B_1L*(NUM-1)
J=I+T_B_1L
E,I,J
*END DO

*DO,NUM,1,B_DIVBY
I=B_DIVEBX+DIVCX+T_B_1L*(NUM-1)
J=I+T_B_1L
E,I,J
*END DO

! EXTENDING COLUMN REINFORCEMENT INTO THE TOP BEAM

*DO,NUM,1,DIVBY
I=N1BEAM+1+TN_BM_1L*(NUM-1)
J=I+TN_BM_1L
E,I,J
*END DO

*DO,NUM,1,DIVBY
I=N1BEAM+DIVCX/2+TN_BM_1L*(NUM-1)
J=I+TN_BM_1L
E,I,J
*END DO

*DO,NUM,1,DIVBY
I=N1BEAM+DIVCX-1+TN_BM_1L*(NUM-1)
J=I+TN_BM_1L
E,I,J
*END DO

*GET,E_L_R_C,ELEM,,NUM,MAX        ! E_L_R_C= Element Number of Last
! Reinforcement Extending from Column into Beam

!***************************
!Reinforcing RIGHT COLUMN
!***************************
REAL,7

ESEL,S,ELEM,,(LENo_RC1-(LR_NCOLM-1)*3+1),LENo_RC1
EGEN,2,No_NCOLM,ALL

! Extending Reinforcement from Right Column into Base Beam and Top Beam

ESEL,S,ELEM,,E_L_R_C-(DIVBY+B_DIVBY)*3+1,E_L_R_C-DIVBY*3
! Selecting the extended reinforcement of Left Column into Base Beam

EGEN,2,NoBrkX*2+DIVCX,ALL
! Extending Reinforcement into Base Beam


ESEL,S,ELEM,,E_L_R_C-DIVBY*3+1,E_L_R_C
! Selecting the extended reinforcement of Left Column into Top Beam

EGEN,2,NoBrkX*2+DIVCX,ALL
! Extending Reinforcement into Top Beam
```

```
!********************************
!Reinforcing Beam
!********************************

REAL,8

! N1BEAM=1st Node of the Beam
! L_BM_N=Last Node of the Beam at the top layer
! TN_BM_1L=Total No. of Nodes in the 1st layer of Beam


! Reinforcing Bottom Layer of Reinforcment in Beam
*DO,NUM,1,TN_BM_1L-1
I=N1BEAM+TN_BM_1L+NUM-1
J=I+1
E,I,J
*END DO

! Reinforcing Top Layer of Reinforcment in Beam
*DO,NUM,1,TN_BM_1L-1
I=N1BEAM+TN_BM_1L*(DIVBY-1)+NUM-1
J=I+1
E,I,J
*END DO


!************************************************
!CREATING A WEDGE AT THE LEFT OF LEFT COLUMN
!************************************************

*GET,LASTNODE,NODE,,NUM,MAX

N1WEDGE=LASTNODE+1

!NODE GENERATION
N,,-CTX-(BDY-2*COVR)/2,WHY+COVR+(BDY-2*COVR)/4              !N1WEDGE
N,,-CTX-(BDY-2*COVR)/2,WHY+BDY/2
N,,-CTX-(BDY-2*COVR)/2,WHY+BDY-COVR-(BDY-2*COVR)/4
N,,-CTX-(BDY-2*COVR),WHY+BDY/2

!ELEMENT GENERATION

N_1LBEAM=(DIVBY+1)*2+NoBrkX*2-1

TYPE,1
REAL,10
MAT,8

I=N1BEAM+N_1LBEAM
J=I+N_1LBEAM
K=N1WEDGE+1
L=N1WEDGE
E,I,J,K,L

I=N1BEAM+N_1LBEAM*2
J=I+N_1LBEAM
K=N1WEDGE+2
L=N1WEDGE+1
E,I,J,K,L
```

```
TYPE,1
REAL,9
MAT,8

I=N1WEDGE
J=N1WEDGE+1
K=N1WEDGE+3
L=N1WEDGE+3
E,I,J,K,L

I=N1WEDGE+1
J=N1WEDGE+2
K=N1WEDGE+3
L=N1WEDGE+3
E,I,J,K,L

!*********************************************
! APPLYING FERROCEMENT IN INFILL
!*********************************************

! Ferrocement is modeled by plane stress elements. 1st Strip of Ferrocement consists of bottom layer
! mortar first layer brick, then again mortar layer(just above the 1st brick layer) and finally, the second
! brick layer. 1st Strip of ferrocement elements are generated along the length of the infill. Then this
! layer is continued upward in the same fashion. If the no. of brick layers is even then only the last
! ferrocement layer will consist of an extra topmost mortar layer. If the no. of brick layers is odd then
! ferrocement strips are generated upto the whole no. of NoBrkY/2 layers. And the last ferrocement
! layer will consist of only a single brick layer with mortar layer at its top and bottom

TYPE,1
MAT,10
REAL,11

I=N1_MRTR
J=I+4
K=J+(NoBrkX*2*2)*4
L=K-4
E,I,J,K,L
ESEL,S,MAT,,10
EGEN,NoBrkX-1,4,ALL,,,

I=N1_MRTR+NoBrkX*2*2-4
J=I+3
K=J+(NoBrkX*2*2)*4
L=K-3
E,I,J,K,L

ODD_EVEN=NoBrkY-(NINT(NoBrkY/2)-1)*2        ! NINT(5/2)=3 Upper Rounding

! Say for EVEN no.s, If NoBrkY=50, Then ODD_EVEN=50-24*2=2
! Say for ODD no.s If NoBrkY=51, Then ODD_EVEN=51-25*2=1

! For ODD no.s of Brick Layers. ODD_EVEN = 1

*IF,ODD_EVEN,EQ,1,THEN
EGEN,NINT(NoBrkY/2)-1,(NoBrkX*2*2)*4,ALL

IL=N1_MRTR+(NoBrkX*2*2)*4*(NINT(NoBrkY/2)-1)
JL=IL+4
KL=JL+(NoBrkX*2*2)*3
LL=KL-4
```

```
E,IL,JL,KL,LL    ! Creating 1st Element of Last Layer of Ferrocement

*GET,FR_ODD,ELEM,,NUM,MAX                    ! 1st Element of Last Layer of Ferrocement
ESEL,S,ELEM,,FR_ODD,FR_ODD
EGEN,NoBrkX-1,4,ALL,,,

I1=IL+NoBrkX*2*2-4
J1=I1+3
K1=J1+(NoBrkX*2*2)*3
L1=K1-3
E,I1,J1,K1,L1

! For EVEN no.s of Brick Layers, ODD_EVEN = 2

*ELSE
EGEN,NoBrkY/2-1,(NoBrkX*2*2)*4,ALL

IL=N1_MRTR+(NoBrkX*2*2)*4*(NoBrkY/2-1)
JL=IL+4
KL=JL+(NoBrkX*2*2)*5
LL=KL-4
E,IL,JL,KL,LL                ! Creating 1st Element of Last Layer of Ferrocement

*GET,FR_EVEN,ELEM,,NUM,MAX          ! 1st Element of Last Layer of Ferrocement

ESEL,S,ELEM,,FR_EVEN,FR_EVEN
EGEN,NoBrkX-1,4,ALL,,,

I1=IL+NoBrkX*2*2-4
J1=I1+3
K1=J1+(NoBrkX*2*2)*5
L1=K1-3
E,I1,J1,K1,L1

*ENDIF


!**************************
!MERGE
!**************************
ALLSEL
NUMMRG,NODE
NUMMRG,ELEM
NUMCMP,NODE
NUMCMP,ELEM

!**********************************
!KILLING ALL THE FERROCEMENT
!**********************************

ESEL,S,MAT,,10
EKILL,ALL              ! Deactivates Ferrocement
ALLSEL

!*********************************************
!SUPPORT CONDITIONS
!*********************************************

NSEL,S,LOC,X,-CTX,-(B_EXT*12+CTX)
NSEL,R,LOC,Y,-B_BDY,-B_BDY
```

```
D,ALL,ALL

NSEL,S,LOC,X,B*12,B_EXT*12+B*12
NSEL,R,LOC,Y,-B_BDY,-B_BDY
D,ALL,ALL

!************************************************
! NUMBERING MATERIAL NUMBERS BY COLORS ONLY
!************************************************

ALLSEL
/NUM,1
/PNUM,MAT,1
/REPLOT
GPLOT

! GRAPHICS DISPLAY OF ALL FORCES AND BOUNDARY CONDITIONS
/PBC,ALL,,1
/PBC,NFOR,,0
/PBC,NMOM,,0
/PBC,RFOR,,0
/PBC,RMOM,,0
/PBC,PATH,,0
/REP

!*************************************************************
!Nonlinear Control and Displacement Steps
!*************************************************************

/SOLU
ANTYPE,STATIC

NLGEOM,ON                ! Turns large-deflection effects on
EQSLV,SPARSE
NROPT,FULL

NEQIT,100
AUTOTS,ON

DEF_STEP=300

*DO,I,1,DEF_STEP

! Now selecting the nodes (except top and bottom) at the face of the
! column, which intersects with beam.

NSEL,S,LOC,X,-CTX-(BDY-2*COVR)
NSEL,R,LOC,Y,WHY+BDY/2

*IF,I,LE,8,THEN
D,ALL,UX,I*0.01                    !***APPLYING DISPLACEMENTS****
ALLSEL
NSUBST,4,20,2

*ELSEIF,I,LE,15
D,ALL,UX,0.08+(I-8)*0.0025      !***APPLYING DISPLACEMENTS****
ALLSEL
NSUBST,8,25,4

*ELSE
```

```
D,ALL,UX,0.0975+(I-15)*0.001    !***APPLYING DISPLACEMENTS****
ALLSEL
NSUBST,8,25,5

*ENDIF

OUTRES,ALL,6
LSWRITE,I

*ENDDO

LSSOLVE,1,DEF_STEP,1

SAVE

!***********************************************
!KILLING ELEMENTS WHOSE STRESS EXCEEDS 400psi
!***********************************************

/POST1                      ! Enter POST1
SET,...
ETABLE,STRESS,S,1           ! Store total equivalent strain in ETABLE
ESEL,S,ETAB,STRESS,400      ! Select all elements with total equivalent stress
                            ! greater than or equal to 400

FINISH
/PREP7
EKILL,ALL                   ! Deactivate selected (overstrained) elements
ALLSEL


!*************************
!UNLOADING
!*************************
!********************************************************************
!Nonlinear Control and Displacement Steps for UNLOADING
!********************************************************************
/SOLU
ANTYPE,STATIC
NLGEOM,ON                 ! Turns large-deflection effects on
EQSLV,SPARSE
NROPT,FULL
NEQIT,100
AUTOTS,ON

DEF_STEP=125

*DO,I,1,DEF_STEP
! Now selecting the nodes (except top, bottom) at the face of the column, which intersects with beam.
NSEL,S,NODE,,3690,3690

*IF,I,LE,150,THEN
D,ALL,UX,0.3825-I*0.001        !***APPLYING DISPLACEMENTS****
ALLSEL
NSUBST,8,25,5

*ELSEIF,I,LE,250
D,ALL,UX,0.2325-(I-150)*0.001  !***APPLYING DISPLACEMENTS****
ALLSEL
NSUBST,8,25,4
*ELSE
D,ALL,UX,0.1325-(I-250)*0.001  !***APPLYING DISPLACEMENTS****
```

```
ALLSEL
NSUBST,8,25,5
*ENDIF
OUTRES,ALL,7
LSWRITE,I
*ENDDO

LSSOLVE,1,DEF_STEP,1
SAVE
FINISH

!**************************************
!ACTIVATE THE FERROCEMENT ELEMENTS
!**************************************
/PREP7
ESEL,S,MAT,,10
EALIVE,ALL              ! Activates Ferrocement
ALLSEL

!*********************************************
!PRE-LOADING WITH DISPLACEMENT STEP CONTROL
!*********************************************
/SOLU
ANTYPE,STATIC
NLGEOM,ON              ! Turns large-deflection effects on
EQSLV,SPARSE
NROPT,FULL
NEQIT,100
AUTOTS,ON

DEF_STEP=300

*DO,I,1,DEF_STEP
! Now selecting the nodes (except top and bottom) at the face of the
! column, which intersects with beam.
NSEL,S,NODE,,3690,3690
*IF,I,LE,150,THEN
D,ALL,UX,0.2575+I*0.001        !***APPLYING DISPLACEMENTS****
ALLSEL
NSUBST,8,25,4

*ELSEIF,I,LE,250
D,ALL,UX,0.4075+(I-150)*0.001  !***APPLYING DISPLACEMENTS****
ALLSEL
NSUBST,8,25,5

*ELSE
D,ALL,UX,0.5075+(I-250)*0.001  !***APPLYING DISPLACEMENTS****
ALLSEL
NSUBST,8,25,6

*ENDIF

OUTRES,ALL,6
LSWRITE,I

*ENDDO

LSSOLVE,1,DEF_STEP,1
SAVE
```

APPENDIX C

```
! ----------------------------------------------------------------------------------------------------
! Author:
!                                   M. Shahria Alam
!                                   Lecturer
!                                   Dept. of Civil Engineering
!                                   BUET, Dhaka-10000.
!----------------------------------------------------------------------------------------------------
! As a part of the thesis work "Numerical Modeling of Masonry Infill Panels Retrofitted with Ferro-
! cement" for the partial fulfillment of M.Sc. in Civil Engineering (Structural).
!*********************************************************************************************
! This is a 3 dimensional FE model of masonry infilled Reinforced Concrete Frame
! This model is used to investigate load-deflection response when subjected to lateral load
!*********************************************************************************************


/PREP7
ANTYPE,STATIC

!*****************PARAMETER*****************
fc=4000                 !psi (fc' of concrete)
NUc=0.15                ! poission's ratio of conc.
Cdens=150/(12**3)       ! #/in^3 (density of conc.)
H=10                    ! ft ( colm height) f/f distance
B=14                    ! ft ( beam length) c/c distance
WWZ=5                   ! in (wall thickness)
CTX=18                  ! in (colm thickness along span length)
CTZ=12                  ! in (colm thinckness |_ to span length also |_ to the computer screen)
BDY=18                  ! in (beam depth)
BTZ=CTZ                 ! in (Beam width)
B_EXT=2                 ! in ft Base Beam Extended upto B-EXT
B_BM_DX=4               ! in inches Base Beam Extended size/Division = 4"
B_BDY=24                ! in (BASE Beam depth)
B_BTZ=CTZ               ! in (BASE Beam width)
COVR=2.5                ! in ( cover = clear cover + 1/2 dia of the bar)
FACE_GAP=0.02           ! in ( Gap between frame and wall consider 0.5mm)

WLX=B*12-CTX                         Colm-Colm clear distance
WHY=H*12-BDY                         Colm clear height
WLX_GAP=B*12-CTX-2*FACE_GAP          ! Wall length considering Gap
WHY_GAP=H*12-BDY-2*FACE_GAP          ! Wall Height Considering Gap

!****BRICK and MORTAR SIZE******
BRKl=20                 ! in (Brick length)
BRKw=6.5                ! in (Brick Width)
BRKh=6                  ! in (Brick height)
MRTR=2.25               ! in (Mortar height)

!*******INFILL ARRANGEMENT******
NoBrkX=NINT((WLX_GAP+MRTR)/(BRKl+MRTR))              ! No of bricks in one layer
NoBrkY=NINT((WHY_GAP+MRTR)/(BRKh+MRTR))              ! No of brick layers in the infill

!*******RESIZING OF BRICKS*********        ! Using NoBrkX and NoBrkY
BRKl=(WLX-(NoBrkX-1)*MRTR)/NoBrkX          ! Brick Length without considering gap
BRKh=(WHY-(NoBrkY-1)*MRTR)/NoBrkY          ! Brick Height without considering gap

BRKl_GAP=(WLX_GAP-(NoBrkX-1)*MRTR)/NoBrkX
BRKh_GAP=(WHY_GAP-(NoBrkY-1)*MRTR)/NoBrkY

!*************LOAD***************
P=10000 ! #                 ! Load applied in the portal
```

```
!*******************CALCULATION***************
EXr=29E6                  ! psi ( Modulus of Elasticity of Mild Steel)
Rdens=2                   ! lb/in^3 ( Density of Mild Steel)
AREAr=0.8                 ! in^2 ( Area of a single bar)
EXc=57000*SQRT(fc)        ! psi ( Modulus of Elasticity of Conc.)
Gc=EXc/(2*(1+NUc))        ! psi (Shearing Modulus of Elasticity of Conc.)
AREAc=CTX*CTZ             ! in^2 (Colm area)
MUc=0.35                  ! Coefficient of friction


! Material Property of Brick
EXb=2.3E6                 ! psi ( Modulus of Elasticity of Mild Steel)
Bdens=0.0695             ! lb/in^3 ( Density of Mild Steel)
Gb=EXb/(2*(1+NUc))       !psi (Shearing Modulus of Elasticity of Conc.)

IZZc=CTZ*(CTX**3)/12             ! in^4 ( Moment of Inertia of Colm about Z axis)
IYYc=CTX*(CTZ**3)/12             ! in^4 ( Moment of Inertia of Colm about X axis)
IXXc=IZZc+IYYc
AREAb=BDY*BTZ                    ! in^2 (Beam area)
IZZb=BTZ*(BDY**3)/12            ! in^4 ( Moment of Inertia of Beam about Z axis)
IYYb=BDY*(BTZ**3)/12            ! in^4 ( Moment of Inertia of Beam about Y axis)
IXXb=IZZb+IYYb


!*************DIVISION****************

NDIVWZ=2                  ! Even
WP=(CTZ-WWZ)/2            ! Wall Position w.r.t colm mid
DIVCX=4                   ! Column is divided into 4 segments along X axis
DIVCZ=DIVCX               ! Column is divided into 4 segments along Z axis
DIVBY=4                   ! Beam is divided into 4 segments along Y axis
DIVBZ=DIVBY               ! Beam is divided into 4 segments along Z axis
B_DIVBY=4                 ! Base Beam Extended portion is divided into 4 segments along Y axis
B_DIVEBX=NINT(B_EXT*12/B_BM_DX)           ! Base Beam Extended portion is divided into
B_DIVEBX
DIV_BBZ=DIVBZ             ! Base Beam is divided into 4 segments along Z axis
DIVWZ=2                   ! Wall is divided into 2 segments along Z axis


!*****************************
! ELEMENTS USED
!*****************************
ET,1,SOLID65,,,,,2        ! Nodal Stress Print Out  KEYOPT(5)=2
ET,2,SOLID45
ET,3,LINK8
ET,4,TARGE170
ET,5,CONTA173


!*****************************
!REAL CONSTANTS
!*****************************
R,3,AREAr
R,4,0,S_Z,1, ,0.001, ,
RMORE, , ,,FACE_GAP, , ,
RMORE, ,


!*****************************
!MATERIAL PROPERTIES
!*****************************
!Column Material Properties
MP,DENS,1,Cdens
MP,EX,1,EXc
```

```
MP,NUXY,1,NUc
MP,GXY,1,Gc
MP,MU,1,MUc

!***Defining  BEAM material properties******
MP,DENS,2,Cdens
MP,EX,2,EXc
MP,NUXY,2,NUc
MP,GXY,2,Gc
MP,MU,2,MUc

!***** Defining BRICK material property
MP,DENS,3,Bdens
MP,EX,3,EXb
MP,NUXY,3,NUc
MP,GXY,3,Gb
MP,MU,3,MUc

!***** Defining material property of MORTAR***********
MP,DENS,4,Cdens
MP,EX,4,EXc
MP,NUXY,4,NUc
MP,GXY,4,Gc
MP,MU,4,MUc

!Defining Material Properties of Reinforcement
MP,DENS,5,Rdens
MP,EX,5,EXr

!***Defining  Base BEAM material properties******
MP,DENS,6,Cdens
MP,EX,6,EXc
MP,NUXY,6,NUc
MP,GXY,6,Gc
MP,MU,6,MUc


!****************COLUMN******************
N,1,-CTX          ! Node 1 at the upper left corner of left column over X axis CTX unit left from origin
N,2,COVR-CTX ! Position of reinforcement
N,3,-CTX/2
N,4,-COVR
N,5                ! So far 5 nodes are declared for left Colm of the base.
NGEN,2,DIVCX+1,1,DIVCX+1,1,0,0,COVR          ! Generating another row of parallel nodes
NSEL,S,LOC,Y,0
NSEL,R,LOC,Z,0                                       Selecting 1st row nodes
NGEN,2,(DIVCX+1)*2,1,DIVCX+1,1,0,0,CTZ/2    ! Generating midplane(X-X) nodes at the base

NSEL,S,LOC,Y,0
NSEL,R,LOC,Z,0                              ! Selecting 1st row nodes
NGEN,2,(DIVCX+1)*3,1,DIVCX+1,1,0,0,CTZ-COVR
NSEL,S,LOC,Y,0
NSEL,R,LOC,Z,0
NGEN,2,(DIVCX+1)*4,1,DIVCX+1,1,0,0,CTZ


ALLSEL

! We will generate nodes for column @ (1 layer Brick + 1 layer Mortar ) upto (NoBrkY-1) layers of bricks.
!  i.e. last layer of brick is not generated. It will be generated later.
```

```
! Generating the 2nd row of nodes
NSEL,S,NODE,,1,(DIVCX+1)*(DIVCZ+1)
NGEN,2,(DIVCX+1)*(DIVCZ+1),ALL,,,0,BRKh,0
! (DIVCX+1)*(DIVCZ+1) = Total nodes of a colm at the base

NGEN,NoBrkY,((DIVCX+1)**2)*2,ALL,,,0,BRKh+MRTR,0
! (DIVCX+1)**2 = Total nodes of a colm at the base

NSEL,S,LOC,Y,((BRKh+MRTR)*(NoBrkY-1)+BRKh)
! Selecting nodes of the column at a height of  the interface of wall and beam

NGEN,2,(DIVCX+1)**2,ALL,,,0,COVR,0
! Generating nodes of the column at a height of bottom layer reinforcement of the beam

NSEL,S,LOC,Y,WHY+COVR
! Selecting nodes of the column at a height of reinforcement of the beam

NGEN,2,(DIVCX+1)**2,ALL,,,0,BDY/2-COVR,0
! Generating nodes of the column at the mid-height of the beam

NSEL,S,LOC,Y,WHY+BDY/2
! Selecting nodes of the column at the mid-height of the beam

NGEN,2,(DIVCX+1)**2,ALL,,,0,BDY/2-COVR
! Generating nodes of the column at a height of top layer reinforcement of the beam

NSEL,S,LOC,Y,H*12-COVR
! Selecting nodes of the column at a height of upper layer reinforcement of the beam

NGEN,2,(DIVCX+1)**2,ALL,,,0,COVR
! Generating nodes of the column at the top most layer

ALLSEL

TYPE,1
MAT,1

! For creating the 1st element of the column we have to name the 8 nodes
! which are 1,6,7,2,26,31,32,27   see node arrangements in the base_nodes of column.txt
I=1
J=I+DIVCX+1
K=J+1
L=I+1
M=I+(DIVCX+1)**2
N=J+(DIVCX+1)**2
O=K+(DIVCX+1)**2
P=L+(DIVCX+1)**2
E,I,J,K,L,M,N,O,P                    ! Creating 1st element at the base
EGEN,4,1,ALL                         ! Creating 1st row of elements
ESEL,S,MAT,,1
EGEN,4,(DIVCX+1),ALL                 ! Creating base layer of elements
ESEL,S,MAT,,1
EGEN,(NoBrkY*2-1+DIVBY),(DIVCX+1)*(DIVCZ+1),ALL
! Creating the whole column with Solid45 elements

!*************CREATING 2ND COLUMN********************

*GET,NMAXC1,NODE,0,NUM,MAX           !NMAXC1= Total no. of nodes of 1st column

NSEL,S,NODE,,1,NMAXC1
```

```
NGEN,2,NMAXC1,ALL,,,B*12              ! Generating nodes of 2nd Column at a distance of B*12 inch
ESEL,S,MAT,,1
EGEN,2,NMAXC1,ALL                     ! Generating elements in the 2nd Column


!*******************BEAM*******************

ALLSEL
*GET,NALL2C,NODE,0,NUM,MAX            ! NALL2C = Total no. of nodes in 2 columns
N1BEAM=NALL2C+1                       ! N1BEAM = 1st node of the Beam
N,N1BEAM,,WHY                         ! Defining 1st beam node at the interface of left column (0,WHY,0)
N,N1BEAM+1,,WHY,COVR
N,N1BEAM+2,,WHY,BTZ/2
N,N1BEAM+3,,WHY,BTZ-COVR
N,N1BEAM+4,,WHY,BTZ


NSEL,S,NODE,,N1BEAM,N1BEAM+DIVBZ      ! Selecting nodes of the 1st row of beam
NGEN,2,DIVBZ+1,ALL,,,,COVR           ! Generating another row above the 1st row
NSEL,S,NODE,,N1BEAM,N1BEAM+DIVBZ      ! Selecting nodes of the 1st row of beam
NGEN,2,(DIVBZ+1)*2,ALL,,,,BDY/2       ! Generating 3rd row of nodes above the 2nd row
NSEL,S,NODE,,N1BEAM,N1BEAM+DIVBZ      ! Selecting nodes of the 1st row of beam
NGEN,2,(DIVBZ+1)*3,ALL,,,,BDY-COVR    ! Generating 4th row of nodes above the 3rd row
NSEL,S,NODE,,N1BEAM,N1BEAM+DIVBZ      ! Selecting nodes of the 1st row of beam
NGEN,2,(DIVBZ+1)*4,ALL,,,,BDY         ! Generating top row of nodes of the beam


NSEL,S,NODE,,N1BEAM,N1BEAM+(DIVBZ+1)*(DIVBY+1)-1
! Selecting the nodes at the left most X-sec of the beam

NGEN,2,(DIVBZ+1)*(DIVBY+1),ALL,,,BRKl/2-MRTR/2
! Generating nodes upto the (1st 1/2 brick-1/2 mortar size)

NSEL,S,NODE,,N1BEAM,N1BEAM+2*(DIVBZ+1)*(DIVBY+1)-1
! Selecting the nodes at the left most two X-sec of the beam

NGEN,NoBrkX*2,(DIVBZ+1)*(DIVBY+1)*2,ALL,,,(BRKl/2+MRTR/2)
! Generating nodes upto the 2nd last brick of a layer

ALLSEL

TYPE,1
MAT,2

I=N1BEAM
J=I+(DIVBZ+1)*(DIVBY+1)
K=J+1
L=I+1
M=I+DIVBZ+1
N=M+(DIVBZ+1)*(DIVBY+1)
O=N+1
P=M+1
E,I,J,K,L,M,N,O,P                     ! Creating 1st beam element
ESEL,S,MAT,,2
EGEN,DIVBZ,1,ALL                      ! Creating 1st row of beam element
EGEN,DIVBY,DIVBZ+1,ALL                ! Creating 1st base beam elements
EGEN,NoBrkX*4-1,(DIVBZ+1)*(DIVBY+1),ALL  ! Creating beam elements upto 2nd last element row

*GET,EMAXBEAM,ELEM,0,NUM,MAX
! Getting the last element no.=EMAXBEAM of the last element of beam
```

!*****************INFILL WALL***************

! NODE GENERATION

*GET,NBEAMLST,NODE,0,NUM,MAX   ! NBEAMLST= Last node of the beam element

N1WALL=NBEAMLST+1   !N1WALL= Starting node of the wall element at the base

N,N1WALL,FACE_GAP,FACE_GAP,(CTZ/2-WWZ/2)   ! 1st Wall Node Location
FACE_GAP,FACE_GAP,(CTZ/2-WWZ/2)
NGEN,DIVWZ+1,1,N1WALL,N1WALL+DIVWZ,1,,,WWZ/DIVWZ
! 1st row of wall nodes at the base(ground) along column face

NSEL,S,NODE,,N1WALL,N1WALL+DIVWZ   ! Selecting 1st row of wall nodes
NGEN,2,DIVWZ+1,ALL,,,BRKl_GAP/2-MRTR/2
! Generating lower part of the nodes of the 1st 1/2brick-1/2mortar at the base
NGEN,NoBrkX*2,(DIVWZ+1)*2,ALL,,,(BRKl_GAP/2+MRTR/2)
! Generating all the nodes of the brick at the lower part
NGEN,2,(DIVWZ+1)*2*NoBrkX*2,ALL,,,BRKh_GAP
! Generating upper nodes of the 1st brick layer

NSEL,S,NODE,,N1WALL,N1WALL+(DIVWZ+1)*2*NoBrkX*2*3-1
! Selecting all brick nodes of the 1st layer
NGEN,NoBrkY,(DIVWZ+1)*2*NoBrkX*2*2,ALL,,,,BRKh_GAP+MRTR
! Generating all the nodes of other brick layers

!ELEMENT GENERATION

TYPE,2
MAT,3

! Now defining a brick with a 8 noded solid element
! Brick layer is composed in this way ---- |_____||_____|M|_____||_____|M|_____ ; M means mortar
! In the vertical direction, in 1 layer it starts with 1 full brick then in the latter layer it starts with a 1/2 brick
! Thus the alternate arrangement continues
! In this way   Starts with Full Brick-> |_____|M|_____|M|_____| ----------------
!   Starts with Half Brick->|__|M|_____|M|_____|M|_____| ------------
! If BRICK Layers are odd number (Say 5 Layers) then it will start with Full size
! AND If BRICK Layers are even number(Say 4 Layers) then it will start with Half size

NoLFLBRK= NINT((NoBrkY+0.5)/2)   ! NoLFLBRK= No. of BRICK Layers starting with Full Brick
                                      ! L=Layer, FL=Full Size Brick
NoLHFBRK= NoBrkY-NoLFLBRK   ! NoLHFBRK= No. of BRICK Layers starting with Half Brick
                                      ! L=Layer, HF=Half Size Brick

! BRICK
! Definition : A Full Brick is composed of six solid elements. Each element is a 8 noded solid45 element.
! Brick Length is divided into 3 segments and Brick Width is divided into 2 segments.
! There is division along Brick Height

I=N1WALL   ! Defining 1st part of a brick
J=I+(DIVWZ+1)
K=J+1
L=I+1
M=I+(DIVWZ+1)*2*NoBrkX*2
N=M+(DIVWZ+1)
O=N+1
P=M+1
E,I,J,K,L,M,N,O,P

```
*GET,E1FLBRK1,ELEM,,NUM,MAX
! E1FLBRK1= Element Number of 1st part of a Full BRICK in the 1st Layer
! E1FLBRK1, Here 1= 1st part of 1st brick, FL = part of a Full Brick, 1 = 1st Layer


ESEL,S,MAT,,3
EGEN,DIVWZ,1,ALL                              ! Generating 1st two leftmost parts of 1st brick
EGEN,3,(DIVWZ+1),ALL                          ! Generating 1st Full BRICK in the base layer
EGEN,NoBrkX,(DIVWZ+1)*4,ALL                   ! Generating 1st brick layer

EGEN,NoLFLBRK,((DIVWZ+1)*2*NoBrkX*2)*2*2,ALL
! Generating all the brick layers starting with Full Size BRICKs


!**********2ND BRICK LAYER***********
! Generating alternate layer or the next layer

I=N1WALL+((NoBrkX*2)*2*(DIVWZ+1))*2  !1st Node at the 2nd brick layer which starts with a 1/2 brick
J=I+(DIVWZ+1)
K=J+1
L=I+1
M=I+(DIVWZ+1)*2*NoBrkX*2
N=M+(DIVWZ+1)
O=N+1
P=M+1
E,I,J,K,L,M,N,O,P                             ! Creating 1st part of a 1/2 brick

*GET,E1HFBRK2,ELEM,,NUM,MAX
! E1HFBRK2= Element Number of 1st part of a Half BRICK in the 2nd Layer
! E1HFBRK2, Here 1= 1st brick, HF = Half Brick, 2 = 2nd Layer

ESEL,S,ELEM,,E1HFBRK2                         ! Selecting the 1st  Half BRICK in the 2nd Layer
EGEN,2,1,ALL


! Creating a Full BRICK after a 1/2 BRICK in the 2nd layer

I=N1WALL+((NoBrkX*2)*2*(DIVWZ+1))*2+(DIVWZ+1)*2

! 1st Node at the 2nd brick layer which starts with a Full BRICK

J=I+(DIVWZ+1)
K=J+1
L=I+1
M=I+(DIVWZ+1)*2*NoBrkX*2
N=M+(DIVWZ+1)
O=N+1
P=M+1
E,I,J,K,L,M,N,O,P

*GET,E2FLBRK2,ELEM,,NUM,MAX
! E2FLBRK2= Element Number of 1st part of a Full BRICK in the 2nd Layer
! E2FLBRK2, Here 2= 2nd brick, FL = part of a Full Brick, 2 = 2nd Layer

ESEL,S,ELEM,,E2FLBRK2                 ! Selecting the 1st  Full BRICK in the 2nd Layer
EGEN,2,1,ALL
EGEN,3,(DIVWZ+1),ALL
EGEN,NoBrkX-1,(DIVWZ+1)*4,ALL        ! Generating 2nd brick layer immediate to the last 1/2 BRICK
ESEL,S,ELEM,,E1HFBRK2,E1HFBRK2+1             ! Selecting the 1st  Half BRICK in the 2nd Layer
EGEN,2,(NoBrkX*2-1)*2*(DIVWZ+1),ALL
! Creating the last brick of the 2nd Layer which is a Half BRICK
```

```
*GET,ELSTBRK2,ELEM,,NUM,MAX
! ELSTBRK2= Element Number of last part of the Half BRICK in the 2nd Layer

! There are "NoLHFBRK" No. of BRICK Layers starting with Half Brick

ESEL,S,ELEM,,E1HFBRK2,ELSTBRK2                    ! Selecting all the bricks in the 2nd Layer
EGEN,NoLHFBRK,((DIVWZ+1)*2*NoBrkX*2)*2*2,ALL
! Generating all the brick layers starting with Half Size BRICKs

ALLSEL

TYPE,2
MAT,4

I=N1WALL+(DIVWZ+1)*3
J=I+(DIVWZ+1)
K=J+1
L=I+1
M=I+(DIVWZ+1)*2*NoBrkX*2
N=M+(DIVWZ+1)
O=N+1
P=M+1
E,I,J,K,L,M,N,O,P                      ! Creating 1st MORTAR element  in the1st BRICK Layer
                                       ! starting with Full Brick
*GET,E1MRTR1,ELEM,,NUM,MAX             ! E1MRTR1= Element Number of 1st  part of mortar
                                       ! in the 1st BRICK Layer starting with Full Brick
ESEL,S,ELEM,, E1MRTR1                  ! Selecting 1st part of 1st MORTAR element of
                                       ! 1st row of BRICK Layers
EGEN,2,1,ALL                           ! Generating 1st MORTAR element of 1st row of
                                       !BRICK Layers
EGEN,NoBrkX-1,(DIVWZ+1)*4,ALL          ! Generating All the MORTAR elements in the 1st BRICK
                                       ! Layers, starting with a Full BRICK

EGEN,NoLFLBRK,((NoBrkX*2)*2*(DIVWZ+1))*4,ALL     ! Generating All the MORTAR elements in
                                                 ! all the BRICK Layers, starting with a Full BRICK

! Creating MORTAR elements in the BRICK layers starting with a Half size Brick

I=N1WALL+((NoBrkX*2)*2*(DIVWZ+1))*2+(DIVWZ+1)
J=I+(DIVWZ+1)
K=J+1
L=I+1
M=I+(DIVWZ+1)*2*NoBrkX*2
N=M+(DIVWZ+1)
O=N+1
P=M+1
E,I,J,K,L,M,N,O,P

*GET,E1MRTR2,ELEM,,NUM,MAX
! E1MRTR2= Element Number of 1st  MORTAR in the 2nd BRICK Layer starting with a Half Brick

ESEL,S,ELEM,, E1MRTR2
! Selecting 1st MORTAR element of 2nd row of BRICK Layers starting with a Half Brick
EGEN,2,1,ALL
! Generating 1st MORTAR element of 2nd row of BRICK Layers starting with a Half Brick

EGEN,NoBrkX,(DIVWZ+1)*4,ALL
! Generating All the MORTAR elements in the 2nd BRICK Layers, starting with a Half BRICK
```

EGEN,NoLHFBRK,((NoBrkX*2)*2*(DIVWZ+1))*4,ALL
! Generating All the MORTAR elements in the BRICK Layers, starting with a Half BRICK

ESEL,S,MAT,,4

! Creating Mortar Layer in between Brick Layers

I=N1WALL+(NoBrkX*2)*2*(DIVWZ+1)
J=I+(DIVWZ+1)
K=J+1
L=I+1
M=I+(DIVWZ+1)*2*NoBrkX*2
N=M+(DIVWZ+1)
O=N+1
P=M+1
E,I,J,K,L,M,N,O,P

*GET,EMRTRBtn,ELEM,,NUM,MAX
! EMRTRBtn= Element Number of 1st part of MORTAR in Between1st and 2nd BRICK Layer

ESEL,S,ELEM,, EMRTRBtn
! Selecting 1st part of MORTAR element in Between1st and 2nd BRICK Layer

EGEN,2,1,ALL   ! Generating 1st MORTAR in Between1st and 2nd BRICK Layer
EGEN,(NoBrkX*4-1),(DIVWZ+1),ALL
! Generating 1st MORTAR Layer in Between 1st and 2nd BRICK Layers

EGEN,NoBrkY-1,(NoBrkX*2)*2*(DIVWZ+1)*2,ALL
! Generating all the MORTAR Layers in Between BRICK Layers

*GET,EMRTRLST,ELEM,,NUM,MAX
! EMRTRLST= Element Number of the Last part of MORTAR

!********************************
!GENERATING BASE BEAM
!********************************

*GET,N_INFLST,NODE,0,NUM,MAX   ! Last Node of Infill

N1B_BEAM=N_INFLST+1   ! 1st Node of Base Beam
N,,-B_EXT*12-CTX,-B_BDY   ! Defining 1st Base beam node
N,,-B_EXT*12-CTX,-B_BDY,COVR
N,,-B_EXT*12-CTX,-B_BDY,B_BTZ/2
N,,-B_EXT*12-CTX,-B_BDY,B_BTZ-COVR
N,,-B_EXT*12-CTX,-B_BDY,B_BTZ

NSEL,S,NODE,,N1B_BEAM,N1B_BEAM+DIV_BBZ
! Selecting nodes of the 1st row of Base Beam

NGEN,2,DIV_BBZ+1,ALL,,,,COVR   ! Generating another row above the 1st row
NSEL,S,NODE,,N1B_BEAM,N1B_BEAM+DIV_BBZ   ! Selecting nodes of the 1st row of Base Beam
NGEN,2,(DIV_BBZ+1)*2,ALL,,,,B_BDY/2   ! Generating 3rd row of nodes above the 2nd row
NSEL,S,NODE,,N1B_BEAM,N1B_BEAM+DIV_BBZ   ! Selecting nodes of the 1st row of Base Beam
NGEN,2,(DIV_BBZ+1)*3,ALL,,,,B_BDY-COVR   ! Generating 4th row of nodes above the 3rd row
NSEL,S,NODE,,N1B_BEAM,N1B_BEAM+DIV_BBZ   ! Selecting nodes of the 1st row of Base Beam
NGEN,2,(DIV_BBZ+1)*4,ALL,,,,B_BDY   ! Generating top row of nodes of the beam

NSEL,S,NODE,,N1B_BEAM,N1B_BEAM+(DIV_BBZ+1)*(B_DIVBY+1)-1
! Selecting 1st Plane Nodes of Base Beam

NGEN,B_DIVEBX+1,(DIV_BBZ+1)*(B_DIVBY+1),ALL,,,B_BM_DX   !
NSEL,S,NODE,,N1B_BEAM+(DIV_BBZ+1)*(B_DIVBY+1)*B_DIVEBX,N1B_BEAM+(DIV_BBZ+1)*(
B_DIVBY+1)*(B_DIVEBX+1)-1
! Selecting a Plane of Nodes at the Column Reinforcement Location

NGEN,2,(DIV_BBZ+1)*(B_DIVBY+1),ALL,,,COVR

NSEL,S,NODE,,N1B_BEAM+(DIV_BBZ+1)*(B_DIVBY+1)*B_DIVEBX,N1B_BEAM+(DIV_BBZ+1)*(
B_DIVBY+1)*(B_DIVEBX+1)-1
! Selecting a Plane of Nodes at the Column Reinforcement Location

NGEN,2,(DIV_BBZ+1)*(B_DIVBY+1)*2,ALL,,,CTX/2

NSEL,S,NODE,,N1B_BEAM+(DIV_BBZ+1)*(B_DIVBY+1)*B_DIVEBX,N1B_BEAM+(DIV_BBZ+1)*(
B_DIVBY+1)*(B_DIVEBX+1)-1
! Selecting a Plane of Nodes at the Column Reinforcement Location

NGEN,2,(DIV_BBZ+1)*(B_DIVBY+1)*3,ALL,,,CTX-COVR

NSEL,S,NODE,,N1B_BEAM+(DIV_BBZ+1)*(B_DIVBY+1)*B_DIVEBX,N1B_BEAM+(DIV_BBZ+1)*(
B_DIVBY+1)*(B_DIVEBX+1)-1
! Selecting a Plane of Nodes at the Column Reinforcement Location

NGEN,2,(DIV_BBZ+1)*(B_DIVBY+1)*4,ALL,,,CTX

*GET,N_B_COLM,NODE,0,NUM,MAX   ! Last Node of Base Beam upto Left Column Lacation

NSEL,S,NODE,,N_B_COLM-(DIV_BBZ+1)*(B_DIVBY+1)+1,N_B_COLM   !Plane of Nodes of the Base
Beam at the Location of last point of Left Column
NGEN,(NoBrkX*2+1),(DIV_BBZ+1)*(B_DIVBY+1),ALL,,,WLX/(NoBrkX*2)   ! Generating nodes
of the Base Beam at the position of the bricks

*GET,N_B_RCOL,NODE,0,NUM,MAX   ! Last Node of Base Beam upto face of Right Column

NSEL,S,NODE,,N_B_RCOL-(DIV_BBZ+1)*(B_DIVBY+1)+1,N_B_RCOL
!Plane of Nodes of the Base Beam at the Location of last point of Left Column

NGEN,2,(DIV_BBZ+1)*(B_DIVBY+1),ALL,,,COVR

NSEL,S,NODE,,N_B_RCOL-(DIV_BBZ+1)*(B_DIVBY+1)+1,N_B_RCOL
!Plane of Nodes of the Base Beam at the Location of last point of Left Column

NGEN,2,(DIV_BBZ+1)*(B_DIVBY+1)*2,ALL,,,CTX/2
NSEL,S,NODE,,N_B_RCOL-(DIV_BBZ+1)*(B_DIVBY+1)+1,N_B_RCOL
!Plane of Nodes of the Base Beam at the Location of last point of Left Column

NGEN,2,(DIV_BBZ+1)*(B_DIVBY+1)*3,ALL,,,CTX-COVR

DIST=B*12+CTX+B_EXT*12   ! Distance Between Extended nodes of Base Beam
B_N_INCR=(DIV_BBZ+1)*(B_DIVBY+1)*B_DIVEBX+(2*DIVCX+1)*(DIV_BBZ+1)*(B_DIVBY+1)+(
NoBrkX*2-1)*(DIV_BBZ+1)*(B_DIVBY+1)

NSEL,S,NODE,,N1B_BEAM,N1B_BEAM+(DIV_BBZ+1)*(B_DIVBY+1)*(B_DIVEBX+1)-1
! Selecting nodes of the 1st row of Base Beam
NGEN,2,B_N_INCR,ALL,,,DIST

ALLSEL

*GET,N_L_B_BM,NODE,0,NUM,MAX   ! N_L_B_BM=Last Node of Base Beam

```
T_N_B_BM=N_L_B_BM-N1B_BEAM+1   ! Total Nodes in a Base Beam
N_1L_BBM=T_N_B_BM/(B_DIVBY+1)    ! Total Nodes in ONE Layer of a Base Beam

T_E_B_BM=N_1L_BBM/(DIV_BBZ+1)-1 !Total No. of Elements in ONE Layer of Base Beam

TYPE,1
MAT,6

I=N1B_BEAM
J=I+(DIV_BBZ+1)*(B_DIVBY+1)
K=J+1
L=I+1
M=I+DIV_BBZ+1
N=M+(DIV_BBZ+1)*(B_DIVBY+1)
O=N+1
P=M+1
E,I,J,K,L,M,N,O,P                          ! Creating 1st BASE Beam element
ESEL,S,MAT,,6
EGEN,DIV_BBZ,1,ALL                         ! Creating 1st row of beam element
EGEN,B_DIVBY,DIV_BBZ+1,ALL                            ! Creating 1st base beam elements
EGEN,T_E_B_BM,(DIV_BBZ+1)*(B_DIVBY+1),ALL
! Creating beam elements upto 2nd last element row


!**********************************************
! Reinforcing two Columns
!**********************************************
TYPE,3
REAL,3
MAT,5

! Reinforcing left Column
*DO,I,1,(NoBrkY*2+DIVBY)-1                 ! Starting a Loop to generate reinforcment
I=I-1
J=(DIVCX+1)+2+(DIVCX+1)*(DIVCZ+1)*I        ! (Generating 1st Reinforcement)
K=J+(DIVCX+1)*(DIVCZ+1)
E,J,K

*IF,I,EQ,0,THEN
*GET,Erodfst1,ELEM,,NUM,MAX
! Erodfst1= Element Number of First part of Reinforcement of the 1st Column
*ENDIF

L=(DIVCX+1)*2-1+(DIVCX+1)*(DIVCZ+1)*I      ! (Generating 2nd Reinforcement)
M=L+(DIVCX+1)*(DIVCZ+1)
E,L,M

N=(DIVCX+1)*(DIVCZ+1)*(I+1)-(DIVCX+1)*2+2 ! (Generating 3rd Reinforcement)
O=N+(DIVCX+1)*(DIVCZ+1)
E,N,O

J1=(DIVCX+1)*(DIVCZ+1)*(I+1)-(DIVCX+1)-1    ! (Generating 4th Reinforcement)
K1=J1+(DIVCX+1)*(DIVCZ+1)
E,J1,K1

*END DO

*GET,Erodlst1,ELEM,,NUM,MAX
! Erodlst1= Element Number of Last part of Reinforcement of the 1st Column
```

```
ESEL,S,ELEM,,Erodfst1,Erodlst1                          ! Selecting all the reinforcement of Left Column
EGEN,2,(NoBrkY*2+DIVBY)*(DIVCX+1)*(DIVCZ+1),ALL
! Generating all the reinforcement of Right Column

!*********************************************
! Reinforcing Beam
!*********************************************

TYPE,3
REAL,3
MAT,5

*DO,I,1,(4*NoBrkX-1)                                    ! Starting a Loop to generate Reinforcement
I=I-1

J=N1BEAM+(DIVBZ+1)+1+(DIVBZ+1)*(DIVBY+1)*I      ! (Generating 1st Reinforcement)
K=J+(DIVBZ+1)*(DIVBY+1)
E,J,K

L=N1BEAM+(DIVBZ+1)*2-2+(DIVBZ+1)*(DIVBY+1)*I    ! (Generating 2nd Reinforcement)
M=L+(DIVBZ+1)*(DIVBY+1)
E,L,M

N=N1BEAM+(DIVBZ+1)*(DIVBY+1)*(I+1)-(DIVBZ+1)*2+1        ! (Generating 3rd Reinforcement)
O=N+(DIVBZ+1)*(DIVBY+1)
E,N,O

J1=N1BEAM+(DIVBZ+1)*(DIVBY+1)*(I+1)-(DIVBZ+1)-2 ! (Generating 4th Reinforcement)
K1=J1+(DIVBZ+1)*(DIVBY+1)
E,J1,K1

*END DO

! Extending Reinforcement into LEFT Column
N1C_LXBM=NMAXC1-(DIVCX+1)*(DIVCZ+1)*DIVBY+(DIVCX+1)+1
N2C_LXBM=N1C_LXBM+(DIVCX+1)*2
N3C_LXBM=NMAXC1-(DIVCX+1)*(DIVCZ+1)*2+(DIVCX+1)+1
N4C_LXBM=N3C_LXBM+(DIVCX+1)*2

*DO,I,1,DIVCX

J=N1C_LXBM+I-1
K=J+1
E,J,K

J1=N2C_LXBM+I-1
K1=J1+1
E,J1,K1

J2=N3C_LXBM+I-1
K2=J2+1
E,J2,K2

J3=N4C_LXBM+I-1
K3=J3+1
E,J3,K3

*END DO
```

```
! Extending Reinforcement into RIGHT Column
N1C_RXBM=2*NMAXC1-(DIVCX+1)*(DIVCZ+1)*DIVBY+(DIVCX+1)+1
N2C_RXBM=N1C_RXBM+(DIVCX+1)*2
N3C_RXBM=2*NMAXC1-(DIVCX+1)*(DIVCZ+1)*2+(DIVCX+1)+1
N4C_RXBM=N3C_RXBM+(DIVCX+1)*2

*DO,I,1,DIVCX

J=N1C_RXBM+I-1
K=J+1
E,J,K

J1=N2C_RXBM+I-1
K1=J1+1
E,J1,K1

J2=N3C_RXBM+I-1
K2=J2+1
E,J2,K2

J3=N4C_RXBM+I-1
K3=J3+1
E,J3,K3

*END DO

!********************************************
! Reinforcing BASE Beam
!********************************************

TYPE,3
REAL,3
MAT,5

*DO,I,1,T_E_B_BM                              ! Starting a Loop to generate Reinforcement
I=I-1

J=N1B_BEAM+(DIV_BBZ+1)+1+(DIV_BBZ+1)*(B_DIVBY+1)*I    ! (Generating 1st Reinforcement)
K=J+(DIV_BBZ+1)*(B_DIVBY+1)
E,J,K

L=N1B_BEAM+(DIV_BBZ+1)*2-2+(DIV_BBZ+1)*(B_DIVBY+1)*I! (Generating 2nd Reinforcement)
M=L+(DIV_BBZ+1)*(B_DIVBY+1)
E,L,M

N=N1B_BEAM+(DIV_BBZ+1)*(B_DIVBY+1)*(I+1)-(DIV_BBZ+1)*2+1       ! (Generating 3rd
Reinforcement)
O=N+(DIV_BBZ+1)*(B_DIVBY+1)
E,N,O

J1=N1B_BEAM+(DIV_BBZ+1)*(B_DIVBY+1)*(I+1)-(DIV_BBZ+1)-2        ! (Generating 4th
Reinforcement)
K1=J1+(DIV_BBZ+1)*(B_DIVBY+1)
E,J1,K1

*END DO

! Extending Reinforcement of Left Column into Base Beam
N1L_B_BM=N1B_BEAM+(B_DIVEBX+1)*(DIV_BBZ+1)*(B_DIVBY+1)+1
N2L_B_BM=N1L_B_BM+DIV_BBZ-2
```

```
N3L_B_BM=N1B_BEAM+(B_DIVEBX+DIVCX-1)*(DIV_BBZ+1)*(B_DIVBY+1)+1
N4L_B_BM=N3L_B_BM+DIV_BBZ-2

*DO,I,1,B_DIVBY

J=N1L_B_BM+(DIV_BBZ+1)*(I-1)
K=J+(DIV_BBZ+1)
E,J,K

J1=N2L_B_BM+(DIV_BBZ+1)*(I-1)
K1=J1+(DIV_BBZ+1)
E,J1,K1

J2=N3L_B_BM+(DIV_BBZ+1)*(I-1)
K2=J2+(DIV_BBZ+1)
E,J2,K2

J3=N4L_B_BM+(DIV_BBZ+1)*(I-1)
K3=J3+(DIV_BBZ+1)
E,J3,K3

*END DO

! Extending Reinforcement of Right Column into Base Beam

N1R_B_BM=N_L_B_BM-(B_DIVEBX+DIVCX)*(DIV_BBZ+1)*(B_DIVBY+1)+2
N2R_B_BM=N1R_B_BM+DIV_BBZ-2
N3R_B_BM=N_L_B_BM-(B_DIVEBX+2)*(DIV_BBZ+1)*(B_DIVBY+1)+2
N4R_B_BM=N3R_B_BM+DIV_BBZ-2

*DO,I,1,B_DIVBY

J=N1R_B_BM+(DIV_BBZ+1)*(I-1)
K=J+(DIV_BBZ+1)
E,J,K

J1=N2R_B_BM+(DIV_BBZ+1)*(I-1)
K1=J1+(DIV_BBZ+1)
E,J1,K1

J2=N3R_B_BM+(DIV_BBZ+1)*(I-1)
K2=J2+(DIV_BBZ+1)
E,J2,K2

J3=N4R_B_BM+(DIV_BBZ+1)*(I-1)
K3=J3+(DIV_BBZ+1)
E,J3,K3

*END DO

!**************************
!INTERFACE ELEMENT
!**************************

! APPLYING TARGET ELEMENT
TYPE,4
REAL,4
TSHAP,QUAD                ! Shape of the target element is quadrilateral

! Defining Interface Element Between Column & Infill
```

```
! TARGET Element on Left Column Face
MAT,1

*DO,Num,1,NoBrkY*2-1

Num=Num-1

I=(DIVCX+1)*2+(DIVCX+1)*(DIVCZ+1)*Num                    ! Node at the ground along column face at
                                                         ! position of Reinforcements on Z axis
J=(DIVCX+1)*2+(DIVCX+1)*(DIVCZ+1)*(Num+1)                ! Node at the next layer along column face
K=(NINT(DIVCZ/2+1))*(DIVCX+1)+(DIVCX+1)*(DIVCZ+1)*(Num+1)    ! Node at the next layer
                                                             ! along column face
L=(NINT(DIVCZ/2+1))*(DIVCX+1)+(DIVCX+1)*(DIVCZ+1)*Num        ! Node at the ground along
                                                             ! column face

E,I,J,K,L

I1=(NINT(DIVCZ/2+1))*(DIVCX+1)+(DIVCX+1)*(DIVCZ+1)*Num        ! Node at the ground along
                                                              ! column face
J1=(NINT(DIVCZ/2+1))*(DIVCX+1)+(DIVCX+1)*(DIVCZ+1)*(Num+1)    ! Node at the next layer
                                                              ! along column face
K1=(DIVCX+1)*DIVCZ+(DIVCX+1)*(DIVCZ+1)*(Num+1)                ! Node at the next layer
                                                              ! along column face
L1=DIVCZ*(DIVCX+1)+(DIVCX+1)*(DIVCZ+1)*Num                    ! Node at the ground along
                                                              ! column face

E,I1,J1,K1,L1

*END DO

! TARGET Element on Rightt Column Face
N1COL2=NMAXC1+1                  ! N1COL2= 1st Node of Column 2

*DO,Num,1,NoBrkY*2-1
Num=Num-1

I=N1COL2+(DIVCX+1)+(DIVCX+1)*(DIVCZ+1)*Num                       ! Node at the ground along Right
                                                                 ! column face
J=N1COL2+(NINT(DIVCZ/2))*(DIVCX+1)+(DIVCX+1)*(DIVCZ+1)*Num        ! Node at the ground along
                                                                 ! Right column face
K=N1COL2+(NINT(DIVCZ/2))*(DIVCX+1)+(DIVCX+1)*(DIVCZ+1)*(Num+1)        ! Node at the next
                                                                 ! layer along Right column face
L=N1COL2+(DIVCX+1)+(DIVCX+1)*(DIVCZ+1)*(Num+1)                    ! Node at the next layer
                                                                 ! along Right column face

E,I,J,K,L

I1=N1COL2+(NINT(DIVCZ/2))*(DIVCX+1)+(DIVCX+1)*(DIVCZ+1)*Num    ! Node at the ground along
                                                              ! Right column face
J1=N1COL2+(DIVCX+1)*(DIVCZ-1)+(DIVCX+1)*(DIVCZ+1)*Num          ! Node at the ground along
                                                              ! Right column face
K1=N1COL2+(DIVCX+1)*(DIVCZ-1)+(DIVCX+1)*(DIVCZ+1)*(Num+1)      ! Node at the next layer
                                                              ! along Right column face
L1=N1COL2+(NINT(DIVCZ/2))*(DIVCX+1)+(DIVCX+1)*(DIVCZ+1)*(Num+1)    ! Node at the next
                                                              ! layer along Right column face
E,I1,J1,K1,L1

*END DO

! Defining Interface Element Between Beam & Infill
! TARGET Element on Beam Face
MAT,2
```

```
*DO,Num,1,NoBrkX*2*2-1

Num=Num-1

I=N1BEAM+1+(DIVBY+1)*(DIVBZ+1)*Num                          ! Node at the Lower edge of beam face
J=N1BEAM+1+(DIVBY+1)*(DIVBZ+1)*(Num+1)                      ! Node at the next section of the Lower edge
                                                           ! of beam face
K=N1BEAM+NINT(DIVBZ/2)+(DIVBY+1)*(DIVBZ+1)*(Num+1)    ! Node at the next section of the
                                                           ! Lower edge of beam face
L=N1BEAM+NINT(DIVBZ/2)+(DIVBY+1)*(DIVBZ+1)*Num        ! Node at the Lower edge of beam face
E,I,J,K,L

I1=N1BEAM+DIVBZ-1+(DIVBY+1)*(DIVBZ+1)*Num            ! Node at the Lower edge of beam face
J1=N1BEAM+NINT(DIVBZ/2)+(DIVBY+1)*(DIVBZ+1)*Num      ! Node at the Lower edge of beam face
K1=N1BEAM+NINT(DIVBZ/2)+(DIVBY+1)*(DIVBZ+1)*(Num+1)      ! Node at the next section of the
                                                           ! Lower edge of beam face
L1=N1BEAM+DIVBZ-1+(DIVBY+1)*(DIVBZ+1)*(Num+1)           ! Node at the next section of the
                                                           ! Lower edge of beam face
E,I1,J1,K1,L1

*END DO

! Defining Interface Element Between BASE Beam & Infill
! TARGET Element over BASE Beam Face
MAT,6

N1_B_TRG=N1B_BEAM+(B_DIVEBX+DIVCX+1)*(DIV_BBZ+1)*(B_DIVBY+1)-DIV_BBZ

*DO,NUM,1,NoBrkX*2

I=N1_B_TRG+(DIV_BBZ+1)*(B_DIVBY+1)*(NUM-1)
J=I+1
K=J+(DIV_BBZ+1)*(B_DIVBY+1)
L=K-1
E,I,J,K,L

I1=N1_B_TRG+(DIV_BBZ+1)*(B_DIVBY+1)*(NUM-1)+1
J1=I1+1
K1=J1+(DIV_BBZ+1)*(B_DIVBY+1)
L1=K1-1
E,I1,J1,K1,L1

*END DO


! APPLYING CONTACT ELEMENT
TYPE,5
REAL,4

! Defining Interface Element Between Column & Infill
! CONTA173 Element on Left Face of INFILL
MAT,3

*DO,Num,1,2*NoBrkY-1

I=N1WALL+(DIVWZ+1)*2*NoBrkX*2*(Num-1)                       ! Wall Node
J=I+1
K=J+(DIVWZ+1)*2*NoBrkX*2
L=K-1
E,I,J,K,L
```

```
I1=N1WALL+(DIVWZ+1)*2*NoBrkX*2*(Num-1)+1          ! Wall Node
J1=I1+1
K1=J1+(DIVWZ+1)*2*NoBrkX*2
L1=K1-1
E,I1,J1,K1,L1

*END DO

! Defining Interface Element Between Column & Infill
! CONTA173 Element on Right Face of INFILL

*DO,Num,1,2*NoBrkY-1

I=N1WALL+(DIVWZ+1)*2*NoBrkX*2*Num-3     ! Wall Node
J=I+1
K=J+(DIVWZ+1)*2*NoBrkX*2
L=K-1
E,I,L,K,J

I1=N1WALL+(DIVWZ+1)*2*NoBrkX*2*Num-2    ! Wall Node
J1=I1+1
K1=J1+(DIVWZ+1)*2*NoBrkX*2
L1=K1-1
E,I1,L1,K1,J1

*END DO

! Defining Interface Element Between BASE Beam & Infill
! CONTA173 Element below INFILL

*DO,Num,1,4*NoBrkX-1

I=N1WALL+(DIVWZ+1)*(Num-1)
J=I+1
K=J+(DIVWZ+1)
L=K-1
E,I,L,K,J

I1=N1WALL+(DIVWZ+1)*(Num-1)+1
J1=I1+1
K1=J1+(DIVWZ+1)
L1=K1-1
E,I1,L1,K1,J1

*END DO

! Defining Interface Element Between Beam & Infill
! CONTA173 Element over INFILL
! NLSTRW1N= 1st Node No. of the Last Layer of the Topmost Brick Layer

NLSTRW1N=N1WALL+(DIVWZ+1)*2*NoBrkX*2*(NoBrkY*2-1)

*DO,Num,1,4*NoBrkX-1

I=NLSTRW1N+(DIVWZ+1)*(Num-1)
J=I+1
K=J+(DIVWZ+1)
L=K-1
E,I,J,K,L
```

```
I1=NLSTRW1N+(DIVWZ+1)*(Num-1)+1
J1=I1+1
K1=J1+(DIVWZ+1)
L1=K1-1
E,I1,J1,K1,L1

*END DO

!***************************
!MERGE
!***************************
ALLSEL
NUMMRG,NODE
NUMMRG,ELEM
NUMCMP,NODE
NUMCMP,ELEM

!******************************
!SUPPORT CONDITION
!******************************

! Support Conditions and loads are given
NSEL,S,LOC,X,0,-(B_EXT*12+CTX)
NSEL,R,LOC,Y,-B_BDY,-B_BDY
D,ALL,ALL

NSEL,S,LOC,X,B*12-CTX,B_EXT*12+B*12
NSEL,R,LOC,Y,-B_BDY,-B_BDY
D,ALL,ALL

!******************************
!LOADS APPLYING
!******************************

!Concentrated Load, P is distributed(P_dis) at all the nodes of the intersection of Beam and Column

P_dis=P/((DIVBY+1)*(DIVCZ+1))

! Now selecting all the nodes at the face of the column which intersects with beam.
NSEL,S,LOC,X,-CTX
NSEL,R,LOC,Y,WHY,H*12
NSEL,R,LOC,Z,0,CTZ

F,ALL,FX,P_dis          ! Applying load in X direction at the joint of portal

!*************************************************
! NUMBERING MATERIAL NUMBERS BY COLORS ONLY
!*************************************************

ALLSEL
/NUM,1
/PNUM,MAT,1
/REPLOT
GPLOT
SAVE
```